SPONTANEOUS PANCREATITIS CAUSED BY TISSUE-SPECIFIC GENE ABLATION OF *HHEX* IN MICE

Mark Ferreira

A DISSERTATION

in

Cell and Molecular Biology

Presented to the Faculties of the University of Pennsylvania

in

Partial Fulfillment of the Requirements for the

Degree of Doctor of Philosophy

2015

Supervisor of Dissertation

_____

Klaus H. Kaestner, Ph.D.
Professor of Genetics

Graduate Group Chairperson

_____

Daniel S. Kessler, Ph.D.
Associate Professor of Cell and Developmental Biology

Dissertation Committee
Michael A. Pack, M.D., Professor of Medicine
Anil K. Rustgi, M.D., Professor of Medicine
Doris A. Stoffers, M.D., Ph.D., Professor of Medicine
Ben Z. Stanger, M.D.,Ph.D., Associate Professor of Medicine (Chair)

ACKNOWLEDGMENTS

First and foremost, I would like to thank my thesis advisers, Drs. Catherine Lee May and Klaus Kaestner, for their immense support and guidance throughout my thesis years. Both are incredible scientists who have a passion for science that is admirable. Each has undoubtedly cultivated my development as a scientist by granting me independence, yet guidance when needed, and for this I am certainly grateful.

Also, I would to acknowledge my thesis committee, Drs. Ben Stanger, Anil Rustgi, Doris Stoffers, and Michael Pack, for their helpful suggestions and guidance to my project throughout the years.

I am indebted to Dr. Maximilian Reichert and Basil Bakir for their immense help with the assays involving primary ductal cells. Although many times the cells decided not to cooperate, Max and Basil were always willing to sacrifice their time to try again.

I would like to thank all members of the Kaestner Lab for welcoming me into the lab midway through my thesis and making the lab such a fun place to work. Everyone has helped me in some way given the vast amount of technical expertise in the lab. I would particularly like to thank: Drs. Jia Zhang and Lindsay McKenna for pioneering the Hhex project and carrying it forward before my arrival; Tia Bernard-Banks for her immense help with mouse husbandry and checking plugs; Dr. Karyn Sheaffer for tolerating my neverending amount of questions, and actually answering them; Dr. John Le Lay for his willingness to provide his technical expertise and knowledge; and Dr. Natalie Terry for her sage advice and help throughout the past several years. Finally, I need to thank all my friends and family who have helped and encouraged me throughout these past few years!

ABSTRACT

SPONTANEOUS PANCREATITIS CAUSED BY TISSUE-SPECIFIC GENE ABLATION OF *HHEX* IN MICE

Mark Ferreira

Klaus H. Kaestner

Background & Aims: Perturbations in pancreatic ductal bicarbonate secretion often result in chronic pancreatitis. Although the physiological mechanism of ductal secretion is known, its transcriptional control is not well characterized. Here, we investigate the role of the transcription factor Hematopoietically-expressed homeobox protein (Hhex) in pancreatic secretion and pancreatitis.

Methods: We derived mice with pancreas-specific, Cre-mediated *Hhex* gene ablation to determine the requirement of Hhex in the pancreatic duct in early life and in adult stages. Histological and immunostaining analyses were used to detect the presence of pathology. Pancreatic primary ductal cells (PDCs) were isolated to discover differentially expressed transcripts upon acute *Hhex* ablation on a cell autonomous level.

Results: Hhex protein was detected throughout the embryonic and adult ductal trees. Ablation of *Hhex* in pancreatic progenitors resulted in postnatal ductal ectasia associated with acinar-to-ductal metaplasia, a progressive phenotype that ultimately resulted in chronic pancreatitis. *Hhex* ablation in adult mice, however, did not cause any detectable pathology. Ductal ectasia in young mice did not result from perturbations of Hnf6,

Hnf1β, or primary cilia expression. RNA-seq analysis of *Hhex*-ablated PDCs indicated the G-protein coupled receptor *Natriuretic peptide receptor 3* (*Npr3*), implicated in paracrine signaling, was upregulated 4.70-fold.

Conclusions: Although Hhex is dispensable for ductal cell function in the adult, ablation of *Hhex* in pancreatic progenitors results in pancreatitis. Our data highlight the critical role of Hhex in maintaining ductal homeostasis in early life and support ductal hypersecretion as a novel etiology of pediatric chronic pancreatitis.

TABLE OF CONTENTS

LIST OF TABLES

LIST OF FIGURES

CHAPTER 1
INTRODUCTION

The pancreas, situated in the abdomen posterior to the stomach and within the duodenal C-loop, is a dual-function organ that plays a necessary role in the digestive process and blood glucose regulation. On a histological level, the pancreas can be divided into two compartments that represent their functions – namely the endocrine (islets of Langerhans, blood glucose homeostasis) and exocrine (acinar and ductal cells, delivery of digestive enzymes) compartments. In this chapter, I will outline the developmental process orchestrating pancreatic development, and more specifically the pancreatic ductal tree, with an emphasis on the role that various transcription factors play in this process (Part I). In addition, I will describe the molecular process by which ductal bicarbonate secretion occurs (Part II), and I will relate this secretory mechanism to current findings regarding pancreatic ductal pathology (Part III), a significant cause of morbidity and mortality in patients worldwide. Finally, I will introduce the transcription factor Hematopoietically-expressed homeobox protein (Hhex) (Part IV), whose role in the pancreatic duct is the main focus of this dissertation.

I. PANCREATIC DEVELOPMENT

Morphological Development of the Pancreas

Pancreatic development, akin to the development of many organs, is a highly regulated process contingent upon the proper input of various extrinsic morphogens and cell-autonomous expression of transcription factors in specified endodermal cells. Due to

the complex interplay of morphological changes occurring in the embryo and the elaboration of different transcription factor networks as progenitor cells differentiate, pancreatic development is generally divided into distinct periods, each with its associated critical milestones. These include: (1) the primary transition (E9.5-E12.5 in the mouse), marked by outgrowth of pancreatic progenitors from the foregut, branching morphogenesis, the emergence of a population of primarily glucagon^{+} endocrine cells, and the initiation of ductal morphogenesis; (2) the secondary transition (E13.5-E16.5), which includes differentiation and expansion of the acinar, ductal, and endocrine lineages; (3) the perinatal period, a time in which all epithelial lineages undergo rapid proliferation and maturation; and (4) adulthood, when the mature pancreas is poised to perform its endocrine and exocrine functions as necessary (see Figure 1). Because the majority of ductal cell differentiation and morphogenesis occurs in the primary and secondary transitions, these periods are discussed below.

The Primary Transition

The first morphological evidence of pancreatic development is detectable at approximately E9.0-E9.5 in the mouse, at which time a thickening of cells develops on the dorsal gut tube and subsequently evaginates dorsally (Wessells and Cohen, 1967); this anlage is termed the "dorsal pancreatic bud" (dorsal bud). Just prior to the evagination of the dorsal bud, the dorsal gut tube loses direct contact with the notochord at E8.5 as the dorsal aortae fuse, which has important ramifications concerning extrinsic morphogenic signals (Pictet et al., 1972). The dorsal bud undergoes elongation into a stalk of stratified, unpolarized epithelium with a stunted lumen continuous with the gut

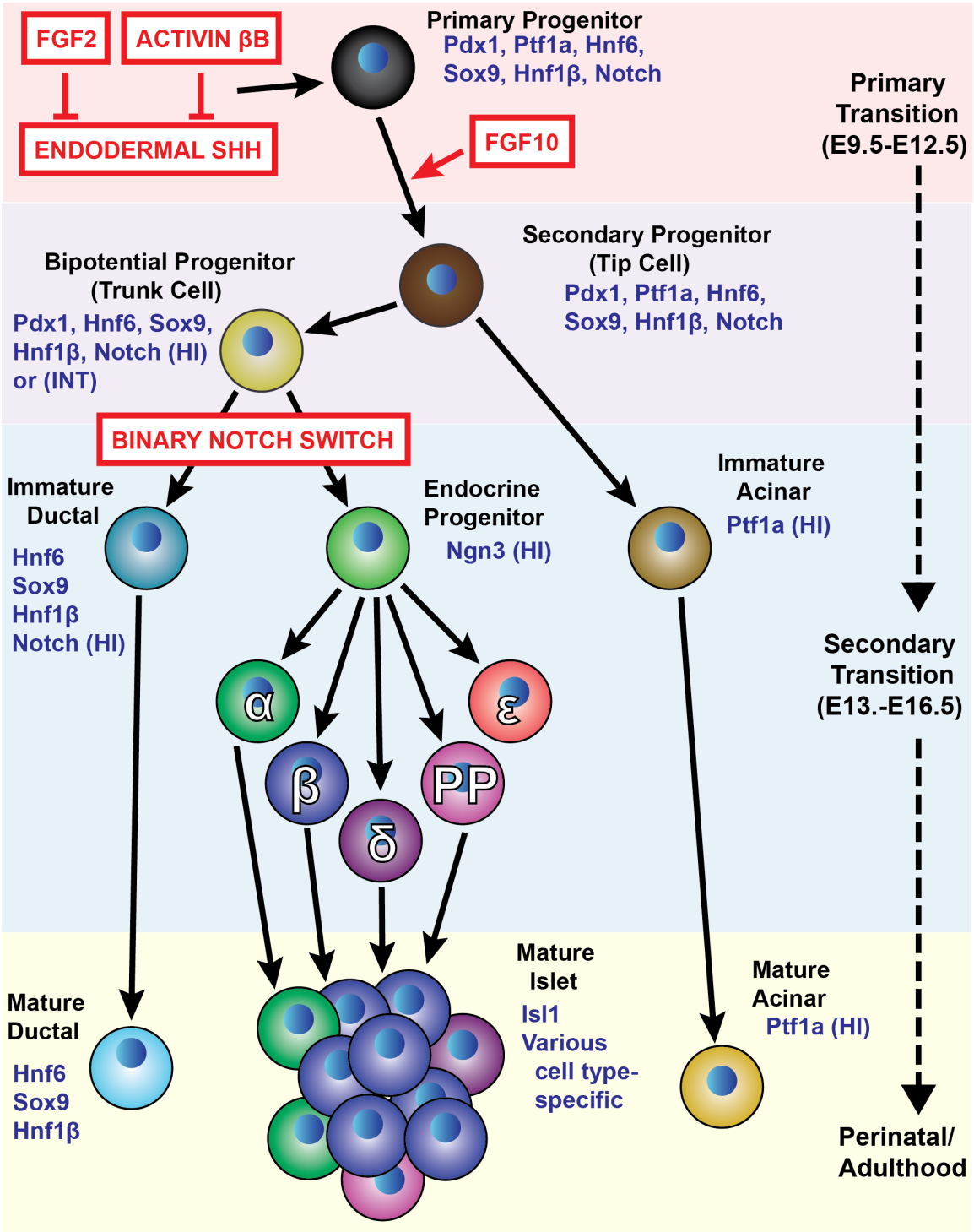

Figure 1. Overview of pancreatic development. At E8.5, prior to the primary transition, the dorsal prepancreatic endoderm receives permissive signals from the notochord that repress *Shh* expression and allow for specification of pancreatic progenitors and stabilization of the pro-pancreatic transcription factor network. The subsequent outgrowth

of pancreatic progenitors is contingent upon FGF10 signals received from the pancreatic mesenchyme. Before the secondary transition commences, tip cells give rise to bipotential progenitors of the epithelial cords (trunk cells). At E13.5, tip cells become restricted progenitors for acinar cells. The bipotential progenitor cells utilize lateral inhibition via Notch signaling to allocate endocrine progenitors. Isolated trunk cells with intermediate levels of Notch activity activate *Ngn3* expression and stabilize a pro-endocrine transcription factor network, while concomitantly repressing this program in neighboring cells (which exhibit HI Notch activity and become ductal progenitors). $Ngn3^+$ cells delaminate in the secondary transition and coalesce to form islets in late gestation. Nascent cells of all three lineages will undergo a maturation process in late gestation and the perinatal period. All epithelial lineages proliferate rapidly in the perinatal period. α = $glucagon^+$ alpha-cell; β = $insulin^+$ beta-cell; δ = $somatostatin^+$ delta-cell; PP = $pancreatic\ polypeptide^+$ PP cell; ε = $ghrelin^+$ epsilon-cell.

tube (referred to as the primary central lumen). Importantly, expansion of pancreatic mesenchyme is intimately associated with this process. Around E10.5-E11, acute-angle branching morphogenesis of the bud initiates, particularly toward the apical region of the bud growing into the mesenchyme.

The development of the ventral pancreatic bud follows a similar pattern to that outlined for the dorsal bud, but it arises approximately 12 hours after in the mouse (E9.5-E10.0) (Spooner et al., 1970). The ventral bud develops at the anterior intestinal portal (AIP) in close proximity to the emerging hepatic diverticulum, which gives rise to the liver, gallbladder, and intra- and extrahepatic biliary ducts. At the 6-somite stage, the endoderm receives pro-pancreatic instructive signals from the lateral plate mesoderm, likely activin, bone morphogenetic protein (BMP), and/or retinoic acid (RA) (Kumar et al., 2003). Foregut endoderm explant studies have demonstrated that subsequent organ specification at the AIP is contingent upon the physical locale of the endodermal cells in relation to the surrounding mesenchymal cells. At this specific timepoint at the AIP, pancreatic specification is considered to be the default pathway of the endoderm, whereas cells of the definitive endoderm in contact with FGF signals released from cardiac mesoderm and BMP signals from the septum transversum are diverted to the liver fate (Jung et al., 1999, Deutsch et al., 2001, Rossi et al., 2001). Morphogenetic repression of pancreatic fate is especially evident in *Hhex*$^{-/-}$ mice. Bort and colleagues described the requirement of the transcription factor Hhex for proliferation of the definitive endoderm beyond the cardiac mesoderm FGF signals (Bort et al., 2006). Thus, in the absence of Hhex, there is a failure of ventral pancreatic specification; this defect is non-autonomous,

however, because *Hhex*$^{-/-}$ explants grown away from cardiac mesoderm express the pancreatic progenitor marker *Pdx1*.

Near the end of the primary transition (E12-E13 in mouse), rotation of the gut tube brings the ventral and dorsal buds together in the C-loop of the duodenum. This results in their fusion into one primordium, with the dorsal bud contributing to the tail and body of the mature pancreas and the ventral bud giving rise to the head and uncus. The ductal systems within each bud typically fuse into one ductal network. The ventral duct fuses to a central portion of the dorsal duct, thereby creating the main pancreatic duct (duct of Wirsung) that runs the entire length of the pancreas and drains into the duodenum via the major papilla. The proximal portion of the dorsal duct forms the accessory duct (duct of Santorini). A common anatomical variant in humans is communication of the accessory duct with the duodenum via a minor papilla in at least 7% of the population (Smanio, 1969, Stimec et al., 1996).

The Secondary Transition

After bud fusion creates one pancreatic primordium, a period of rapid outgrowth into the pancreatic mesenchyme ensues, termed the "secondary transition," that is marked by a divergence in the differentiation potential of progenitor cells and the onset of differentiation of acinar, ductal, and endocrine lineages (see Figure 1). On a histological level, the epithelium begins to resemble a tree-like network. Cells at the tip of the branches ("tip cells") have been identified as multipotential progenitors at E12.5 and before, but exclusively acinar cell progenitors at E13.5 and thereafter (Zhou et al., 2007). "Trunk cells" are the progenitors for both ductal and endocrine lineages; this divergence

of the multipotent progenitor pool has been supported by lineage tracing analysis using a variety of *CreER* lines driven by regulatory elements of different loci that show regionalized expression (Zhou et al., 2007, Solar et al., 2009, Kopp et al., 2011). Induction of *Neurogenin3* (*Ngn3*) in isolated trunk cells permits differentiation toward an endocrine fate, and these endocrine progenitors delaminate from the epithelium via an epithelial-to-mesenchymal transition (Rukstalis and Habener, 2007). Tip cells begin to differentiate toward the acinar lineage in this time period, acquiring ultrastructural characteristics of zymogen granules and increasing expression of digestive enzymes, such as carboxypeptidase I, elastase, amylase, and trypsinogen (Pictet et al., 1972, Petrucco et al., 1990).

Development of the Ductal Tree

How the pancreatic ductal tree develops in the midst of the significant morphological changes of the primary transition and the wave of endocrine differentiation in the secondary transition is truly a fascinating question. Moreover, it is imperative that all differentiating acinar cells and ductal segments communicate so that digestive enzymes are not trapped in blind-ends. Although developmental biologists have made great inroads into explaining the basis of ductal development, there are many questions left unanswered.

Similar to tube-like structures of all organs (e.g. glandular tissue, lungs, blood vessels, etc.), the ductal epithelium displays apical-basal polarity that is required for its formation and functioning. The apical pole of the cell is the site of bicarbonate secretion and faces the ductal lumen, which will contain the exocrine secretions; the basal surface

makes contact with the basement membrane and extracellular matrix; and finally, intercellular junctional complexes with neighboring ductal cells are established on the lateral surfaces. Proper acinar and ductal cell polarity, as well as intercellular junctions, is required for maintenance of pancreatic homeostasis. Conditional pancreatic ablation of *Lkb1* in mice demonstrates this fact in that mutant mice rapidly suffer from pancreatitis soon after birth as a result of defective polarity and tight junctions (Hezel et al., 2008).

Apical-basal polarity in the pancreas is first established at E10.5-E11.5 during the primary transition; notably, determination of cellular polarity occurs prior to the process of tubulogenesis (Kesavan et al., 2009, Villasenor et al., 2010). Unlike other organs that employ a typical branching pattern to form a tree-like network of tubes (for example, the lung), the pancreas follows a model of "spreading" apical-basal polarity to establish interspersed microlumina (Metzger et al., 2008). Using high-resolution three-dimensional microscopy, the laboratory of Ondine Cleaver established that one of the first signs of polarization in the dorsal bud was apical localization of Zonula occludens-1 (ZO-1, a typical apical marker in mature tissues) in isolated cells throughout the predominantly unpolarized, stratified epithelium (Villasenor et al., 2010). This finding corroborates earlier work reported by Kesavan and colleagues, who observed the apical targeting of Mucin-1 in isolated cells by E11.5 (Kesavan et al., 2009). In both studies, analysis at timepoints immediately thereafter indicated that although this process initiated stochastically in single cells, the cells neighboring the apical pole of the polarizing cell in turn polarized, with the cells' apical poles abutting. Subsequently, a microlumen would form. By E12.5, the microlumina interspersed throughout the bud connect to form a complex plexus, which undergoes remodeling during the secondary transition. The timing

of plexus formation is coincident with gut rotation and bud fusion at the end of the primary transition – this likely explains how the ductal network of each bud can fuse to form a single network in the adult. The first evidence of a *bona fide* tube, defined by a single-cell layer in contact with basement membrane with a central clearing, is finally evident at E13.5.

To define a molecular mechanism for establishment of apical-basal polarity, Kesavan and colleagues investigated the involvement of the Rho-GTPase Cdc42, which is known to play a role in lumen formation of 3D organotypic MDCK and Caco-2 cell lines *in vitro* (Martin-Belmonte et al., 2007, Jaffe et al., 2008). In pancreata of mice with conditional ablation of *Cdc42*, pancreatic progenitor cells lost the ability to establish proper microlumina (Kesavan et al., 2009). Instead, apical proteins (Mucin-1, tight junction proteins, etc.) localized to intracellular and intercellular lumina without inducing polarization in neighboring cells. This led to a failure of plexus formation, thereby precluding tubulogenesis and disrupting subsequent endocrine and ductal differentiation. Additionally, the authors defined several downstream aspects of this process, such as signaling through kinases Par3, Par6, ROCK, and phosphorylated atypical Protein Kinase C (aPKC). Intriguingly, pharmacologic inhibition of aPKC alone was sufficient to inhibit tubulogenesis and plexus remodeling, yet microlumina and apical polarity developed seemingly unperturbed. The process of plexus remodeling, however, is likely complex and highly regulated, so aPKC is only one required component. Villasenor and colleagues determined Ephrin B (EphB) signaling is also required for proper plexus remodeling, as $EphB2^{lacZ/lacZ}/EphB3^{-/-}$ compound mutant mice failed to organize the ductal arbor into a hierarchical network (Villasenor et al., 2010).

Although these data highlight the early role of Cdc42 and EphrinB signaling in pancreatic duct development, it is still unclear how this process initiates stochastically within the pancreatic buds. Additionally, *Cdc42* ablation disrupted only apical polarity, as basolateral markers were unaffected in mutants. Future work is needed to determine mechanisms of establishing polarity of these domains and how the epithelial cells are able to undergo drastic reorganization from a stratified layer into a simple layer. Finally, the mechanisms by which nascent ductular tubes are able to establish contacts with all differentiating acinar cells and the primary central lumen opening into the duodenum remain to be elucidated.

Developmental Signaling Cascades

The development of an organ from a germ layer is a highly dynamic, complex process that relies on timely activation or repression of various signaling pathways in a context-specific manner. In some cases, these signals alter gene expression and thus transcription factor networks; in other cases, they affect the physical processes of the cell, such as cytoskeleton remodeling in cellular migration. These critical spatiotemporal cues are generally provided by surrounding tissues (either secreted morphogens or membrane-bound ligands) so that organ development proceeds in a coordinated, controlled fashion. A great deal of work has outlined many of the morphogenetic interactions between the developing pancreatic epithelium and surrounding structures, particularly the notochord, dorsal aorta, lateral plate mesoderm, cardiac mesoderm, and septum transversum during specification, and the pancreatic mesenchyme for organ outgrowth.

Importantly, pancreatic development proceeds upon a backdrop of endodermal regionalization, thus providing the requisite context for patterning signals. Similar to other germ layers, anterior-posterior patterning of the endoderm is established by the expression of *Hox* genes [reviewed in (Deschamps et al., 1999)]. In addition, other transcription factors, such *Sox2* in the anterior endoderm, *Pdx1* in the pancreaticoduodenal region, and *Cdx2* in the hindgut, are expressed regionally and establish broad fields of possible organ fate that will ultimately be determined by the morphogenetic inputs from surrounding tissue (Jonsson et al., 1995, Que et al., 2007, Gao et al., 2009). Here, I provide a brief overview of the contributions of several signaling pathways to pancreatic development (see Figure 1).

Hedgehog (Hh)

Sonic hedgehog (Shh) is expressed throughout the developing endoderm, as it is required for the differentiation of the mesodermally-derived smooth muscle layer surrounding the gut tube. Prior to dorsal pancreatic bud formation, contact of the presumptive prepancreatic endoderm with the notochord is required for induction of pancreatic genes, such as *Pdx1* (Kim et al., 1997). Follow-up studies in the Melton Lab identified that the signals released from the notochord, specifically activin-βB and FGF2, are sufficient to repress *Shh* expression in the prepancreatic endoderm (Hebrok et al., 1998). Thus, this established that repression of Shh signaling is a required event early in pancreatic development. Due to the fact that caudal endoderm co-cultured with notochord did not activate expression of pancreatic genes, it was concluded that the notochord establishes only permissive signaling for pancreatic development (Kim et al., 1997). The

field of *Shh* repression in the dorsal gut tube endoderm ultimately defines the domain that is competent to become pancreas; this is highlighted by the fact that exposure of chick embryos to cyclopamine, an inhibitor of Hh signaling, was sufficient to expand the pancreatic field within the *Pdx1*-expressing endoderm (Kim and Melton, 1998). Conversely, ectopic expression of *Shh* under the *Pdx1* promoter drives the differentiation of pancreatic mesoderm toward a smooth muscle fate and leads to a mixed pancreatic-intestinal differentiation of the epithelium (Apelqvist et al., 1997).

Hh signaling beyond initial specification of the prepancreatic endoderm is more complex. Hebrok and colleagues characterized the pancreatic phenotype of mice lacking components of the signaling pathway, specifically *Shh*, *Indian Hedgehog* (*Ihh*), or the receptor *Patched1* (*Ptc1*) (Hebrok et al., 2000). Notable findings include: $Shh^{-/-}$ mice exhibited significantly reduced body weight yet increased relative pancreatic size and increased relative number of endocrine cells; 42% of $Ihh^{-/-}$ mice displayed an annular pancreas, a defect associated with defective morphogenesis of the ventral pancreatic bud; $Ptc1^{-/-}$ mice failed to induce *Pdx1* expression at E9.0-E9.5; and $Ptc1^{+/-}$ male mice exhibited glucose intolerance in adulthood. Although these results confirm that Shh indeed has a repressive effect on pancreatic development, data from the $Ptc1^{+/-}$ mice implicate Hh signaling, in some capacity, in endocrine cell function and/or differentiation.

Fibroblast growth factor (FGF)

FGF signaling, mediated by greater than 20 soluble FGF proteins and four FGF tyrosine kinase receptors in humans (of which there are also multiple isoforms due to

alternative splicing), serves a critical function throughout embryonic development. Its earliest function in pancreatic development is evident at gastrulation, at which time FGF4 signals released from the mesectoderm render the dorsal foregut competent to respond to pro-pancreatic signals from the notochord (Wells and Melton, 2000). The notochord, as noted previously, releases FGF2, which represses *Shh* expression in the prepancreatic endoderm, establishing a requirement for FGF signaling in dorsal bud morphogenesis. For the ventral bud, FGF signaling plays an opposite role; FGF1 and FGF2 released by the cardiac mesoderm diverts the definitive endoderm at the anterior intestinal portal toward a hepatic fate (Jung et al., 1999).

During the primary and secondary transitions, FGF signaling mediated by the pancreatic mesenchyme is crucial to organ outgrowth. For instance, in *Fgf10*$^{-/-}$ embryos, pancreatic budding proceeds in a similar fashion to controls, yet subsequent growth, differentiation, and branching morphogenesis are prematurely arrested due to decreased proliferation of pancreatic progenitors (Bhushan et al., 2001). Fgf10 signaling was subsequently shown to maintain Notch activation in pancreatic progenitors and thus the size of the progenitor pool (discussed below) (Hart et al., 2003, Norgaard et al., 2003). Unsurprisingly, loss of *Fgf10* results in pancreatic hypoplasia, as pancreatic size is determined by an intrinsic program contingent upon the number of pancreatic progenitors (Stanger et al., 2007).

Notch

Notch signaling is mediated through cell-cell interactions at the plasma membrane and is important for lateral inhibition. In 1999, Helena Edlund's laboratory reported that

mice deficient for Notch signaling, either by deletion of the ligand *Delta-like gene 1* or the intracellular mediator *RBP-Jκ*, exhibit precocious endocrine cell differentiation at the expense of organ outgrowth and branching morphogenesis (Apelqvist et al., 1999). These data are further supported by mice deficient for the Notch target *Hes1*, a transcriptional repressor; these mice exhibit pancreatic hypoplasia due to increased terminal differentiation of endocrine cells (Jensen et al., 2000). Thus, the importance of Notch signaling in pancreatic development appears to be at least two-fold – it is required for maintenance and expansion of the pancreatic progenitor pool, and it is required for proper allocation of endocrine progenitor number.

As previously discussed, FGF10 is required for expansion of the pancreatic progenitor pool (Bhushan et al., 2001). Notch, however, is a necessary downstream mediator of this signaling cascade since γ-secretase inhibitors suppress the effect of FGF10, thereby establishing an epistatic relationship (Miralles et al., 2006). The molecular basis of this relationship is likely predicated upon the fact that the cell cycle inhibitor p57 is a direct target of transcriptional repression by the Notch effector Hes1 in pancreatic progenitors (Georgia et al., 2006).

The studies presented above demonstrate that downregulation of Notch signaling is sufficient for *Ngn3* induction and endocrine differentiation. Conversely, forced misexpression of the Notch intracellular domain (NICD), the transcriptional effector of active Notch signaling, in pancreatic progenitors blocks acinar and endocrine cell differentiation (Murtaugh et al., 2003). Moreover, forced misexpression of NICD in $Pax4^{+}$ endocrine progenitors shunts their fate toward the ductal lineage (Greenwood et al., 2007). Thus, it appears Notch signaling allows for a binary switch of endocrine vs.

ductal cell fate in trunk cells. In agreement with this, Shih and colleagues discovered that *Hes1* and *Sox9* are both transcriptional targets of Notch signaling, but at different thresholds (Shih et al., 2012). They present a model in which high levels of Notch signaling in bipotential ductal progenitors results in *Hes1* and *Sox9* expression, yet intermediate levels only activate *Sox9*. In the latter case, *Sox9* induces *Ngn3*, which in turn represses *Sox9*, thus allowing for exit from the bipotential state.

Transcription Factors in Development

As outlined above, communication between adjacent structures in the developing embryo is of paramount importance, as this provides critical spatiotemporal feedback. In order for a particular organ to develop, specific transcription factor networks must be stabilized for cell fate decisions to occur. Regionalization merely poises the endoderm for a specific organ fate; however, the pathways described above contribute to the expression and/or repression of various transcription factors that will be the determinants of cell fate. It is important to note that this is a dynamic process, as the required transcription factor networks change throughout development and upon cellular differentiation. Below, I highlight several of the key transcription factors required for outgrowth of the pancreas and discuss their role in the pancreatic ductal lineage.

Pdx1

As previously discussed, induction of *Pdx1* at E8.5 requires repression of endodermal *Shh* expression (Apelqvist et al., 1997, Hebrok et al., 1998, Kim and Melton, 1998). *Pdx1*$^{-/-}$ mice display a rudimentary dorsal bud, indicating that the process of bud

formation is Pdx1-independent; however, subsequent organogenesis is halted in both mice and humans (Jonsson et al., 1994, Stoffers et al., 1997b). This phenotype underscores the fact that Pdx1 is a critical node in the pancreatic progenitor transcription factor network, and pancreatic size is coupled to the number of $Pdx1^{+}$ progenitors (Stanger et al., 2007). The early expression pattern of *Pdx1* has been exploited to drive expression of *Cre* recombinase in pancreatic progenitors under control of Pdx1 regulatory elements (Gu et al., 2002).

Postnatal Pdx1 expression is restricted predominantly to insulin-producing β-cells of the islets. Heterozygous mutations of PDX1 are associated with mature onset diabetes of the young, type 4 (MODY4) (Stoffers et al., 1997a). Using mice homozygous for a hypomorphic *Pdx1* allele, Oliver-Krasinski and colleagues identified Pdx1 as an important regulator of the pro-endocrine transcription factor network that regulates *Ngn3* expression (Oliver-Krasinski et al., 2009). Because the authors did not observe any differences in organ size, which could have been attributed to a decreased pool of pancreatic progenitors given the hypomorphic allele, they were able to establish a cell-autonomous role for Pdx1 in the *Ngn3* regulome in endocrine progenitors.

Ptf1a

Ptf1a is expressed slightly after *Pdx1* induction in pancreatic progenitors; unlike *Pdx1*, however, which is also expressed in the rostral duodenum and antral stomach, *Ptf1a* is confined to the pancreatic anlagen (Krapp et al., 1998, Burlison et al., 2008). Supporting its role as a crucial factor in the pancreatic progenitor transcription factor network, $Ptf1a^{-/-}$ mice exhibit only a rudimentary dorsal bud and fail to undergo

pancreatic organogenesis (Krapp et al., 1998). In contrast to the phenotype observed in *Pdx1*$^{-/-}$ mice, *Ptf1a*$^{-/-}$ mice develop an endocrine population that populates the embryonic mesentery and ultimately spleen at later stages of development (Krapp et al., 1998).

The cooperation of Ptf1a and Pdx1 in maintenance of the pro-pancreatic program is demonstrated by ectopic endodermal expression of *Ptf1a* driving the *Pdx1*$^{+}$ field toward a pancreatic fate (Afelik et al., 2006). Moreover, regulatory crosstalk between these two factors leads to self-stabilization of the pro-pancreatic network. Although *Ptf1a* expression does not require *Pdx1* expression and vice versa, Ptf1a can bind and activate Area III of the *Pdx1* promoter (Kawaguchi et al., 2002, Wiebe et al., 2007).

After the primary transition, *Ptf1a* expression is restricted to acinar cells, in which it participates in a heterotrimeric transcription complex that regulates the expression of various functional genes, including amylase, trypsin, and elastase (Cockell et al., 1989, Petrucco et al., 1990).

Hnf1β

Also known as *Tcf2*, *Hnf1β* is expressed broadly in the endoderm in early development, prior to pancreas specification. *Hnf1β*$^{-/-}$ mice exhibit pancreatic agenesis; although *Pdx1* is expressed in a rudimentary dorsal pancreatic bud, no ventral bud forms, and gastric and duodenal *Pdx1* expression is perturbed (Haumaitre et al., 2005). Pancreatic agenesis is likely a result of a lack of *Ptf1a* expression, thus leading to a failure of self-stabilization of the pro-pancreatic transcription factor network. Moreover, *Hnf1β* expression is maintained by Pdx1 and Hnf6 after pancreatic specification (Oliver-Krasinski et al., 2009). It is presumed that MODY5 results from disruptions of endocrine

cell allocation in development, as *Hnf1β* expression becomes restricted to the ductal lineage postnatally and is not expressed appreciably in mature islets. Using lineage tracing analysis in *Hnf1β-CreER* mice, Solar and colleagues determined that *Hnf1β* expression is confined to the bipotential trunk cells during the secondary transition, which is in agreement with previous staining analyses (Maestro et al., 2003, Solar et al., 2009). Lineage-labeling at E18.5 and beyond resulted in labeling of ductal cells exclusively.

Hnf1β is also critical for renal development; patients heterozygous for mutations of the *HNF1β* locus suffer not only from MODY5 but also renal cysts (Bohn et al., 2003). Hnf1β has been placed atop a transcriptional network of genes in the kidney that are involved in primary ciliogenesis and that have previously been implicated in renal cystogenesis (Gresh et al., 2004). This finding has been exploited in models of pancreatic *Hnf6* gene ablation, which exhibit pancreatic cysts devoid of primary cilia (Pierreux et al., 2006, Zhang et al., 2009). *Hnf6*$^{-/-}$ pancreata have reduced Hnf1β expression in bipotential progenitors at the secondary transition, so the authors concluded cystogenesis at this time was mediated by Hnf6-dependent regulation of the *Hnf1β* locus (Pierreux et al., 2006). The direct contribution of Hnf1β to this phenotype, however, necessitates future study with genetic models of *Hnf1β* ablation.

Hnf6

Hnf6 is expressed in the foregut endoderm prior to pancreatic specification (Jacquemin et al., 2003). Interestingly, *Hnf6*$^{-/-}$ mice show a delay in *Pdx1* expression in the prospective dorsal and ventral pancreatic buds (Jacquemin et al., 2003). This results

in pancreatic hypoplasia due to delayed specification of pancreatic progenitors, thus reducing the progenitor pool (Jacquemin et al., 2003, Stanger et al., 2007).

Later developmental roles for Hnf6 have also been established by several groups. Jacquemin and colleagues described the regulation of the *Ngn3* locus by Hnf6 in bipotential progenitors; the near-complete loss of *Ngn3* expression in *Hnf6*$^{-/-}$ mice suggested a role for Hnf6 in endocrine allocation beyond the non-autonomous effects on organ size (Jacquemin et al., 2000). Indeed, the authors supported this notion by showing direct binding of Hnf6 to the *Ngn3* promoter and that *Hnf6*$^{-/-}$ mice are glucose-intolerant, a finding corroborated by conditional *Hnf6* ablation (Jacquemin et al., 2000, Zhang et al., 2009).

Hnf6 is a critical factor for normal ductal development; mice with either germline or conditional ablation of *Hnf6* develop ductal cysts during late gestational timepoints and the perinatal period (Pierreux et al., 2006, Zhang et al., 2009). As described in the previous section, the current understanding of this phenotype centers on decreased expression of *Hnf1β* in the trunk cells during the secondary transition, which in turn abrogates elaboration of primary cilia resulting in cysts. Pancreatic deletion of primary cilia, which serve as a node of various signaling pathways in various epithelial cells [reviewed in (Fry et al., 2014)], have been shown to result in polycystic pancreata (Cano et al., 2004, Cano et al., 2006). Furthermore, 10% of patients suffering from polycystic kidney disease have polycystic pancreata, thus highlighting the relevance of this organelle to pancreatic pathology (Pirro et al., 2003).

Sox9

Similar to Hnf6 and Hnf1β, Sox9 is expressed early in pancreatic development, is required for normal endocrine development, and is restricted to the ductal lineage postnatally (Seymour et al., 2007, Seymour et al., 2008, Dubois et al., 2011). Sox9 maintains the pool of pancreatic progenitors via its interaction with the Notch pathway; in addition to the *Sox9* locus itself being a target of Notch signaling, the population of $Hes1^{+}/Pdx1^{+}$ progenitor cells at E10.5 was reduced by 43% upon conditional ablation of *Sox9*, suggesting that Sox9 may regulate Notch activity (Seymour et al., 2007, Shih et al., 2012). Moreover, Sox9 cell-autonomously regulates expression of *Fgfr2*, which renders progenitor cells responsive to Fgf10 pro-proliferative signals secreted by the mesenchyme (Bhushan et al., 2001, Seymour et al., 2012).

Studies of *Sox9* conditional ablation demonstrate perturbed ductal development in that induced ablation at E12.5 resulted in dilated lumina in mutants at E15.5 and a polycystic pancreas in mutant adults (Shih et al., 2012). To elucidate the molecular mechanism, the authors used microarray analysis to compare a gene set enriched in P23 ducts vs. the Sox9-regulated genes at E15.5 (Shih et al., 2012). The gene *Pkd2*, of which mutations cause autosomal-dominant polycystic kidney disease in humans and result in disruption of primary ciliogenesis, was reduced in *Sox9*-ablated pancreas (Wu et al., 1998, Wu et al., 2000); furthermore, the cystic ductal epithelium was devoid of Pkd2 or primary cilia.

II. MOLECULAR MECHANISM OF PANCREATIC DUCTAL SECRETION

Overview of Ductal Function

The primary function of the ductal network is duodenal transport of both digestive enzymes released from acini and bicarbonate to neutralize acidic chyme. To accomplish this, the ductal cells actively secrete bicarbonate against an immense concentration gradient – the bicarbonate concentration of pancreatic juice in humans can reach as high as 140mM, approximately 7-fold higher than that found in tissues (Whitcomb and Ermentrout, 2004). Moreover, bicarbonate secretion creates an osmotic gradient to draw in water, which aids in flushing pancreatic zymogens to the duodenum; an overwhelming majority of the two liters of pancreatic juice produced per day in humans is a result of ductal secretion.

The process of secretion is highly regulated by enterohormonal and neural inputs to ensure a coordinated postprandial response of the exocrine pancreas. This coordination is highlighted by the high density of gap junctions between acinar cells, as electrical coupling provides for a coordinated response [(Meda et al., 1983) and reviewed in (Petersen and Findlay, 1987)]. Below, I will describe the molecular mechanisms by which bicarbonate is actively secreted by the ductal cell and how this secretion is regulated in concert with acinar cell secretion.

Basic Mechanism of Bicarbonate Secretion

Similar to all epithelial cells, basolateral membrane localization of the Na^+-K^+-ATPase pump in ductal cells establishes an electrochemical gradient due to movement of two K^+ ions into the cell and coupled extrusion of three Na^+ ions (see Figure 2)

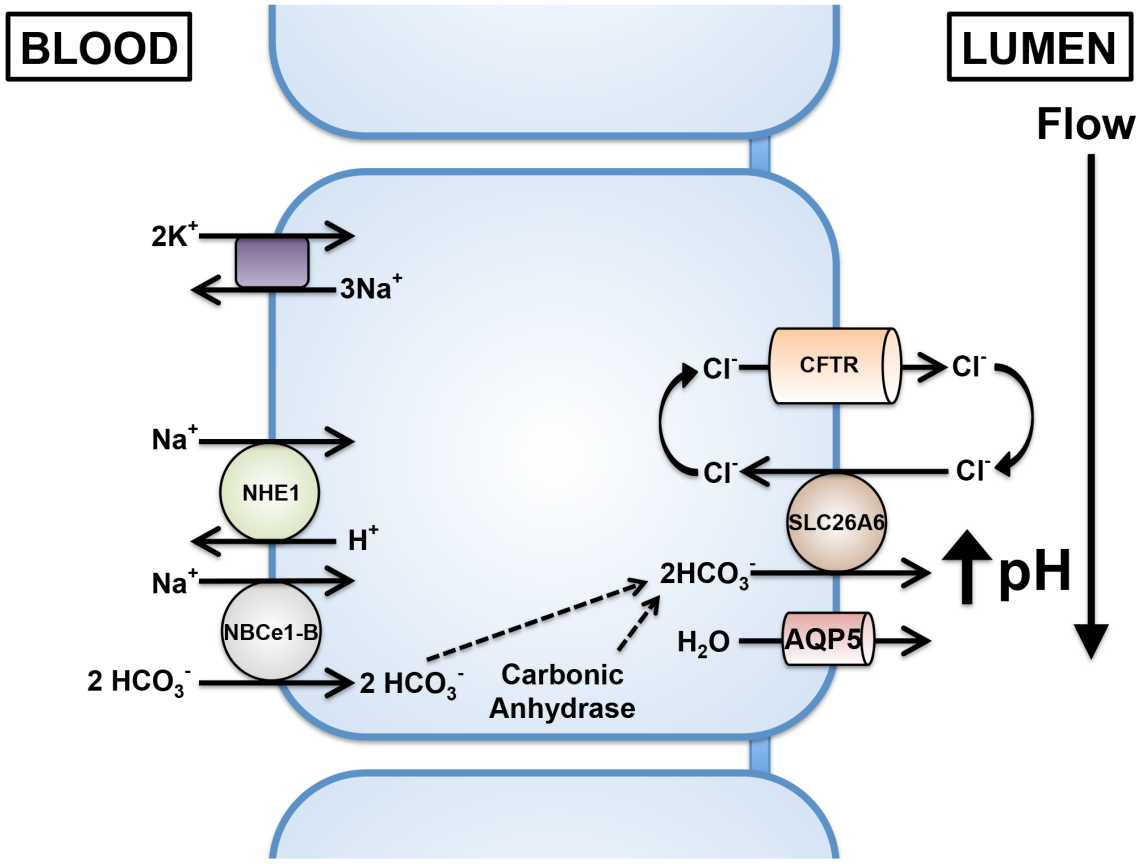

Figure 2. Molecular mechanism of ductal bicarbonate secretion. The electrochemical gradient established by the Na^+-K^+-ATPase pump is coupled to intracellular HCO_3^- transport via NBCe1-B. Upon stimulation of the ductal cell, the open probability of CFTR increases, driving chloride extrusion. Chloride is then recycled in exchange for HCO_3^- transport into the lumen of the duct. This creates an osmotic gradient that mobilizes water transport by mass action through aquaporin channels and paracellular pathways.

(Smith et al., 1987). A high conductance K^+ channel, likely the MaxiK channel, maintains the resting membrane potential close to the equilibrium potential of K^+; the MaxiK channel is an attractive candidate for this role, as it exhibits a high conductance (125-250pS) and is regulated by the cAMP/PKA pathway, which regulates ductal secretion (Gray et al., 1990). The electrochemical gradient established by the Na^+-K^+-ATPase pump is then exploited by a basolateral Na^+-HCO_3^- symporter to drive HCO_3^- transport and alkalinize the intracellular envrionment (Zhao et al., 1994). This transporter, identified as NBCe1-B (originally called pancreatic NBC1 or pNBC1), was cloned from a cDNA library derived from human pancreas using a probe designed from the NBC expressed sequence tag (Abuladze et al., 1998). Conductance of NBCe1-B is enhanced by increased concentration of cAMP and exhibits a $1Na^+$:$2HCO_3^-$ stoichiometry (Gross et al., 2003). Additionally, the electroneutral, basolateral Na^+/H^+ transporter (NHE1) may contribute to increasing intracellular pH, but this contribution is minor given that inhibition of NHE1 with amiloride does not affect secretin-induced intracellular alkalinization (Veel et al., 1992). Thus, NBCe1-B mediates the majority of basolateral influx of HCO_3^- during ductal secretion (Ishiguro et al., 1996a, Ishiguro et al., 1996b).

In order for ductal secretion to occur, the increase in intracellular pH must be converted to bicarbonate extrusion into the lumen of the duct. To this end, the ductal cell utilizes two transporters on the apical surface, namely cystic fibrosis transmembrane conductance regulator (CFTR) and solute carrier 26a6 (SLC26A6), to tether bicarbonate secretion to the cycling of chloride ions (Zeng et al., 1997, Lee et al., 1999a, Lee et al.,

1999b, Stewart et al., 2009). CFTR (ABCC7) is an ATP-binding cassette transporter that functions as a small conductance chloride channel (Tabcharani et al., 1991). Acinar cell secretions also contribute to the luminal pool of chloride in the proximal ducts. The electrogenic antiporter SLC26A6 subsequently transports bicarbonate into the lumen and chloride into the cell in a 2:1 ratio, respectively (Wang et al., 2006, Stewart et al., 2009). This establishes an osmotic gradient, thus providing a driving force for water transport through aquaporin-1 (basolateral and luminal surfaces) and aquaporin-5 (luminal surface) (Ko et al., 2002, Burghardt et al., 2003).

Regulation of Ductal Secretion

To link the pancreatic response with digestion, exocrine secretion is coupled to vagal and hormonal inputs with significant crosstalk between signaling pathways. The first evidence of a coordinated digestive response was provided by Bayliss and Starling over 100 years ago; in their seminal work, they noted that the application of acid to the duodena of dogs evoked an increase in pancreatic secretion (Bayliss and Starling, 1902). Their identification of the hormone secretin pioneered the field of endocrinology. Secretin signals via a G-protein coupled receptor (GPCR), resulting in an increase in cyclic AMP (cAMP) concentration and activation of Protein Kinase A (PKA) (Ulrich et al., 1998). In ductal cells, increased cAMP/PKA signaling augments the activity of several transporters (Figure 3) (Tabcharani et al., 1991, Gross et al., 2003). The open probability of CFTR is low in the absence of PKA-mediated phosphorylation of the regulatory domain, as this is a requisite modification for nucleotide binding

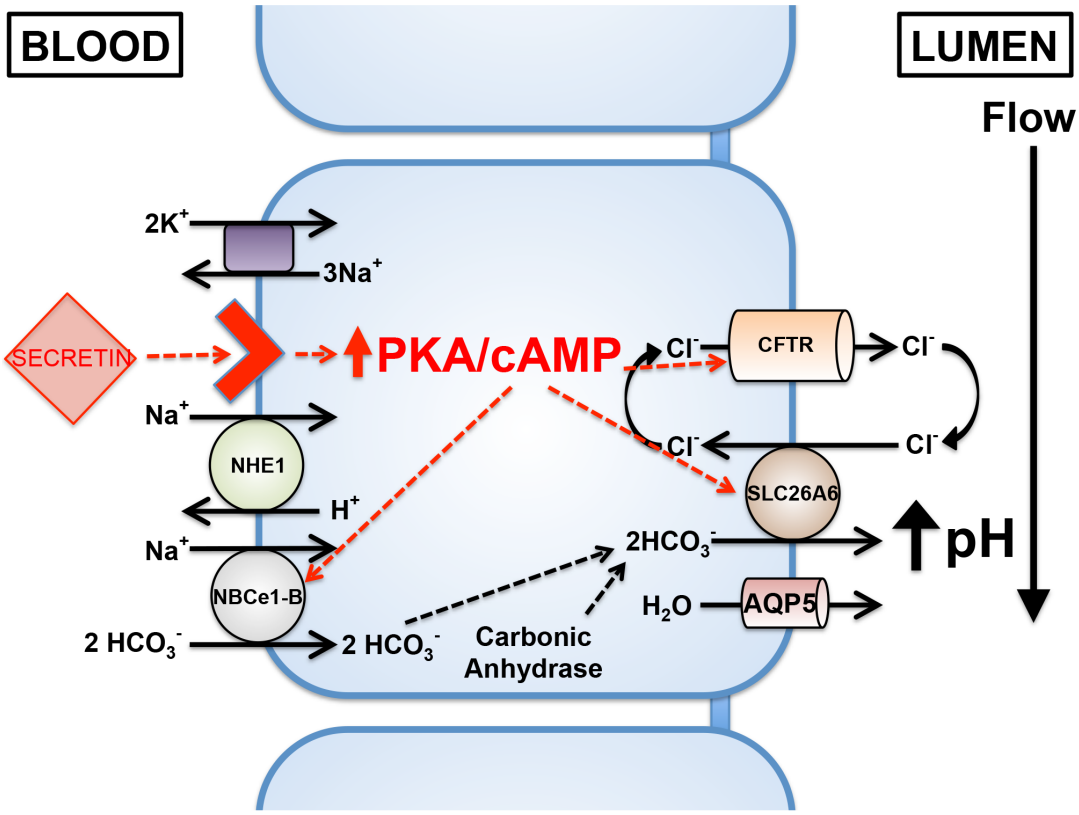

Figure 3. Effects of secretin-mediated signaling in ductal cells. Binding of secretin to its G-protein couple receptor initiates the formation of cAMP and activation of Protein Kinase A second messengers. This increases the flux through the indicated transporters, leading to a drastic increase in bicarbonate movement across the ductal epithelium into the ductal lumen.

(Anderson et al., 1991, Anderson and Welsh, 1992). In fact, mutations of the regulatory domain have been identified as one of many causes of cystic fibrosis (Vankeerberghen et al., 1998).

Additionally, ductal cells are sensitive to Gq-coupled receptors, such as the muscarinic M3 receptors, that are tethered to phospholipase-Cβ (PLCβ)-dependent cleavage of phosphatidylinositol (Folsch et al., 1980, Ashton et al., 1993). In the ductal cell, production of inositol trisphosphate (IP_3) by PLCβ leads to a synergistic increase in ductal secretion when coupled with secretin signaling (Park et al., 2013). The mechanism for this synergism is dependent upon the displacement of the scaffolding protein IP_3 receptor binding protein (IRBIT) from IP_3 receptors by IP_3 (Park et al., 2013). IRBIT can then associate with and sequester the With no lysine kinase (WNK) and Ste20-related proline alanine rich kinase (SPAK). In the resting state, WNK/SPAK kinases phosphorylate NBCe1-B, CFTR, and SLC26A6, reducing their expression at the plasma membrane (Yang et al., 2009, Yang et al., 2011). Therefore, Gq-mediated increases in IP_3 levels ultimately disinhibit these critical transporters, which are also activated by PKA/cAMP signaling (Figure 4). Furthermore, the affinity of IP_3 receptors for IP_3, and thus IRBIT release, is increased by PKA-mediated phosphorylation (Park et al., 2013).

The synergism between PLCβ- and PKA-mediated second messengers is important for acinar-ductal crosstalk. First, the predominant hormone that regulates acinar cell secretion, cholecystokinin (CCK), is released by the presence of fatty acids in the duodenum. In addition to binding CCK_A receptors located on acinar cells, CCK activates CCK_B receptors in the central nervous system, which leads to acetylcholine release from vagal efferents in the pancreas after feeding. Therefore, the actions of both

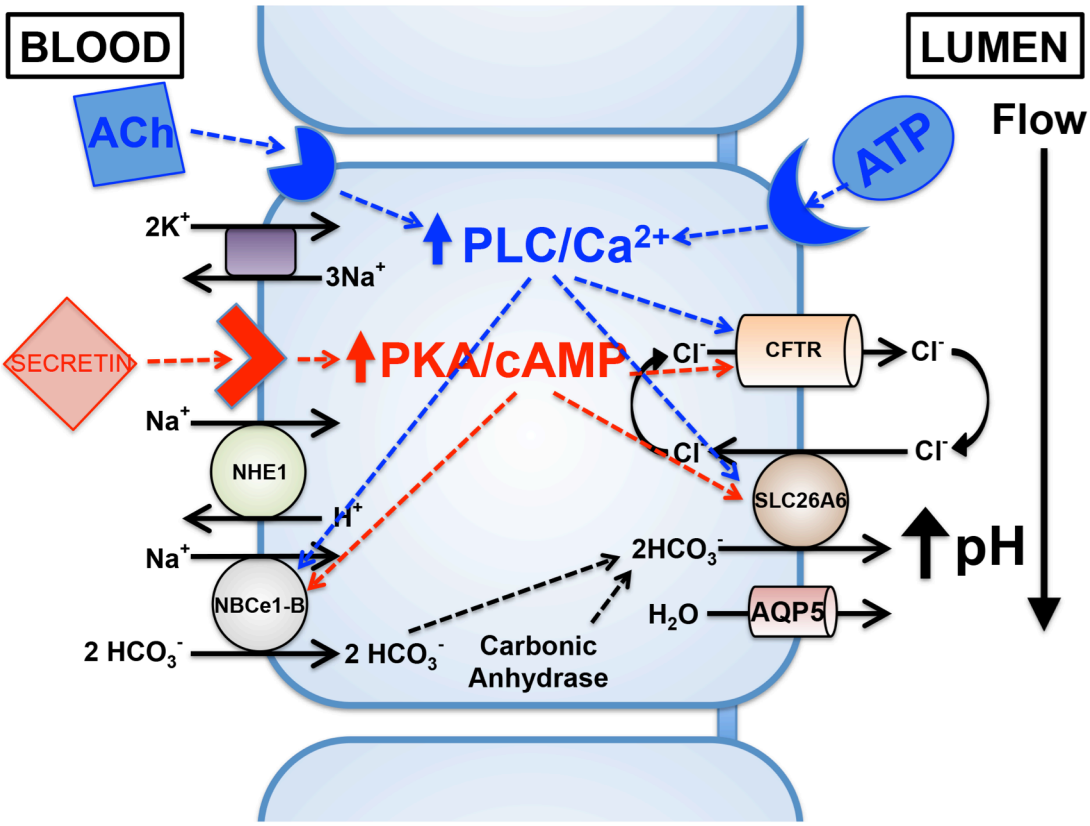

Figure 4. Synergism between Gs- and Gq-coupled signaling pathways in ductal cells. The PLCβ (Gq) and PKA (O'Reilly et al.) signaling pathways interact on a number of levels to enhance ductal secretion. Conceptually, these pathways intersect upon the critical transporters NBCe1-B, CFTR, and SLC26A6. Acetylcholine is given as an example of a basolateral Gq-coupled receptor (signaling via vagal input), and ATP is an example of a paracrine signal released by acinar cells that will activate a Gq-coupled receptor.

secretin and vagal output from CCK will enhance ductal secretion, as acetylcholine signals through M3 (Gq) muscarinic receptors in ductal cells (Ashton et al., 1993). Secondly, both the direct and indirect actions of CCK will stimulate acinar cell secretion. Secretions of acinar cells contain various paracrine factors, such as Ca^{2+} and ATP, which activate Gq receptors on the surface of the ductal cell (Hede et al., 1999, Racz et al., 2002). Together, hormonal and neural inputs ensure that the exocrine pancreas secretes as a coordinated unit.

III. PANCREATIC DUCTAL PATHOLOGY

Cystic diseases

The etiology of true pancreatic cysts includes a wide range of causes, but those most relevant to the subject matter at hand include the primary ciliopathies. As noted, 10% of patients with polycystic kidney disease also exhibit polycystic pancreata (Pirro et al., 2003). Additionally, genetic mouse models of pancreatic perturbation of primary cilia support a causative role of primary cilia dysfunction in cystogenesis (Cano et al., 2004, Cano et al., 2006). This is further supported by analysis of *Hnf6*-null, *Hnf6*-conditional null, and *Sox9*-conditional null pancreata; all three of these models exhibited polycystic pancreata devoid of primary cilia (Pierreux et al., 2006, Zhang et al., 2009, Shih et al., 2012).

Cystic Fibrosis

Cystic fibrosis was named in 1938 in reference to its pancreatic pathology, which includes inspissated secretions obstructing proximal ducts, leading to dramatic

parenchymal destruction caused by interstitial fibrosis, cyst formation, and lipomatosis (Andersen, 1938). After the discovery and cloning of the causative gene, *Cystic fibrosis transmembrane conductance regulator* (*CFTR*), a number of groups attempted to solve the mystery pertaining to its function (Riordan et al., 1989). Ultimately, it was determined to be predominantly a chloride channel that is regulated in the pancreatic ductal epithelium by PKA-mediated phosphorylation, PLCβ second messengers, and nucleotide binding (as it is ATP-binding cassette channel) (Lee et al., 1999a, Lee et al., 1999b, Stewart et al., 2009). Therefore, the primary pancreatic defect in cystic fibrosis is a failure of the ductal cell to secrete adequate bicarbonate; secretion of bicarbonate is intimately tied to chloride recycling (Figure 2). Because bicarbonate secretion also provides the driving force for drawing water into ductal lumina, it becomes clear how inspissated protein plugs form in the ducts. As ductal plugging continues, obstruction will invariably lead to entrapment of zymogens and recurrent bouts of pancreatitis. Given the large size of the CFTR locus (>180 kilobases), a plethora of mutations have been identified, but it is important to note that mutations differ considerably in regards to penetrance and severity of a phenotype (Ferec and Cutting, 2012).

Pancreatitis

Pancreatitis subsumes several related diseases that are on a spectrum regarding chronicity and histopathological changes; these include acute, recurrent acute, and chronic pancreatitis. The differential etiology of acute and chronic pancreatitis is vast (Figures 5 and 6), but irrespective of the cause, a common feature is autoactivation of trypsinogen resulting in parenchymal digestion and inflammation. This autoactivation is

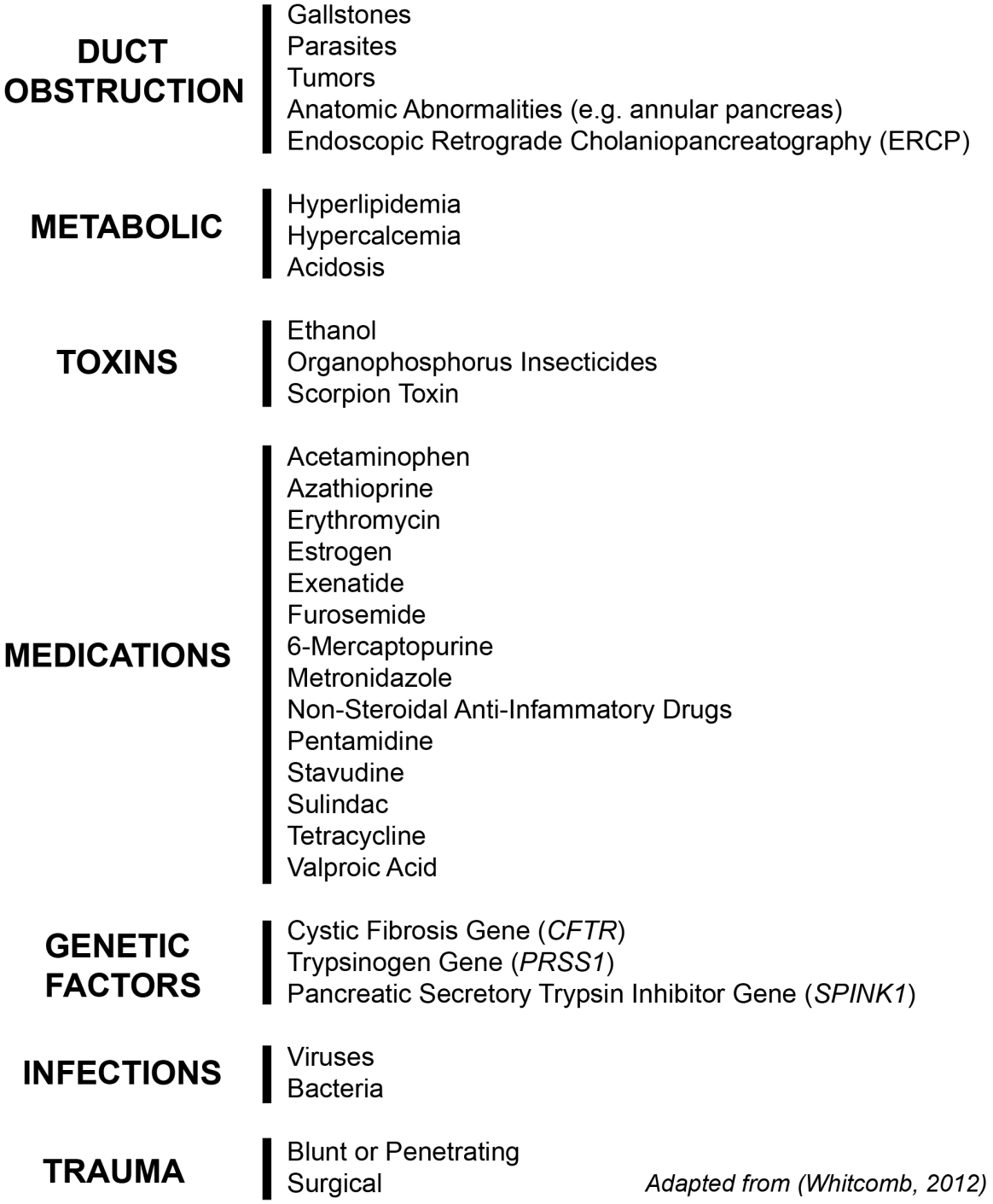

Figure 5. Causes of acute pancreatitis.

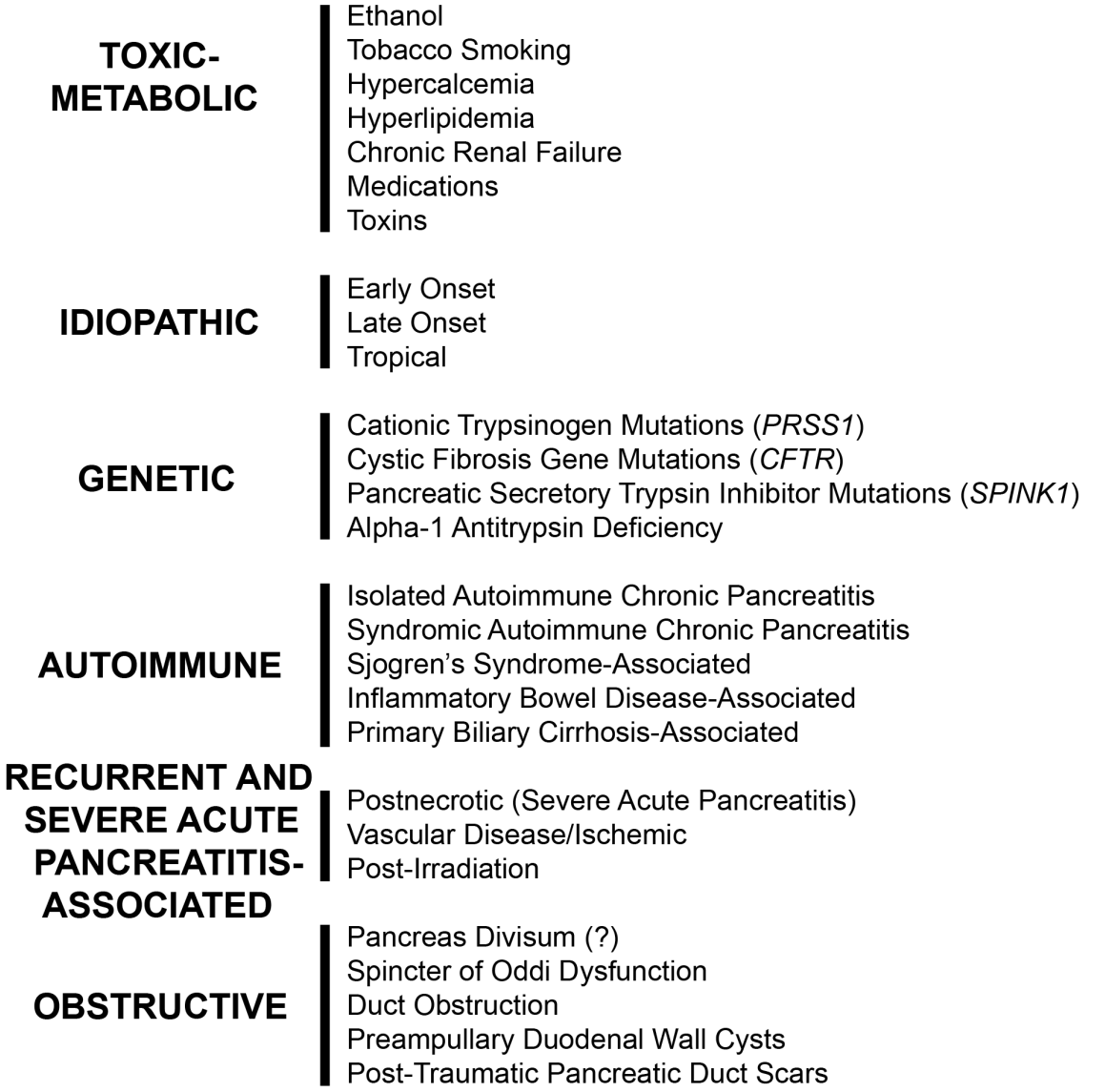

Figure 6. Causes of chronic pancreatitis.

particularly evident in patients who harbor mutations in the trypsinogen gene (PRSS1).

IV. HEMATOPOIETICALLY-EXPRESSED HOMEOBOX PROTEIN

As noted above, proper ductal development and function is critical in maintaining pancreatic homeostasis. The relative dearth of knowledge regarding the role transcription factors play in regulating secretion highlights the need to explore further potential contributions of transcriptional dysregulation to pancreatic ductal pathology. Recently, the Kaestner Lab has identified the transcription factor Hematopoietically-expressed homeobox protein (Hhex) to be expressed in the adult pancreatic ductal epithelium (Zhang et al., 2014). Additionally, *Hhex* expression has been utilized as a "pan-epithelial" marker in the secondary transition of the embryonic pancreas, firmly establishing its expression in this tissue after outgrowth of the anlagen (Zhou et al., 2007). The roles of Hhex in pancreatic development and mature ductal function, however, have not been elucidated.

HHEX Protein

The transcription factor Hhex, originally termed Proline-rich homeodomain protein (Prh), was identified in 1992 by Crompton and colleagues via a PCR screen of Antennapedia-like homeobox sequences of a cDNA library constructed from avian monoblasts (Crompton et al., 1992). Since its discovery, *HHEX* orthologs have been identified in vertebrates and invertebrates alike, including *C. elegans* but not yeast (Hromas et al., 1993, Morck et al., 2004). In humans, the *HHEX* locus is at 10q23.33 (19 32.28cM in mice) and encodes a ~37kD protein comprised of 270 amino acids that is

highly conserved with other species. Relative to murine Hhex, the human orthologue differs by only one amino acid in the DNA-binding homeodomain and is 94% identical across the entire sequence (Bedford et al., 1993).

HHEX protein can be divided into three functional domains: an N-terminal proline-rich domain important for transcriptional repression, a DNA-binding homeodomain, and a C-terminal acidic activation domain (Figure 7). Importantly, Hhex can serve as a repressor or activator of transcription depending on context. The full-length protein was identified to bind the consensus motif 5'-YWATTAAR-3' (Y=C/T, W=A/T, R=A/G), which contains the core ATTA motif characteristic of homeobox transcription factors (Crompton et al., 1992); however, truncation analysis combined with electrophoretic mobility shift assays using randomized oligonucleotides revealed the homeodomain itself is more promiscuous, binding 5'-TAAT-3', 5'CAAG-3', or 5'-ATTAA-3' (Pellizzari et al., 2000). This finding indicates that the abutting domains help enhance specificity of protein:DNA interactions.

Transcriptional activation by Hhex is coordinated by the C-terminal acidic domain, as evidenced by its requirement (in conjunction with the homeodomain) for direct regulation of the sodium-dependent bile acid cotransporter (Denson et al., 2000, Kasamatsu et al., 2004). Moreover, this domain has been reported to interact with TATA-box binding protein, suggesting that it may interact with general activators of transcription (Guiral et al., 2001).

The ability of Hhex to repress transcriptional targets is mediated via the N-terminal, proline-rich domain. One canonical mechanism of transcriptional repression that has been described is a Hhex-dependent recruitment of Groucho/TLE (transducin-

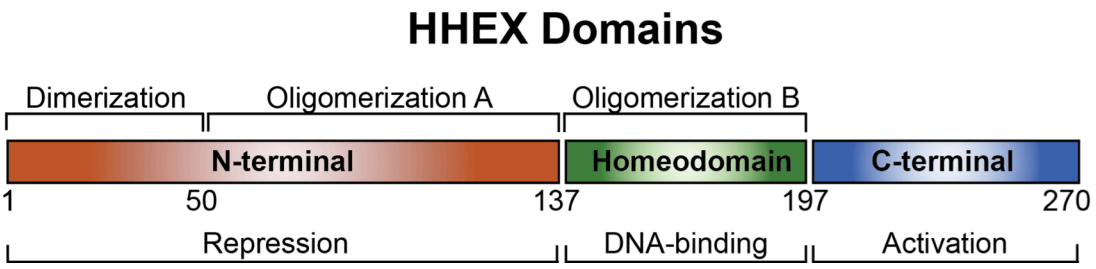

Figure 7. Schematic of HHEX protein domains. The N-terminus mediates the repressive transcriptional functions of HHEX, the homeodomain DNA-binding, and the C-terminus transcriptional activation. The N-terminal 50 amino acids mediate dimeric interactions of HHEX protein, whereas Oligomerization Domain A of one dimer interacts with Oligomerization Domain B of another dimer. A model has been put forth that suggests HHEX can participate in an octameric complex.

like enhancer of split) via an interaction motif at amino acids 30-39 of Hhex for repression of reporter activity in the human K562 lymphoblastic cell line (Swingler et al., 2004). Groucho/TLE establishes a transcriptional complex that recruits chromatin remodeling enzymes, such as histone deacetylases, that aid in repression [reviewed in (Chen and Courey, 2000)]. Another mechanism of Hhex-dependent repression that has been described is via its interaction with eukaryotic initiation factor 4E (eIF-4E), a protein that is required for nucleocytoplasmic transport of specific transcripts. Interaction of eIF-4E with the N-terminus of Hhex (amino acids 18-24) inhibits the capability of eIF-4E to transport *Cyclin D1* transcripts to the cytoplasm for translation, thereby decreasing Cyclin D1 protein levels and cellular proliferation in myeloid cells (Topisirovic et al., 2003).

Intriguingly, the N-terminal domain has also been implicated in Hhex self-association. Using a multitude of biochemical methods, such as gel-filtration, analytical ultracentrifugation, electron microscopy, and protein cross-linking, Soufi and colleagues performed an in-depth biochemical characterization of the Hhex protein (Soufi et al., 2006). Their findings suggest that Hhex exists as an oligomeric complex within cells. Truncation analysis supported the conclusion that amino acids 1-50 of the N-terminus foster dimerization, yet not oligomerization. Oligomerization of Hhex dimers was dependent on coordination of the N-terminal domain (amino acids 50-137; Figure 7 Oligomerization Domain A) of one dimer with the homeodomain of another (Figure 7 Oligomerization Domain B), thereby bridging dimers; together, the authors put forth a model in which Hhex self-assembles into an octamer. The significance of this finding for Hhex functioning is not yet established. It is important to note that self-assembly in this

context may be an artifact of overexpression in cell lines, misfolding of recombinant proteins, and/or lack of a native post-translational modification that may frequently be present on Hhex protein *in vivo*. If true, however, one may expect tandem Hhex consensus motifs to be present in Hhex-binding sites identified by high-throughput sequencing of chromatin immunoprecipitation. It is also possible that Hhex octamers may have the capacity to mediate long-range chromatin interactions. Clearly, the possibility of functional consequences will need to be studied further before any conclusions can be formulated.

Expression Dynamics in Development and Adulthood

In vertebrates, Hhex exhibits a dynamic expression pattern throughout development. *Hhex* transcript is first seen in the mouse as early as E4.5 in the primitive endoderm, preceding primitive streak formation (Thomas et al., 1998). At E7.0 (midstreak stage), *Hhex* transcripts are detectable in all three germ layers, including the ectoderm and presumptive definitive endoderm at the site of the prospective node, anterior visceral endoderm, and extraembryonic blood islands of the yolk sac (Thomas et al., 1998). This expression pattern directly correlates with phenotypes observed by other groups in *Hhex*$^{-/-}$ mice, which display abnormalities in liver, thyroid, forebrain, heart, hematopoietic progenitor, and endothelium development (Martinez Barbera et al., 2000, Guo et al., 2003, Hallaq et al., 2004).

Following gastrulation, endodermal *Hhex* expression is localized to the anterior endoderm and the ventral-lateral foregut, the site of ventral pancreatic and liver organogenesis (Thomas et al., 1998). *Hhex* mRNA is expressed at E10.0 in precursors of

the thymus, liver, thyroid, dorsal pancreatic bud, and gallbladder (Bogue et al., 2000). By E13.5, endodermal *Hhex* expression is limited to the thyroid, liver, epithelial cells of the pancreatic and extra-hepatic biliary ducts, and most cell types of the lung, and it is notably high in the epithelia of the extra-hepatic bile ducts and pancreas at E18.5 (Bogue et al., 2000). In the adult mouse, Hhex gene activity has been previously described in the lung, thyroid, and liver (Bogue et al., 2000); moreover, Hhex has been shown to regulate directly functional genes in various mature cell types, such as somatostatin in δ-cells, the sodium-dependent bile acid cotransporter in immortalized cell lines, the sodium-iodide symporter in lactating mammary tissue, and endothelial cell-specific molecule 1 in endothelial cells (Denson et al., 2000, Kasamatsu et al., 2004, Cong et al., 2006, Puppin et al., 2006, Zhang et al., 2014).

The expression pattern of Hhex in the ventral-lateral foregut prior to pancreas specification suggests that it may serve an essential function in pancreatic development. Indeed, *Hhex*$^{-/-}$ mice fail to specify the ventral pancreatic bud, as well as exhibit variable forebrain truncation, thyroid hypoplasia, and cannot expand the hepatic primordium (Martinez Barbera et al., 2000, Bort et al., 2004, Bort et al., 2006). Importantly, the failure of ventral pancreatic morphogenesis was determined to be a result of a lack of proliferation of the definitive endoderm, thus compromising cell positioning and subjecting these cells to morphogenetic inhibition by the cardiac mesoderm (Bort et al., 2004). This cell-extrinsic mechanism was confirmed by the proper induction of the pancreatic progenitor gene *Pdx1* and the pro-endocrine genes *Isl1*, *Ngn3*, and *NeuroD* when *Hhex*$^{-/-}$ endodermal explants were grown away from the cardiac mesoderm (Bort et

al., 2004). Embryonic lethality of *Hhex*$^{-/-}$ mice, however, precluded any further analysis of the role of Hhex in pancreatic development or function.

V. SUMMARY AND SPECIFIC AIMS

Our understanding of the molecular mechanism governing pancreatic ductal secretion has progressed dramatically in the past couple decades. This has lent novel insight into the etiology of pathogenic mechanisms of disease, particularly cystic fibrosis and pancreatitis, and in some cases has improved therapeutic interventions. Although our understanding of secretion and its hormonal regulation has improved, there is a lack of data elucidating the role transcriptional regulation plays in this process, and more importantly, whether aberrant transcriptional regulation of secretion may contribute to human ductal pathology.

The following chapters aim to clarify the role of the homeobox transcription factor Hhex in pancreatic development and mature ductal function. The results shown in these chapters attempt to: **(1) identify whether Hhex is required for proper ductal development, and if so, what its molecular mechanism of action is, and (2) to determine whether Hhex is necessary to maintain functioning of the mature pancreatic duct.** Together, these findings will elucidate the role of Hhex in the context of the pancreatic duct and may uncover novel insights into the pathogenesis of human pancreatic ductal pathology.

CHAPTER 2
MATERIALS & METHODS

Mice

The derivation of the *Hhex*^{loxP} allele has been described previously (see Figure 8 for overview) (Hunter et al., 2007). *Pdx1-Cre*^{Early} mice were kindly provided by Dr. Guoqiang Gu and Dr. Doug Melton, and *Sox9-CreER*^{T2} mice were kindly provided by Dr. Maike Sander (Gu et al., 2002, Kopp et al., 2011). Mice were maintained on a 129SvEv/C57BL/6 mixed background. Genotyping was performed by PCR analysis using genomic DNA isolated from toe snips of newborn mice. Genotyping primers are provided in Table 1, and thermocycler conditions were as follows: *Hhex*^{loxP} and *CreER*^{T2}: 94°C 4 minutes, [94°C 35 seconds, 60°C 35 seconds, 72°C 50 seconds] 33 times, 72°C 7 minutes, 4°C indefinitely; *Cre*: 94°C 5 minutes, [94°C 30 seconds, 56°C 45 seconds, 72°C 60 seconds] 30 times, 72°C 10 minutes, 4°C indefinitely. Experimental mice were derived from crossing *Hhex*$^{loxP/loxP}$ animals with either *Hhex*$^{loxP/loxP}$*;Pdx1-Cre*^{Early} or *Hhex*$^{loxP/loxP}$*;Sox9-CreER*^{T2} mice; *Hhex*$^{loxP/loxP}$ littermates were used as controls for all experiments. For timed matings, the morning at which a vaginal plug was present was considered day E0.5.

For experiments with tamoxifen induction, adult mice (>9 weeks of age) were administered 5mg tamoxifen (Sigma, T5648, Lot SLBF8049V) per 40g body mass for 3 consecutive days by oral gavage. Tamoxifen was suspended in a 10% ethanol;90% sunflower seed oil (Sigma, S5007) (v/v) mixture at 20mg/ml and rotated at 42°C for 2

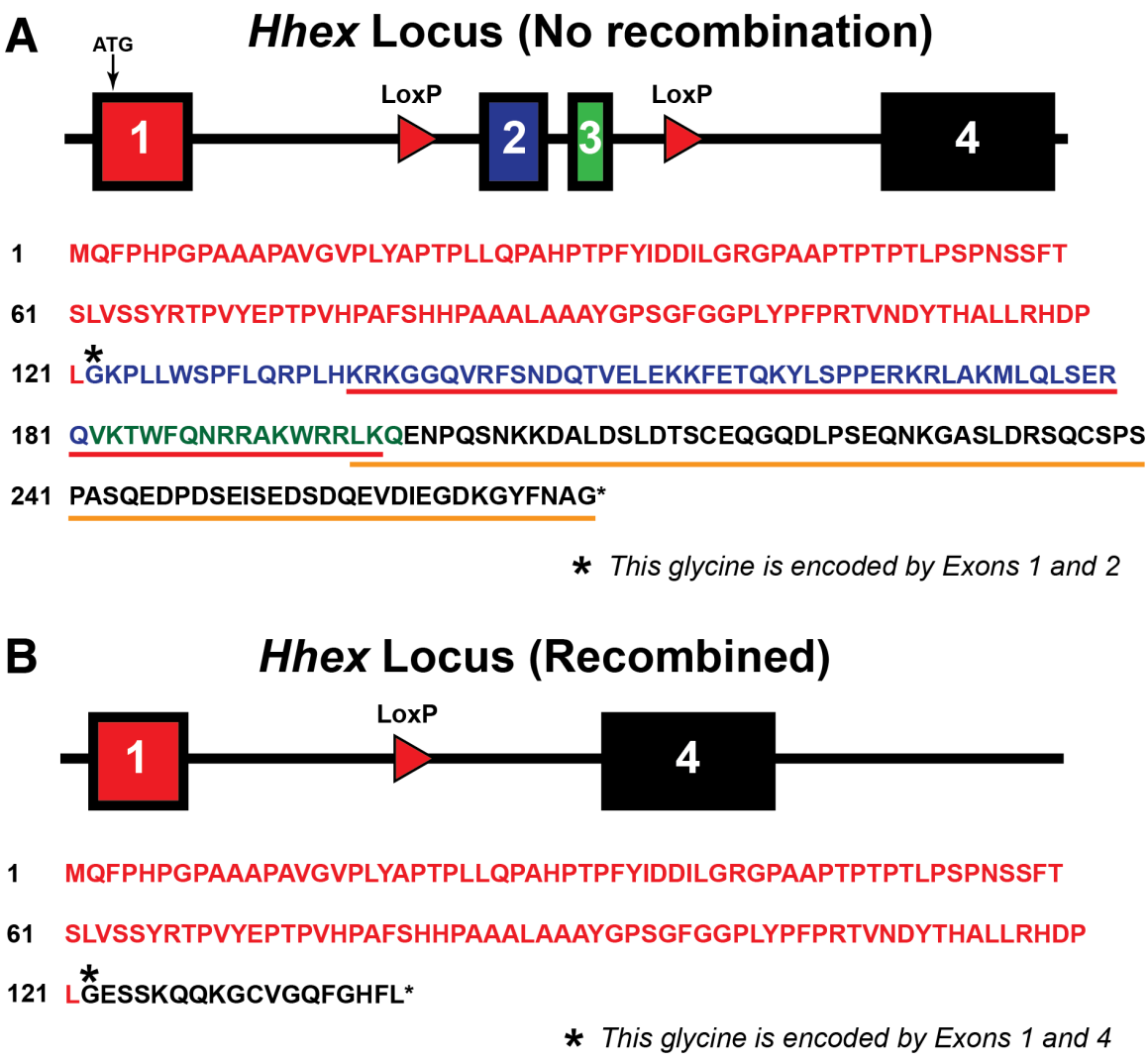

Figure 8. Schematic of *Hhex* ablation. (A) *LoxP* sites were inserted into the *Hhex* locus flanking genomic regions encoding exons 2 and 3, which code for the DNA-binding homeodomain of Hhex (*red underline in sequence*) (Hunter et al., 2007). The 76-amino acid C-terminus used for production of an α-Hhex polyclonal antibody is indicated (*orange underline*) (Ghosh et al., 2000). (B) In the presence of Cre recombinase, the *LoxP* sites recombine, thereby excising exons 2 and 3. This results in a frameshift mutation downstream of exon 1 and therefore a truncated protein.

Primer	Sequence (5'→3')	Product Size (bp)
Hhex-F	ATTGACGGAAATGTTGCCATA	WT: 473 loxP: 605
Hhex-R	CCAAGTGACACGATCCAGAAC	
CreERT2-F	TTTCAATACCGGAGATCATGC	550
CreERT2-R	ATTCCTGTCCAGGAGCAAGTT	
Cre-F	GCGGCATGGTGCAAGTTGAAT	232
Cre-R	CGTTCACCGGCATCAACGTTT	

Table 1. Primers used for genotyping analysis.

hours until completely dissolved. All procedures involving mice were approved by the University of Pennsylvania Institutional Animal Care and Use Committee.

Histological Analysis

For studies with adult mice, pancreata were dissected and fixed in 4% paraformaldehyde (PFA)/phosphate-buffered saline (PBS) (w/v) for 16 hours at 4°C, followed by three 10 minute washes with 1x PBS. Pancreata were laid flat in tissue cassettes for paraffin embedding. Fixation times for embryonic/perinatal mice were adjusted as follows: E13.5-E18.5, 1 hour; P3, 2 hours; P10, 4 hours; P21, 10 hours. Paraffin sections with the maximal footprint were used for all experiments.

For all histological studies, slides were dewaxed/rehydrated in a xylene-ethanol series, followed by antigen retrieval in citric acid buffer pH 6.0 in a 2100 Classic Clinical Autoclave (Prestige Medical) if needed (Table 2). After 2 hours of cooling, slides were rinsed for 10 minutes in running tap water. For immunohistochemistry, endogenous peroxidase activity was blocked by placing slides in 3% hydrogen peroxide for 15 minutes, followed by a five minute wash in water. Slides were then blocked with Avidin D and Biotin blocking reagents (Vector Laboratories, SP-2001) for 15 minutes each at room temperature, with a quick rinse of PBS in between. Slides were blocked with CAS-Block (Invitrogen, 008120) for 30 minutes at room temperature. Primary antibodies (Table 2) were diluted in CAS-Block and incubated overnight at 4°C, followed by species-specific biotinylated secondary antibody (Table 3; 1:200 in PBS/0.1% Triton X-100) incubation for 40 minutes at 37°C. Signals were developed using the

Primary Antisera					
Antigen	**Species**	**Dilution**	**Antigen Retrieval**	**Source**	**Lot No.**
Ac-Tub	Mouse	1:1000	Yes	Sigma (T7451)	103M4772V
GFP	Goat	1:500	Yes	Abcam (ab6673)	10
Hhex	Rabbit	1:250	Yes	Dr. Clifford Bogue (Ghosh et al., 2000)	
Hnf1β	Goat	1:100	Yes	Santa Cruz (sc-7411)	E1010
Hnf6	Guinea Pig	1:1000	Yes	Kind gift from Dr. Patrick Jacquemin (Prevot et al., 2012)	
Muc1	Armenian Hamster	1:200	Yes	NeoMarkers (MAbHM-1630-P1Abx)	1630X1210A
Ngn3	Guinea Pig	1:1000	Yes	Kind gift from Dr. Maike Sander	
Npr3	Rabbit	1:50	No	Thermo Scientific (PA5-22080)	PH1894881J
Phospho-p38	Mouse	1:200	Yes	Santa Cruz (sc-7973)	H2007
SMA	Rabbit	1:200	Yes	Abcam (ab5694)	GR110346-1
Sox9	Goat	1:100	Yes	Santa Cruz (sc-17340)	L0408
Sox9	Rabbit	1:1000	Yes	Millipore (AB5535)	LV1762669

Table 2. Primary antibodies used for immunostaining analysis.

Secondary Antisera				
Raised against	**Raised in**	**Conjugate**	**Dilution**	**Source**
Goat IgG	Horse	Biotin	1:200	Vector Laboratories (BA-9500)
Guinea Pig IgG	Goat	Biotin	1:200	Vector Laboratories (BA-7000)
Mouse IgG	Goat	Biotin	1:200	Vector Laboratories (BA-9200)
Rabbit IgG	Goat	Biotin	1:200	Vector Laboratories (BA-1000)
Rabbit IgG	Donkey	Cy2	1:500	Jackson ImmunoResearch (711-225-152)
Rabbit IgG	Donkey	Cy3	1:500	Jackson ImmunoResearch (711-165-152)
Armenian Hamster IgG	Goat	Cy2	1:500	Jackson ImmunoResearch (127-225-160)
Armenian Hamster IgG	Goat	Cy3	1:500	Jackson ImmunoResearch (127-165-160)
Mouse IgG	Goat	Cy2	1:500	Jackson ImmunoResearch (115-225-166)
Mouse IgG	Goat	Cy3	1:500	Jackson ImmunoResearch (115-165-166)
Guinea Pig IgG	Donkey	Cy2	1:500	Jackson ImmunoResearch (706-485-148)
Goat IgG	Bovine	Cy2	1:500	Jackson ImmunoResearch (805-545-180)
Goat IgG	Bovine	Cy3	1:500	Jackson ImmunoResearch (805-165-180)
Goat IgG	Bovine	Cy5	1:500	Jackson ImmunoResearch (805-605-180)

Table 3. Secondary antibodies used for immunostaining analysis.

VECTASTAIN Elite ABC Kit (Vector Laboratories, PK-6100) and peroxidase substrate 3,3'diaminobenzidine (Derikx et al.) Kit (Vector Laboratories, SK-4100) according to manufacturer's instructions. For immunofluorescence, slides were blocked with CAS-Block for 30 minutes at room temperature after antigen retrieval and then incubated with primary antibody (Table 2) diluted in CAS-Block overnight at 4°C, followed by species-specific fluorescently-conjugated secondary antibody (Table 3; 1:500 in CAS-Block) for 2-4 hours at room temperature. Slides were mounted with Fluorescent Mounting Medium (KPL, 71-00-16) or Vectashield mounting medium with DAPI (Vector Laboratories, H-1200). All histological images were obtained using a Nikon Eclipse 80i microscope with a Q-imaging Retiga 2000R camera using iVision software (BioVision Technologies). Numerical apertures of objectives were as follows (mag/NA): 4x/0.13, 10x/0.30, 20x/0.50, 40x/0.75.

To determine the presence of pathology, histological slides were assessed by a pathologist in a blinded manner. For measurement of duct diameter, slides were scanned and all luminal diameters present on the pancreatic footprint were measured; data are presented as means of the average diameter of each animal for each genotype. For luminal contents score, a pathologist assigned each animal a single score in a blinded manner on a scale of 0-10, with 0 representing no luminal contents on average and 10 representing virtually all ducts completely occluded by inspissated, eosinophilic contents; data are presented as the mean score of each genotype.

Elastase1 ELISA

Approximately 220µl blood was collected from the tail vein of each mouse using heparinized blood collecting tubes (Fisher Scientific, 02-668-10). After centrifugation in plasma separator tubes with lithium heparin (BD Biosciences, 365958), plasma was diluted 1:1 with PBS, and 100µl was used per well in the Elastase1, Pancreatic (ELA1) BioAssay ELISA kit (Mouse) (US Biological, 024760) according to manufacturer's instructions. The assay was performed in technical duplicate for each animal. Absorbance at 450nm was measured using a Multiskan FC Microplate Photometer (Thermo Scientific, 51119000).

RNA Extraction, qRT-PCR, and Transcriptome Analysis

For animal studies, dorsal pancreata were dissected in ice-cold PBS and homogenized in TRIzol (Ambion, 15596-026). For *in vitro* studies, cells were washed twice with ice-cold PBS and scraped in 1ml PBS. After brief centrifugation at maximum speed, cells were lysed in TRIzol. Total cellular RNA was extracted using the RNeasy Mini Kit (QIAGEN, 74104). Reverse transcription and qPCR were performed as previously described.(Le Lay et al., 2009) Expression levels were normalized to those of *TATA-box binding protein* (*Tbp*) as an internal control. Primer sequences for qPCR are provided in Table 4.

For high throughput RNA sequencing, total RNA quantity and quality were assayed with an Agilent 2100 Bioanalyzer (Agilent Technologies). Libraries were prepared using the TruSeq RNA sample prep kit v2 (Illumina). Single-read sequencing

Transcript	Forward Primer Sequence (5'→3')	Reverse Primer Sequence (5'→3')
Cys1	AAAGGCAACCCTGAAGACAG	GCCATGAGCTCCTCTTCTGA
Hhex	TCAGAATCGCCGAGCTAAAT	CTGTCCAACGCATCCTTTTT
Hnf1β	CATCTGCAATGGTGGTCACAG	GGCTTGCAGTGGACACTGTTT
Hnf6	CAAATCACCATCTCCCAGCAG	CAGACTCCTCCTCCTGGCATT
Kif3a	GAGAAGGGACCAAGCAGGTAAA	TCCTCGTCAATTTTCGCTTGC
Npr3	GCAAATCATCAGGTGGCCTA	CCATTAGCAAGCCAGCACCTA
Pkd1	CAAGGAGTTCCGCCACAAAG	AACTGGGGATGACTTGGAGC
Pkd2	CTGGATGTTGTGATTGTCGTGT	TAGCAGCCCCTCTGCATTTG
Pkhd1	AAGTCAAGGGCCATCACATC	ATGTTTCTGGTCAACAGCCC
Polaris	AACAGCGCATAAAATCGGGC	GGCACTCAGTCGTTCACTCT
Prkcsh	CCACAGAGGATGAGAAGATGC	TTTCAAGGACCGTTCGACTT
Sec63	GCTCTTCTGGAGACCAAGTCA	AAAGCCACCACCACTCTTGT
Sst	CCCAGACTCCGTCAGTTTCT	GGGCATCATTCTCTGTCTGG
Tbp	CCCCTTGTACCCTTCACCAAT	GAAGCTGCGGTACAATTCCAG

Table 4. Primers used for gene expression analysis by qRT-PCR.

was performed on an Illumina hiSeq2000 (100-bp reads) with Casava1.7 software used for basecalling (Illumina). Low quality reads, as well as ribosomal and repeat sequences, were filtered out. Remaining reads were aligned to the mouse reference genome (NCBI build 37, mm9) using RUM alignment software (Grant et al., 2011). Differential expression analysis was carried out using EdgeR software (Robinson et al., 2010).

Pancreatic Ductal Cell Sorting and Culture

Isolation of pancreatic duct cells and culture conditions have been described previously (Reichert et al., 2013). Briefly, pancreata of uninduced 9-week-old *Hhex*$^{loxP/loxP}$ and *Hhex*$^{loxP/loxP}$*;Sox9-CreER*^{T2} mice were digested in collagenase, and duct cells were isolated via ductal-specific *Dolichos biflorus* agglutinin lectin labeling followed by magnetic bead separation. For recombination experiments, 4-hydroxytamoxifen (Sigma, H7904) was solubilized in ethanol and added to the growth medium at a final concentration of 500nM.

Cloning of HHEX overexpression construct and Lentiviral Transduction

HHEX (Myc-DDK-tagged) ORF (Origene, RC204815; accession number NM_002729) was PCR amplified for subcloning into the pLU.1-IRES-eGFP lentiviral vector using *BamHI* and *AgeI* restriction sites. Primers were BamHI-HHEX-F: 5'-CACGGATCCGGTACCGAGGAGATC-3' and AgeI-DDK-R: 5'-GTGACCGGTTTAAACCTTATCGTCGTCATCCTTG-3'. Thermocycler conditions were as follows: 96°C 2 minutes, [96°C 30 seconds, 63°C 30 seconds, 72°C 60 seconds]

30 times, 72°C 10 minutes, 4°C indefinitely. The cloned construct was confirmed by sequencing at the NAPCore Facility at the Children's Hospital of Philadelphia. Lentiviral particles were prepared at the Protein Expression Facility at the Wistar Institute and concentrated by ultracentrifugation. Primary ductal cells were transduced by spin transduction at a multiplicity of infection of 1000.(Reichert et al., 2013) GFP^+ cells were sorted by FACS 72 hours post-transduction at the Flow Cytometry and Cell Sorting Resource Laboratory at the University of Pennsylvania.

Data Access

All RNA-seq data has been deposited to Gene Expression Omnibus (GEO) and can be retrieved using accession number GSE63526.

Statistical Analysis

At least three animals of each genotype were used for all statistical analyses, as indicated in each experiment. To determine differences between groups, a two-tailed homoscedastic Student's t-test was performed using Microsoft Excel software; p-values <0.05 were considered significant. Variation measurements are given as standard error of the mean.

CHAPTER 3

HHEX FUNCTION IN THE PANCREATIC DUCT

INTRODUCTION

The exocrine pancreas, comprised of acinar and ductal cells, plays a crucial role in digestion by delivering alkaline, isotonic pancreatic juice containing digestive enzymes to the duodenum. Pancreatic zymogens, released from acini in response to postprandial enterohormonal and neural signals, traverse an intricate network of ducts of increasing size (Matthews et al., 1973, Petersen and Ueda, 1975, Reichert and Rustgi, 2011). Rather than merely serving as conduits, the pancreatic ducts actively aid in digestion by secreting bicarbonate against an immense concentration gradient (Whitcomb and Ermentrout, 2004). Similar to acinar cells, ductal cells are stimulated to secrete in response to enterohormonal and neural inputs via the cyclic AMP/PKA and calcium/PLCβ signaling pathways (Folsch et al., 1980, Ashton et al., 1990, 1991, Ashton et al., 1993, Gray et al., 1993). Additionally, various paracrine factors released from acinar cells have been identified that augment ductal cell stimulation, ensuring a coordinated pancreatic response (Ishiguro et al., 1999, Haanes and Novak, 2010).

Bicarbonate secretion serves to solubilize intraluminal zymogens and neutralize acidic chyme in the duodenum (Freedman and Scheele, 1993). Impairment of ductal cell functioning, such as what is frequently observed in patients who harbor mutations in the cystic fibrosis transmembrane conductance regulator (CFTR), contributes to the pathogenesis of pancreatic insufficiency and chronic pancreatitis, an important risk factor for pancreatic ductal adenocarcinoma (Kopelman et al., 1988, Riordan et al., 1989,

Raimondi et al., 2010). Although the mechanism by which bicarbonate is transported across the pancreatic ductal epithelium has been elucidated, the transcriptional control governing this process remains poorly understood.

Recently, the Kaestner Lab reported that the transcription factor Hhex is expressed in the pancreatic ductal epithelium (Zhang et al., 2014); however, due to embryonic lethality of *Hhex*$^{-/-}$ mice, its function in this cell type and its potential contribution to pancreatic disease pathogenesis have not been determined (Martinez Barbera, 2000 #12). Therefore, we sought to characterize the expression dynamics of Hhex within the ductal compartment of the pancreas and determine its requirement for ductal development and function by employing conditional gene ablation in mice. Ablation of *Hhex* in pancreatic progenitors resulted in postnatal ductal ectasia that progressed to chronic pancreatitis later in life, consistent with a published model of ductal hypertension (Yamamoto et al., 2006). Moreover, we identified the G-protein coupled receptor *Npr3*, of which activation is reported to potentiate secretin signaling to increase pancreatic flow rate, as regulated by Hhex and likely contributing to the pathogenesis of chronic pancreatitis in this genetic model (Sabbatini et al., 2003).

RESULTS

Hhex is expressed throughout developing and mature ducts.

In order to determine the function of Hhex in the pancreatic duct, we first characterized its expression dynamics and localization. At E13.5-E18.5, Hhex protein was present in nuclei within $Sox9^+$ cells of the epithelium, yet excluded from $Ngn3^+$ endocrine progenitors during the secondary transition ($n \geq 3$ animals for each timepoint examined) (Figure 9A-D and data not shown). These data indicate that Hhex is expressed in ductal progenitors throughout development, as the $Sox9^+$ domain becomes progressively more restricted to ductal progenitors during the secondary transition (Kopp et al., 2011). In postnatal and adult pancreata, Hhex was expressed in all segments of the ductal tree, including centroacinar cells, intercalated ducts, intralobular ducts, interlobular ducts, and interlobar/main ducts, as well as endocrine δ-cells (Figure 9E-G and data not shown).

Ablation of Hhex in pancreatic progenitors, but not mature ductal cells, results in chronic pancreatitis.

Because embryonic lethality of $Hhex^{-/-}$ mice precluded analysis at later stages, we derived two genetic models for conditional *Hhex* ablation to assess the requirement for Hhex in the maintenance of pancreatic duct function at different timepoints. Pancreata of 18-week-old mice with *Hhex* ablated in pancreatic progenitors ($Hhex^{loxP/loxP}$;$Pdx1\text{-}Cre^{Early}$, n=3) exhibited severe diffuse chronic pancreatitis (40-85% of footprint affected) with duct ectasia, interstitial and periductal fibrosis, acinar dropout, acinar-to-ductal

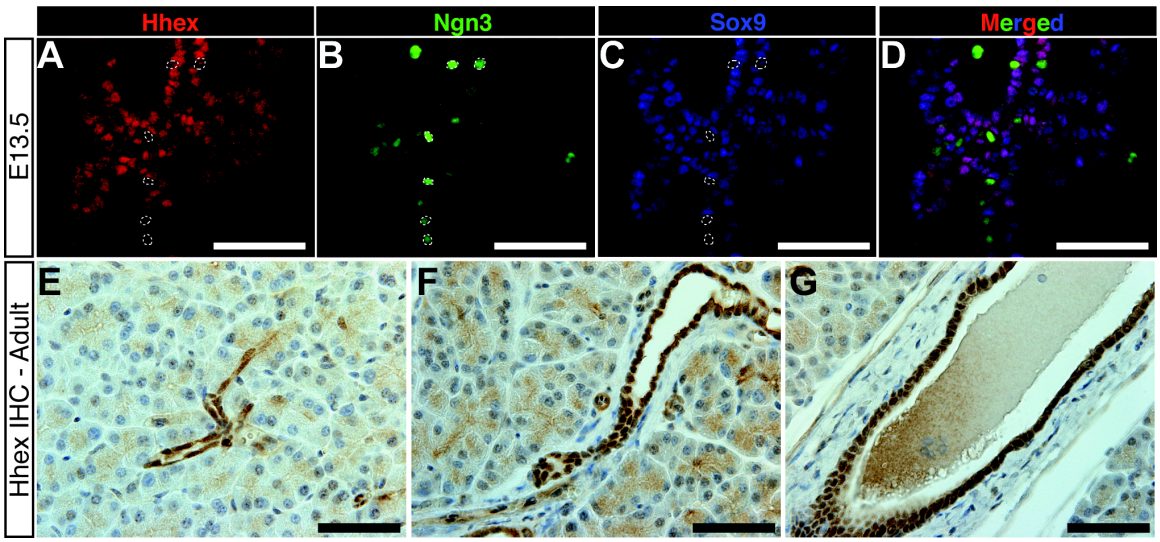

Figure 9. Hhex is expressed throughout embryonic and mature ducts. (A-D) Hhex (A,D, *red*) is expressed in the Sox9^{+} (C,D, *blue*) pancreatic epithelium at E13.5, yet excluded from Ngn3^{+} endocrine progenitors (B,D, *green*). Several Ngn3^{+} cells are outlined (A-C). (E-G) Immunohistochemical staining for Hhex expression (Thomas et al.) in the adult pancreas: (E) intercalated duct; (F) intralobular duct; (G) interlobar/main duct. *Scale bars*, 50µm.

metaplasia (ADM), and numerous aggregates of lymphocytes, plasma cells, and some neutrophils (Figure 10B vs. 10A). Ducts were severely ectatic and tortuous with luminal eosinophilic proteinaceous granular material and cellular debris. Remaining acini were separated into variably sized lobules dissected by variably dense fibrous connective tissue (Figure 10D). Consistent with these histological findings of chronic pancreatitis, plasma levels of Elastase1 were elevated 4.2-fold in 8-week-old *Hhex*$^{loxP/loxP}$*;Pdx1-Cre*^{Early} mice (n=4) relative to age-matched controls (n=3; $p<0.001$) (Figure 10E), reflective of acinar cell injury. These data indicate that Hhex is required for proper functioning of the exocrine pancreas.

Given the striking pancreatic pathology of *Hhex*$^{loxP/loxP}$*;Pdx1-Cre*^{Early} mice, we next tested the hypothesis that Hhex is required for maintenance of homeostasis of the exocrine pancreas in the adult. Nine- to 12-week-old *Hhex*$^{loxP/loxP}$*;Sox9-CreER*^{T2} and *Hhex*$^{loxP/loxP}$ littermate control mice were treated with tamoxifen for three consecutive days to induce CreER-mediated deletion of the *Hhex* gene and then analyzed for pancreatic pathology at two weeks or 12 weeks later (Figure 11A). Quantification of Hhex expression in *Hhex*$^{loxP/loxP}$*;Sox9-CreER*^{T2} mice two weeks post-induction indicated 95.7% ± 0.8% (n=6 mice) of duct cells had lost Hhex expression as intended, with similar ablation efficiency at 12 weeks post-induction (n=5 mice) (Figure 11B-D). Analysis of H&E stained sections yielded no overt pancreatic pathology at either timepoint in *Hhex*$^{loxP/loxP}$*;Sox9-CreER*^{T2} mice compared to littermate controls (Figure 12A-D). Moreover, no significant difference in average duct diameter or luminal contents was detected at two weeks post-induction (Figure 12E,F, p=0.454 and p=0.453, respectively). Finally, measurement of plasma Elastase1 levels by ELISA at 10 weeks post-induction

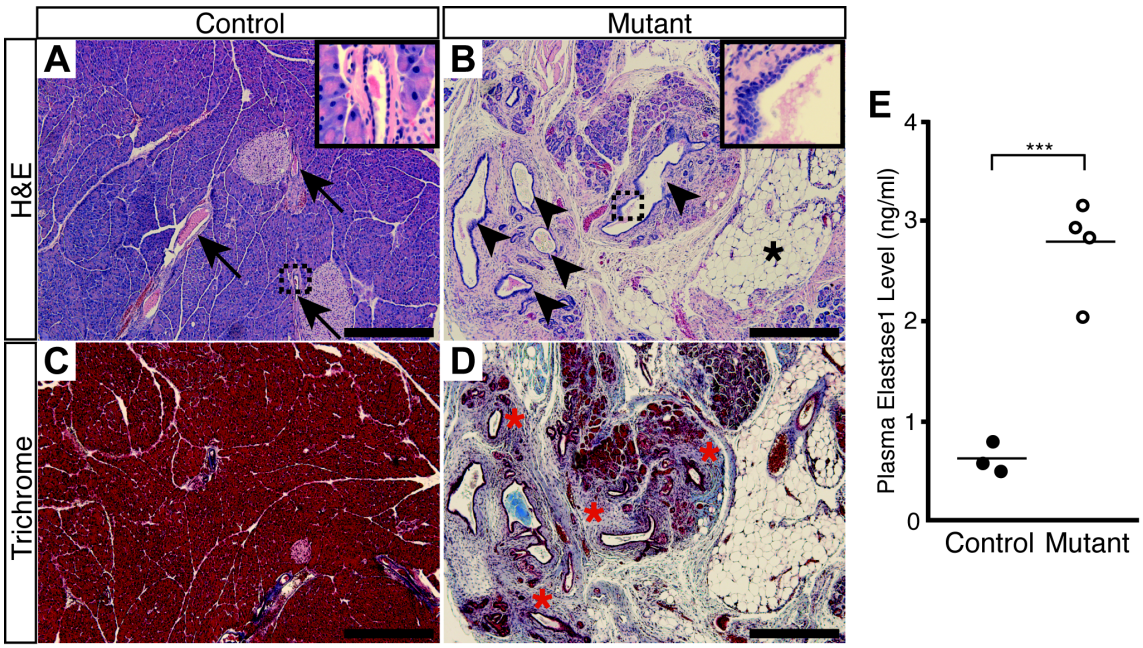

Figure 10. Ablation of *Hhex* in pancreatic progenitors results in chronic pancreatitis. (A,B) Representative H&E images of 18-week-old control (*Hhex*$^{loxP/loxP}$) and mutant (*Hhex*$^{loxP/loxP}$*;Pdx1-Cre*^{Early}) pancreata (n=3). (A) Ducts of control pancreata (*arrows*) are of typical caliber and consist of simple cuboidal epithelium (*inset*). (B) Mutant ducts display tortuous, ectactic ducts (*arrowheads* and *inset*) with parenchymal fibrosis and adipose infiltration (*black asterisk*). (C,D) Trichrome staining highlights periductal and interstitial fibrosis in mutant pancreata (*red asterisks*). (E) Measurement of plasma Elastase1 levels by ELISA indicate an approximate 4.2-fold elevation in 8-week-old mutants (n=4, mean 2.8 ng/ml) compared to age-matched controls (n=3, mean 0.65 ng/ml). Mean of each group is indicated. *Scale bars*, 400μm; *** p<0.001, Student's t-test; *Insets*, 400x.

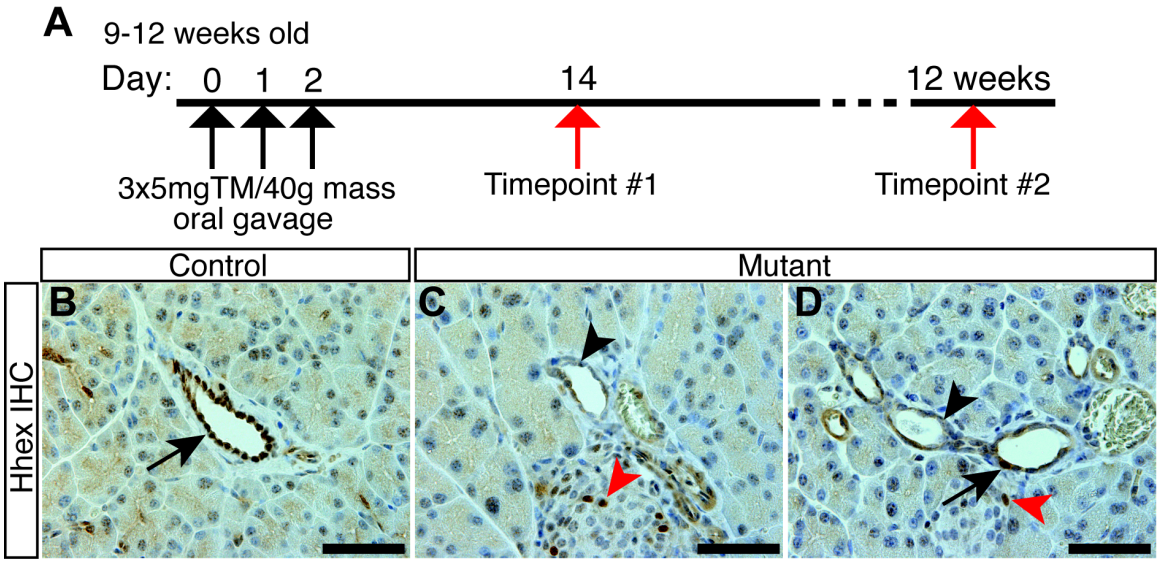

Figure 11. Efficient *Hhex* ablation in *Hhex*$^{loxP/loxP}$;*Sox9-CreER*^{T2} mice. (A) Schematic of tamoxifen induction in 9- to 12-week-old mice. (B-D) Representative Hhex IHC at two weeks post-induction. (B) Littermate controls (*Hhex*$^{loxP/loxP}$, n=4) exhibit ducts with nuclear Hhex expression (*black arrow*). (C, D) In mutant mice (*Hhex*$^{loxP/loxP}$;*Sox9-CreER*^{T2}, n=6), rare escape cells were detected (*black arrow*); 95.7% ± 0.8% of duct cells do not express Hhex (*black arrowheads*), whereas Hhex expression was retained within δ-cells (*red arrowheads*). *Scale bars*, 50μm.

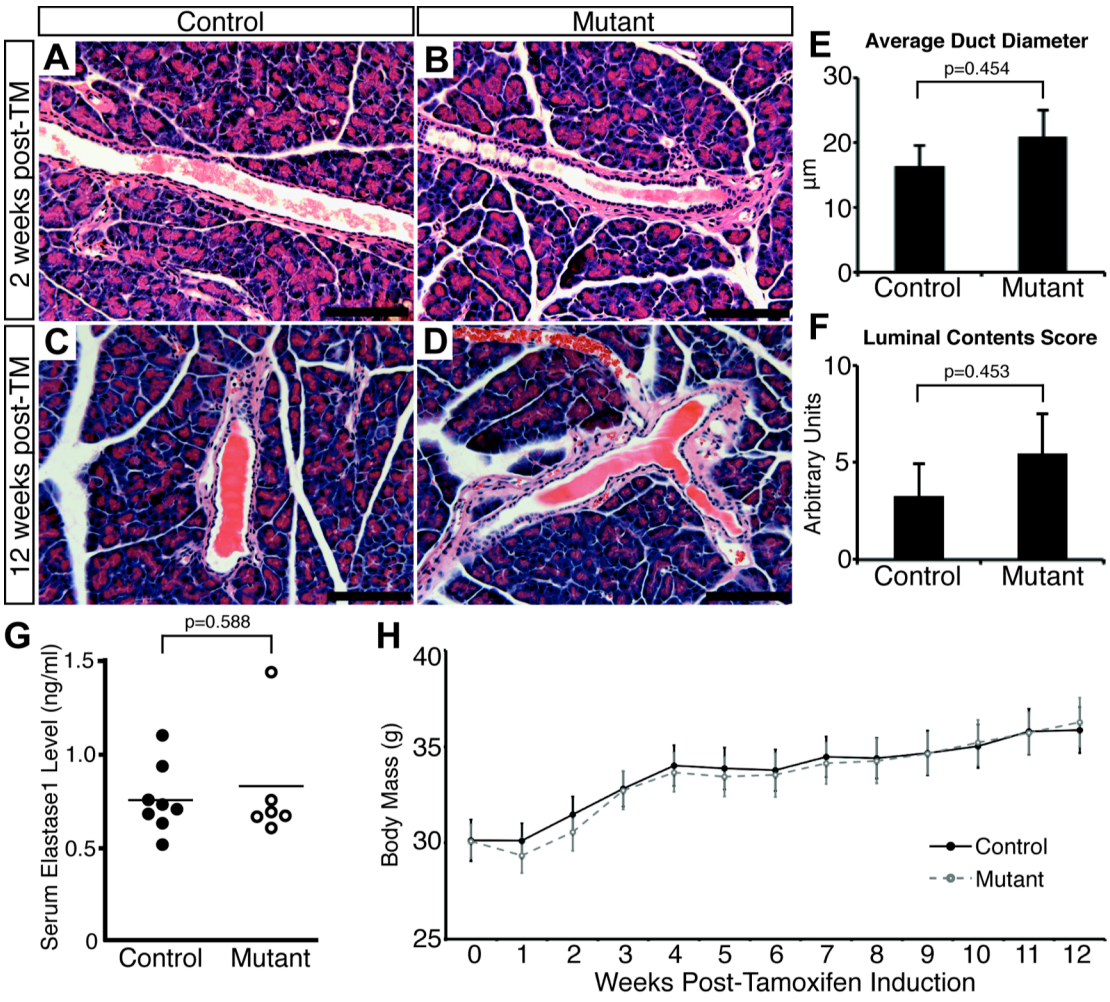

Figure 12. Hhex is not required for maintenance of exocrine compartment homeostasis in the mature pancreas. (A-D) Representative H&E images from littermate control (*Hhex*$^{loxP/loxP}$, n≥4 animals for each timepoint) and mutant pancreata (*Hhex*$^{loxP/loxP}$*;Sox9-CreER*^{T2}, n≥6 animals for each timepoint) display indistinguishable histology at two weeks (A,B) and 12 weeks (C,D) post-induction. *Scale bars*, 100µm. (E) Control (n=4, mean 16.4 ± 3.1µm) and mutant (n=6, mean 20.9 ± 4.1µm) pancreata exhibit similar ductal diameter two weeks post-induction (p=0.454, Student's t-test). Data are presented as means of the average diameter of each animal for each genotype ± S.E.M. (F) Grading of luminal contents (0-10) indicated no significant difference between control (n=4, mean 3.25 ± 1.70) and mutant (n=6, mean 5.5 ± 2.01) pancreata two weeks post-induction (p=0.453, Student's t-test). (G) Similar levels of Elastase1 were detected by ELISA in serum of control (n=8, mean 0.74ng/ml) and mutant (n=6, mean 0.83ng/ml) male mice 10 weeks post-induction (p=0.588, Student's t-test). Mean of each group is indicated. (H)

Control (n=8) and mutant (n=6) male mice were weighed for 12 weeks post-induction, with no significant differences in body mass observed at any timepoint ($p>0.05$, Student's t-test).

showed similar levels between *Hhex*$^{loxP/loxP}$*;Sox9-CreER*^{T2} (n=5) and littermate control mice (n=8; p=0.588) (Figure 12G), and no differences in body mass were detectable between these groups for the duration of the study (Figure 12H). Together, these data demonstrate that Hhex is not required to maintain homeostasis of the mature pancreatic ductal tree.

Embryonic loss of Hhex leads to rapid postnatal ductal ectasia associated with periductal fibrosis and ADM.

Chronic pancreatitis is a final manifestation of myriad causes of exocrine dysfunction. Therefore, we analyzed *Hhex*$^{loxP/loxP}$*;Pdx1-Cre*^{Early} mice at earlier timepoints to determine the most proximal defect, which we reasoned would uncover the specific function(s) of Hhex in ductal epithelial cells. At E18.5, pancreata of *Hhex*$^{loxP/loxP}$*;Pdx1-Cre*^{Early} mice appeared histologically indistinguishable from those of littermate *Hhex*$^{loxP/loxP}$ controls (n≥3 animals for each genotype) (Figure 13A-C). At P3, however, focal areas of ectatic ducts with periductal fibrosis were evident only in mutants (n≥3 animals for each genotype) (Figure 13E vs. 13D). Moreover, these regions were associated with the presence of ADM (Figure 13E,F,I,K,L), a finding never observed in control animals. The focal nature of this phenotype is likely resultant of the mosaic pattern of *Hhex* ablation in *Hhex*$^{loxP/loxP}$*;Pdx1-Cre*^{Early} mice (Figure 14). Analysis of pancreata at P10 and P21 (n≥3 animals for each genotype at each timepoint) indicated that dilation of the exocrine system and extracellular remodeling in mutant mice became progressively more severe (Figure 13G-L); strikingly, the most severely affected mice

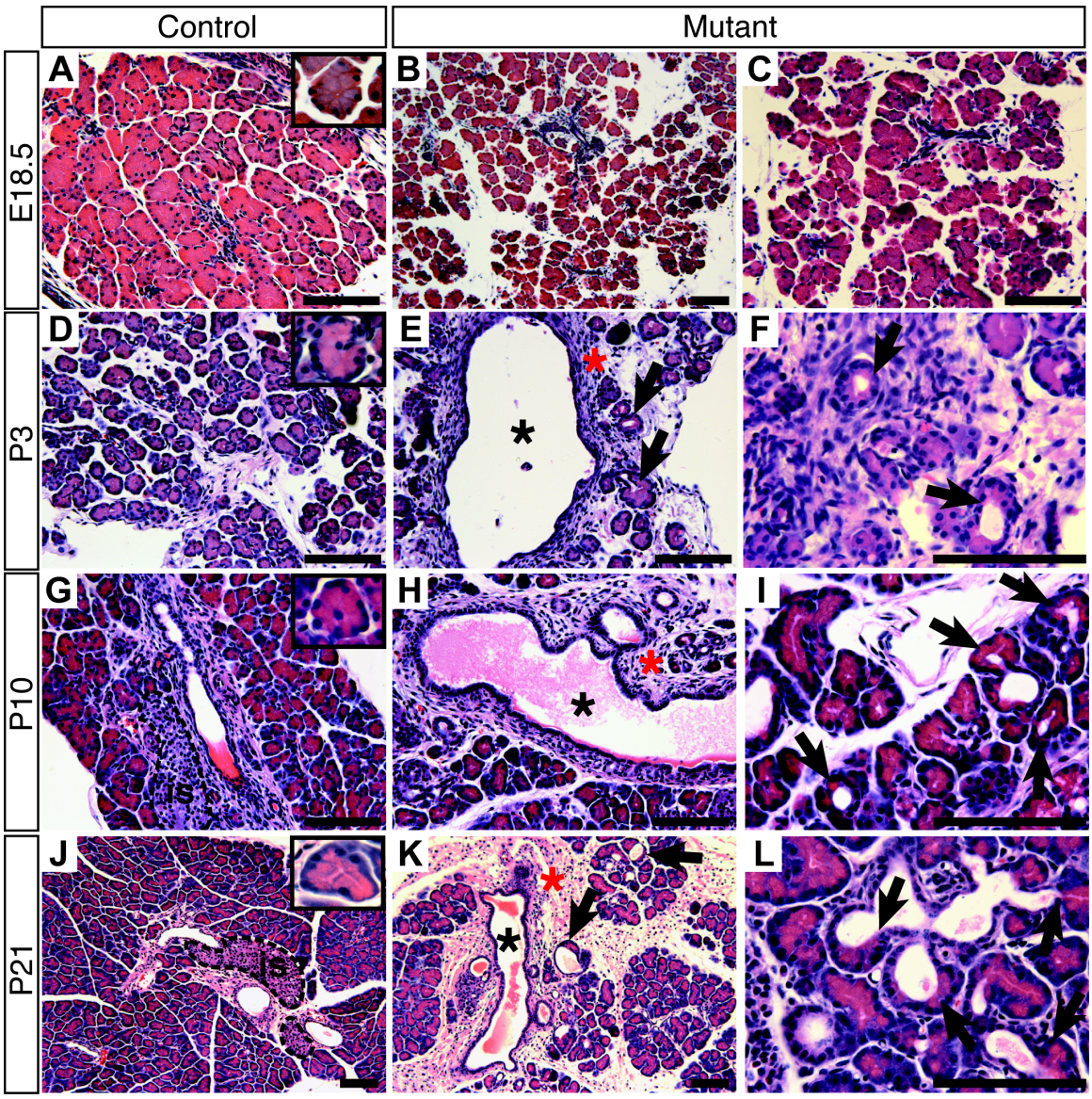

Figure 13. Perinatal ductal ectasia and ADM in *Hhex*$^{loxP/loxP}$*;Pdx1-Cre*^{Early} mice. (A-L) Representative H&E images at several developmental timepoints; *insets*: high magnification view of an acinus from control pancreas at specific age is shown. (A-C) At E18.5, control (*Hhex*$^{loxP/loxP}$, n≥3 animals) and mutant (*Hhex*$^{loxP/loxP}$*;Pdx1-Cre*^{Early}, n≥3 animals) pancreata displayed similar histology. (D-F) Soon after birth at P3, however, mutants (E, n≥3 animals) showed ectatic ducts (*black asterisk*) with associated periductal fibrosis (*red asterisk*). Moreover, these regions were associated with ADM (*arrows*, E and F), a finding only observed in mutants. (G-I) Histological features of periductal fibrosis, ductal ectasia, and ADM in mutants became more prominent at P10. (J-L) At P21, severely affected mutant mice exhibited an exacerbated phenotype with concomitant interstitial fibrosis. *Scale bars*, 100μm; *insets*, 400x; *is*, islet.

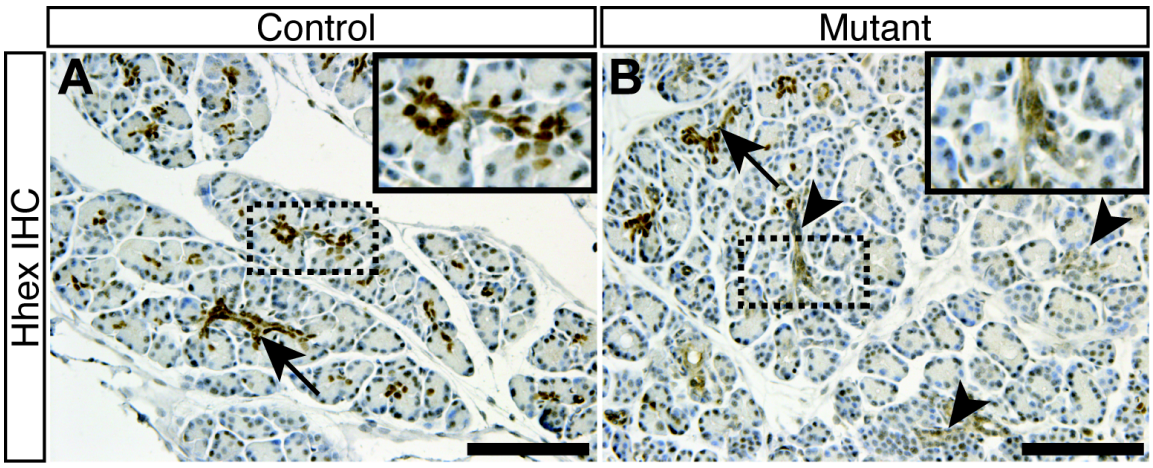

Figure 14. Mosaic Hhex expression in *Hhex*$^{loxP/loxP}$*;Pdx1-Cre*^{Early} mice at P10. (A) Representative Hhex IHC staining in control pancreata (*Hhex*$^{loxP/loxP}$, n≥3 animals) highlights nuclear Hhex expression in ductal cells (*black arrows*). (B) Hhex expression in mutant pancreata (*Hhex*$^{loxP/loxP}$*;Pdx1-Cre*^{Early}, n≥3 animals) was predominantly a pattern of regional mosaicism in that specific ducts either expressed (*black arrow*) or did not express (*black arrowheads*) Hhex. Similar patterns of mosaicism were observed at P3 and P21. *Scale bars*, 100μm; *Insets*, 400x.

(n=2) exhibited diffuse interstitial fibrosis by P21 (Figure 13K). This progressive pattern of ductal ectasia with concomitant fibrosis in mutants likely accounts for the exocrine dysfunction that leads to chronic pancreatitis in adults.

Hhex does not cell autonomously regulate expression of Hnf6, Hnf1β, or primary cilia in ductal cells.

Analysis of $Hhex^{loxP/loxP};Pdx1\text{-}Cre^{Early}$ pancreata in early life indicated that ductal ectasia was likely a primary cause of subsequent exocrine dysfunction. We therefore reasoned that ectasia was a direct consequence of *Hhex* ablation. Conditional ablation of *Hhex* in embryonic liver has been reported to result in dilated ducts and polycystic liver disease in adulthood (Hunter et al., 2007). Moreover, expression of the genes encoding the transcription factors Hnf6 and Hnf1β, both of which are known to regulate the elaboration of primary cilia in the pancreas and other organs, was downregulated in the *Hhex*-ablated liver (Gresh et al., 2004, Pierreux et al., 2006, Hunter et al., 2007, Zhang et al., 2009). Because pancreas-specific disruption of primary cilia in genetic mouse models results in severe ductal ectasia and subsequent chronic pancreatitis, we hypothesized that Hhex may regulate a transcription factor cascade that includes Hnf6, Hnf1β, and genes necessary for functioning of primary cilia (Cano et al., 2004, Cano et al., 2006).

Typically, primary cilia are present exclusively on ductal and islet cells in the pancreas from mid-gestation onward. Therefore, we determined the expression pattern of primary cilia both before (E18.5) (n=3 for each genotype) and after (P10) (n=3 for each genotype) the emergence of ductal ectasia (Figure 15A,B). At both timepoints, primary cilia were clearly evident on the luminal surface of ductal cells in our *Hhex* ablation

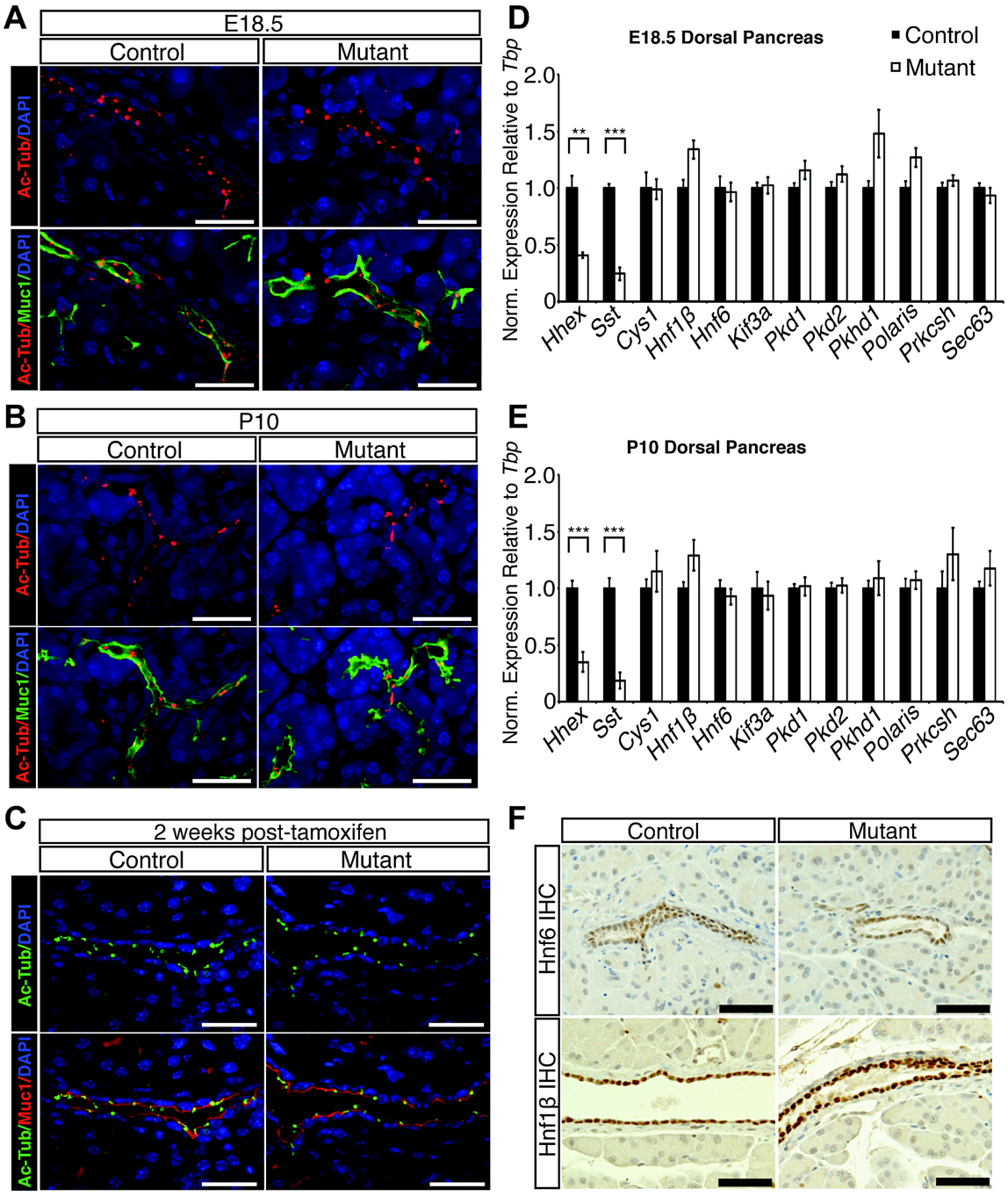

Figure 15. Hhex is not required for expression of Hnf6, Hnf1β, or primary cilia. (A-C) Immunofluorescence staining for acetylated-tubulin, a marker of primary cilia, in the ductal epithelium. (A,B) Acetylated-tubulin (*red*) is visualized within the ductal lumina of both control (*Hhex*$^{loxP/loxP}$) and mutant (*Hhex*$^{loxP/loxP}$*;Pdx1-Cre*^{Early}) pancreata at E18.5 and P10 (n≥3 animals for each genotype at each timepoint). Mucin1 (*green*) was stained to mark the luminal surface of acinar and ductal cells. *Scale bars*, 25μm. (C) A similar expression pattern of acetylated-tubulin (*green*) was observed between adult control

(*Hhex*$^{loxP/loxP}$) and mutant (*Hhex*$^{loxP/loxP}$*;Sox9-CreER*^{T2}) pancreata two weeks post-induction (n≥3 animals for each genotype). Mucin1 (*red*) highlights ductal lumina. *Scale bars*, 25μm. (D,E) qRT-PCR gene expression analysis of dorsal pancreata at E18.5 (D) and P10 (E) show similar levels between littermate control (*Hhex*$^{loxP/loxP}$, n≥3 animals, *black bars*) and mutant (*Hhex*$^{loxP/loxP}$*;Pdx1-Cre*^{Early}, n≥3 animals, *white bars*) mice for an array of genes previously implicated in primary cilia formation and function. Somatostatin (*Sst*) was used as a positive control for downregulation of an established Hhex target gene in the pancreas. *Tbp* levels were used to quantify relative gene expression, and the mean of the control group for each gene was normalized to a value of 1. Data are presented as mean ± S.E.M. **p<0.01, ***p<0.001, Student's t-test. (F) Representative IHC for Hnf6 (*top panels*) and Hnf1β (*bottom panels*) indicate similar levels of protein between controls (*Hhex*$^{loxP/loxP}$, n=3 animals) and mutants (*Hhex*$^{loxP/loxP}$*;Sox9-CreER*^{T2}, n=3 animals) two weeks post-induction in the ductal epithelium. *Scale bars*, 50μm.

model. Additionally, we assayed for the presence of primary cilia in the adult model of *Hhex* ablation and observed similar numbers of primary cilia between *Hhex*$^{loxP/loxP}$;*Sox9-CreER*^{T2} and *Hhex*$^{loxP/loxP}$ littermate control mice (n=3 for each genotype) (Figure 15C).

Although primary cilia were present on ductal cells of mutant pancreata in both genetic models of *Hhex* ablation, the possibility remains that the functioning of these organelles was compromised. To address this possibility, we performed gene expression analysis at E18.5 and P10 for an array of genes that have previously been implicated in primary cilia formation and/or function in both the pancreas and other organs (Gresh et al., 2004, Pierreux et al., 2006). At both ages, no significant decrease in the mRNA levels of any of these genes was detected (Figure 15D,E).

Notably, transcript levels of *Hnf6* and *Hnf1β* were similar between mutants and littermate controls at both E18.5 and P10 (Figure 15D,E), in contrast to what has been reported for protein expression in embryonic liver-specific *Hhex* ablation (Hunter et al., 2007). It is important to note that these two factors are nearly duct-specific in the P10 pancreas, excluding the possibility that residual expression in other cell types accounted for the lack of alteration in gene expression (Coffinier et al., 1999, Kopp et al., 2011, Kopp et al., 2012, Prevot et al., 2012). Moreover, a similar level of each protein was detected in mutant *Hhex*$^{loxP/loxP}$;*Sox9-CreER*^{T2} pancreata (n=5) relative to littermate controls two weeks post-induction (Figure 15F).

To further support the finding that Hnf6 is not a cell-autonomous target of Hhex, pregnant dams were induced at E13.5 for Hnf6 expression analysis at E15.5 in *Hhex*$^{loxP/loxP}$;*Sox9-CreER*^{T2};*Rosa26*$^{LSL-YFP}$ embryos (n=3). Hnf6 protein expression was most notable in the epithelial cords in both mutants and controls, consistent with its

expression in ductal progenitors (Pierreux et al., 2006), and the expression pattern was indistinguishable between the two genotypes (Figure 16A,B). Further, no difference in Hnf6 expression level was detectable between YFP^- (Figure 16B',D' cells 1 and 2) and YFP^+ (cells 3 and 4) cell populations, demonstrating that Hnf6 is not a cell-autonomous target of Hhex. Together, these data indicate that *Hhex* ablation in the pancreas does not affect expression of *Hnf6*, *Hnf1β*, or primary cilia in a cell-autonomous manner, which points toward a different function of Hhex in the pancreas compared to the liver.

Hhex ablation results in changes consistent with ductal hypertension.

Given the coincident onset of ductal ectasia with postnatal exocrine activation in $Hhex^{loxP/loxP};Pdx1\text{-}Cre^{Early}$ mice, and the fact Hhex regulates functional genes in a variety of mature cell types, we next hypothesized that Hhex directly contributes to the regulation of ductal cell function – that is, secretion. Importantly, the progressive manner of the pathologic changes of $Hhex^{loxP/loxP};Pdx1\text{-}Cre^{Early}$ mice closely resembles that of the primary pancreatic ductal hypertension model (Yamamoto et al., 2006). In this model, the pancreatic duct of rats was cannulated and attached to a pump to cause primary ductal hypertension by physical means, while the common bile duct was diverted directly to the duodenum to avoid hepatic hypertension. The first-observed pathologic changes in the pancreas were ectatic ducts with periductal fibrosis, which ultimately proceeded to interstitial fibrosis and chronic pancreatitis, with an overall pathogenesis similar to that seen in Hhex-deficient mice (Figure 13). Therefore, we hypothesized that *Hhex* ablation in the ductal epithelium results in hypersecretion and its sequelae.

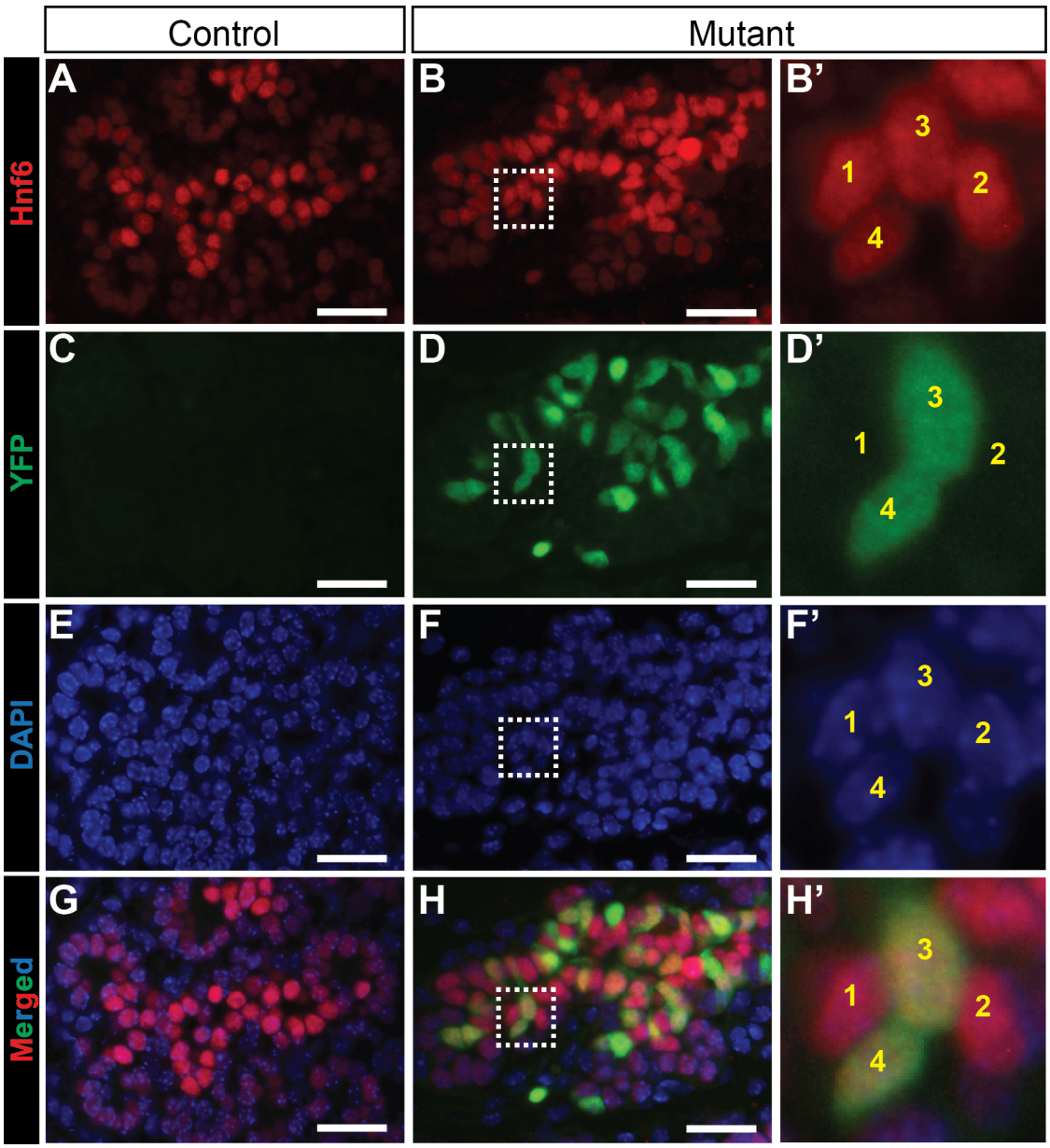

Figure 16. Cell autonomous expression analysis of Hnf6 in *Hhex*-ablated mice. Pregnant dams were injected with tamoxifen at E13.5, and embryos were dissected 48 hours after. Control (*Hhex*$^{loxP/loxP}$;*Rosa26*$^{LSL\text{-}YFP}$) and mutant (*Hhex*$^{loxP/loxP}$;*Sox9-CreER*^{T2};*Rosa26*$^{LSL\text{-}YFP}$)pancreata were immunostained for Hnf6 (A,B) and YFP (C,D). (E,F) DAPI was used to visualize nuclei. (B',D',F',H') Higher magnification views of respective boxed areas. *Scale bars*, 25μm.

To test this hypothesis directly, we attempted to cannulate the Ampulla of Vater for direct volumetric assessment of pancreatic secretions; unfortunately, these attempts were unsuccessful due to the extremely small diameter of the ampulla. As a surrogate for barostress, we therefore assayed for the presence of activated pancreatic stellate cells (PSCs). PSCs have been shown to be activated directly by increased pressure via phosphorylation of the stress kinase p38, and consistent with this finding, widespread activation of PSCs was observed in the ductal hypertension model by staining for smooth muscle actin (Whitcomb et al.) (Yamamoto et al., 2006, Asaumi et al., 2007). Concordantly, pancreata of P21 *Hhex*$^{loxP/loxP}$*;Pdx1-Cre*^{Early} mice (n=2) exhibited SMA^{+} cells most prominently within fibrotic areas of ectatic ducts (Figure 17B,C), abutting histologically normal-appearing acini adjacent to affected regions (Figure 17B), and within areas of interlobar fibrosis (data not shown). In contrast, control pancreata (n=2) showed SMA reactivity only in the vasculature (Figure 17A). Moreover, immunostaining for phosphorylated p38 (p-p38) in P21 tissue showed a similar pattern as that for SMA in that only mutant pancreata had p-p38^{+} fibroblastic-type cells within areas of periductal fibrosis and surrounding acini (Figure 17D-G); these data are consistent with widespread activation of PSCs as a consequence of ductal hypertension.

Hhex cell-autonomously represses Npr3 in ductal cells.

In order to determine the molecular basis of ductal ectasia, we performed transcriptome analysis using *Hhex*-ablated primary ductal cells (PDCs). Due to numerous secondary effects evident in *Hhex*$^{loxP/loxP}$*;Pdx1-Cre*^{Early} mice, such as inflammatory infiltrates, PSC activation, and remodeling of extracellular matrix, we elected to use an *ex*

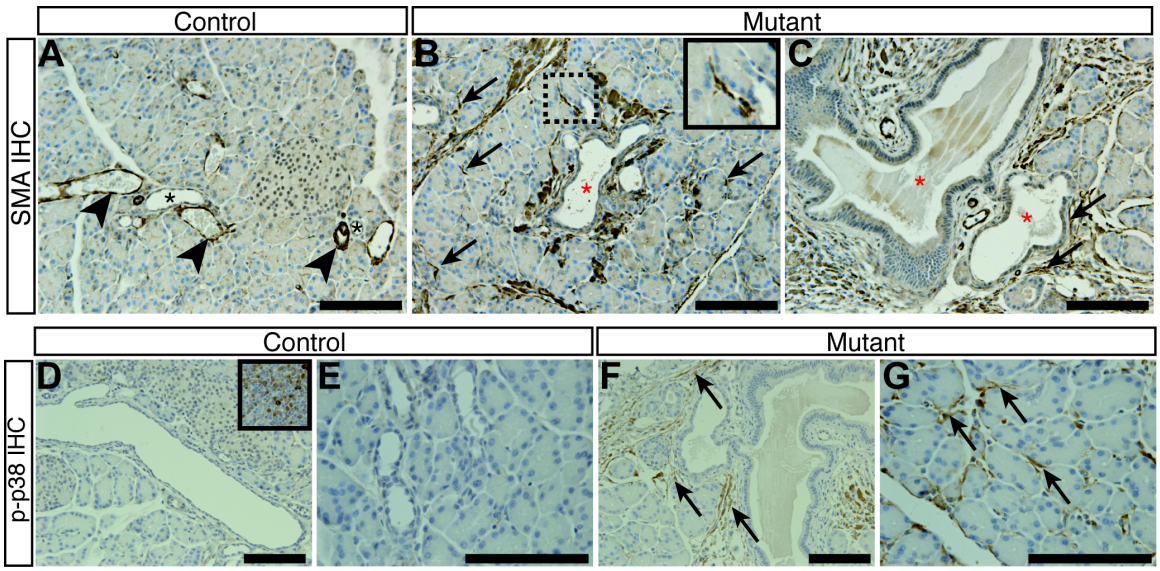

Figure 17. Activated pancreatic stellate cells (PSCs) are present in pancreata of *Hhex*$^{loxP/loxP}$*;Pdx1-Cre*^{Early} mice. (A-C) Immunostaining for smooth muscle actin (Whitcomb et al.) was used as a marker for activated PSCs. (A) In P21 control mice (*Hhex*$^{loxP/loxP}$, n=2), SMA expression was evident exclusively in the vasculature of the pancreas (*arrowheads*). *Black asterisks*, ducts. (B,C) P21 mutant pancreata (*Hhex*$^{loxP/loxP}$*;Pdx1-Cre*^{Early}, n=2), however, exhibited significant SMA expression (*black arrows*) within the parenchyma surrounding ectatic ducts (*red asterisks*) and histologically normal acini. *Inset*, fibroblastic-type SMA^{+} cell abutting an acinus. (D-G) Immunostaining for phosphorylated p38 (p-p38) stress kinase in P21 pancreata. (D,E) p-p38 parenchymal reactivity was not observed within control tissue (n=2). *Inset*, immune cells within an intrapancreatic lymph node were used as an internal positive control. (F,G) p-p38 immunoreactivity within mutant pancreata (n=2) demonstrated a similar pattern as that for SMA in that p-p38^{+} fibroblastic-type cells (*black arrows*) were observed surrounding ectatic ducts and adjacent acini. *Scale bars*, 100µm.

vivo system to ablate *Hhex* acutely in PDCs to ascertain the most proximal gene expression changes. PDCs were isolated from uninduced control $Hhex^{loxP/loxP}$ and mutant $Hhex^{loxP/loxP}$;*Sox9-CreER*^{T2} mice to establish PDC lines (Figure 18A; n=2 for each genotype). Upon 4-hydroxytamoxifen administration *in vitro*, both $Hhex^{loxP/loxP}$;*Sox9-CreER*^{T2} mutant lines showed dramatically reduced levels of *Hhex* transcript relative to control lines (Figure 18B). High throughput sequencing of RNA-derived libraries yielded a total of 216 differentially expressed transcripts (152 upregulated, 64 downregulated; FDR<0.10) in *Hhex*-ablated PDCs vs. controls. Of these, we focused on genes that could be implicated in ductal secretion (i.e. G-protein coupled receptors, ion transporters/channels, and regulators of G-protein coupled receptor downstream signaling) (Figure 18C).

We selected the gene *Natriuretic peptide receptor 3* (*Npr3*) for follow-up analysis because it showed a 4.70-fold increase in *Hhex*-ablated PDCs, is expressed at a higher level than other differentially-regulated G-protein coupled receptors in PDCs (Figure 18C), and has previously been shown to potentiate secretin signaling to enhance pancreatic flow *in vivo* (Sabbatini et al., 2003). Increased levels of *Npr3* transcript were detected in an independent experiment, validating results from the transcriptome analysis (Figure 18D). Immunostaining for Npr3 in both genetic models confirmed increased Npr3 protein levels specifically in the *Hhex*-ablated ductal epithelium, while Npr3 levels within the acinar cells remained unchanged (Figure 18E,F). To support the hypothesis that Hhex functions to repress the *Npr3* locus, we performed the converse experiment to our aforementioned approach, reasoning that Hhex overexpression should reduce *Npr3* levels. Thus, PDCs were transduced with a HHEX-IRES-GFP lentiviral construct and

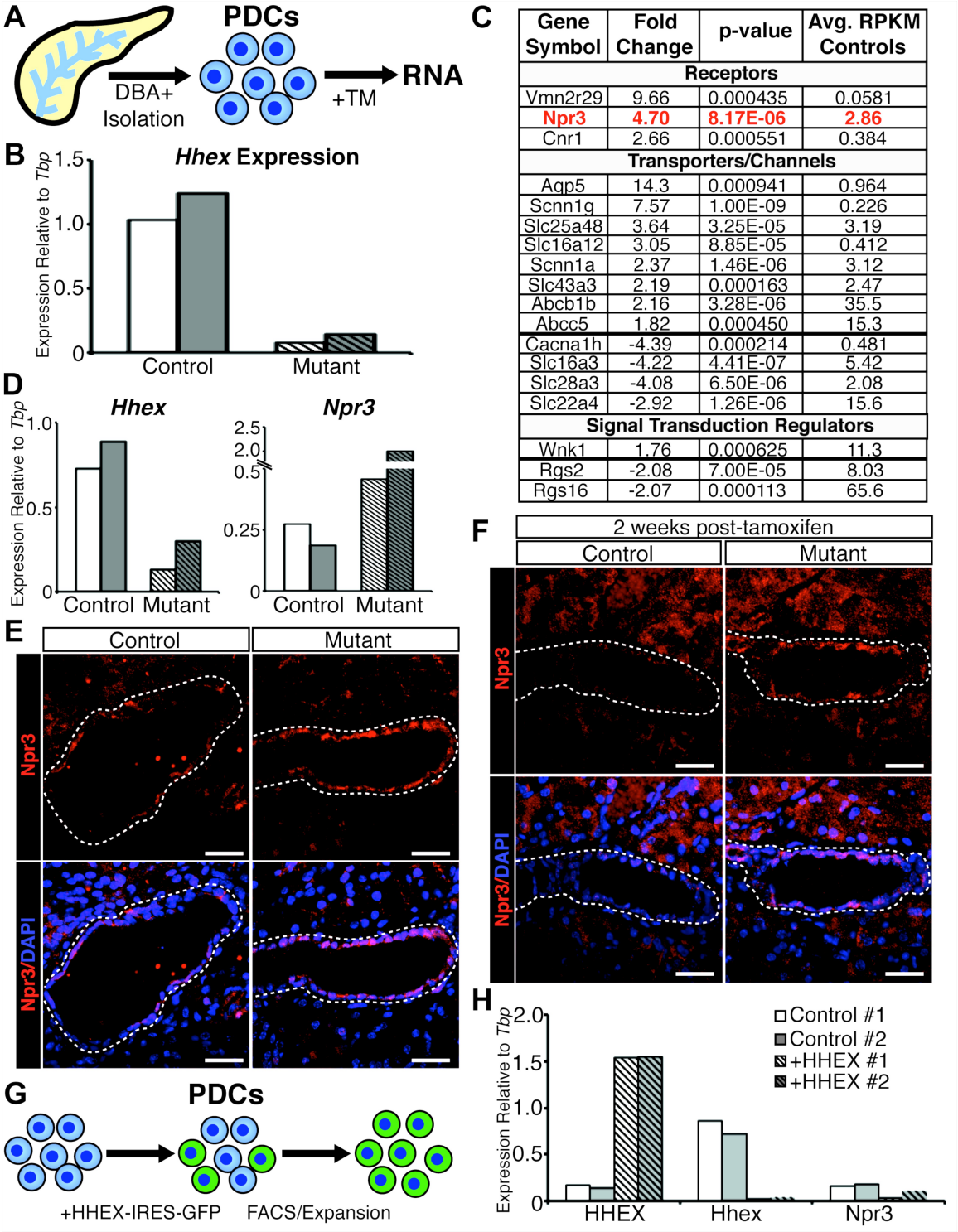

Gene Symbol	Fold Change	p-value	Avg. RPKM Controls
Receptors			
Vmn2r29	9.66	0.000435	0.0581
Npr3	4.70	8.17E-06	2.86
Cnr1	2.66	0.000551	0.384
Transporters/Channels			
Aqp5	14.3	0.000941	0.964
Scnn1g	7.57	1.00E-09	0.226
Slc25a48	3.64	3.25E-05	3.19
Slc16a12	3.05	8.85E-05	0.412
Scnn1a	2.37	1.46E-06	3.12
Slc43a3	2.19	0.000163	2.47
Abcb1b	2.16	3.28E-06	35.5
Abcc5	1.82	0.000450	15.3
Cacna1h	-4.39	0.000214	0.481
Slc16a3	-4.22	4.41E-07	5.42
Slc28a3	-4.08	6.50E-06	2.08
Slc22a4	-2.92	1.26E-06	15.6
Signal Transduction Regulators			
Wnk1	1.76	0.000625	11.3
Rgs2	-2.08	7.00E-05	8.03
Rgs16	-2.07	0.000113	65.6

Figure 18. Hhex regulates Npr3 expression cell-autonomously in pancreatic ductal cells. (A) Schematic of approach to identify cell autonomous targets of Hhex. DBA^{+} ductal cells were isolated from pancreata of nine-week-old control (*Hhex*$^{loxP/loxP}$, n=2 animals)

or mutant (*Hhex*$^{loxP/loxP}$;*Sox9-CreER*^{T2}, n=2 animals) mice to establish primary ductal cell (PDC) lines. Treatment with 4-hydroxytamoxifen was used to induce recombination *in vitro*. (B) Gene expression analysis for *Hhex* transcript levels four days after 4-hydroxytamoxifen treatment. (C) Partial list of the 217 transcripts identified to be differentially regulated in *Hhex*-ablated PDCs by RNA-seq (FDR<0.10). Genes were selected based on their potential to regulate ductal secretion via receptor signaling, ion transport, or signal transduction capability. Fold change is presented as mutant/control. RPKM values of the two control lines were averaged to give an indication of relative expression level. (D) An independent experiment was performed to validate gene expression changes identified by transcriptome analysis. RNA was collected 48 hours after 4-hydroxytamoxifen treatment. *Hhex* and *Npr3* expression levels are both presented relative to *Tbp*. (E,F) Immunofluorescence staining for Npr3 shows higher levels specifically within the ductal epithelium of mutants. (E) P21 mutant (*Hhex*$^{loxP/loxP}$;*Pdx1-Cre*^{Early}, 2 animals) versus control (*Hhex*$^{loxP/loxP}$, 2 animals) mice. DAPI was used to visualize nuclei. Ductal epithelium is outlined. *Scale bars*, 25μm. (F) Adult mutant (*Hhex*$^{loxP/loxP}$;*Sox9-CreER*^{T2}, n=2) versus control (*Hhex*$^{loxP/loxP}$, 2 animals) mice two weeks post-induction with tamoxifen. DAPI was used to visualize nuclei. Ductal epithelium is outlined. *Scale bars*, 25μm. (G) Schematic of HHEX overexpression approach. Two primary ductal cell lines were transduced with a lentivirus containing a HHEX-IRES-GFP construct. GFP^{+} cells were sorted by FACS 72 hours post-transduction to establish HHEX-overexpressing PDC lines. (H) Gene expression analysis of control (n=2) and HHEX-overexpressing (n=2) PDC lines for *HHEX*, *Hhex*, and *Npr3*. Expression levels are presented relative to *Tbp* and are indicated above each bar.

sorted by FACS to establish HHEX-overexpressing PDC lines (Figure 18G). Gene expression analysis indeed showed a reduction of *Npr3* levels relative to control lines (0.104 and 0.029 for HHEX overexpressers, vs. 0.173 and 0.155 for controls) (Figure 18H). Intriguingly, overexpression lines showed a concomitant, dramatic reduction of murine *Hhex* transcript (0.0349 and 0.0212 vs. 0.722 and 0.859), suggesting that Hhex may participate in an autoregulatory feedback loop in pancreatic ductal epithelial cells.

DISCUSSION

The results presented above support a model in which the homeobox transcription factor Hhex serves an essential role in maintenance of exocrine homeostasis in early life by dampening the response of ductal cells to stimulatory signals, thus preventing hypersecretion (see model in Figure 19). According to our model, *Hhex* ablation in pancreatic progenitors results in increased expression of the G-protein coupled receptor (GPCR) Npr3 specifically in ductal cells; this raises the effective concentration of paracrine natriuretic peptide signals, which produces a primary hypersecretion defect of the ductal epithelium. The resultant ductal hypertension leads not only to ductal ectasia, but also to activation of pancreatic stellate cells, which can mediate the processes of periductal fibrosis, inflammation, and immune cell recruitment (Andoh et al., 2000, Shek et al., 2002). The interstitial pressure within pancreata from human patients with chronic pancreatitis has been reported to be over 10-fold higher than normal (Jalleh et al., 1991); thus, we contend that the fibrotic process exhibited in perinatal life initiates a cascade of events that serve as a positive feedback loop, further increasing intraductal pressure and extracellular remodeling, ultimately manifesting as chronic pancreatitis later in life.

Natriuretic peptide signaling is best characterized for its role in cardiovascular homeostasis (Brenner et al., 1990, de Bold et al., 1996); however, most of the gastrointestinal tract has been described as a site of production of atrial natriuretic peptide (ANP) (Gower et al., 1994, Vollmar et al., 1997). Fluctuations of ANP expression in the gastrointestinal tract in fed versus fasted states support its role as a paracrine signaling mediator (Gower et al., 2000). In the pancreas, ANP is most highly expressed in acinar

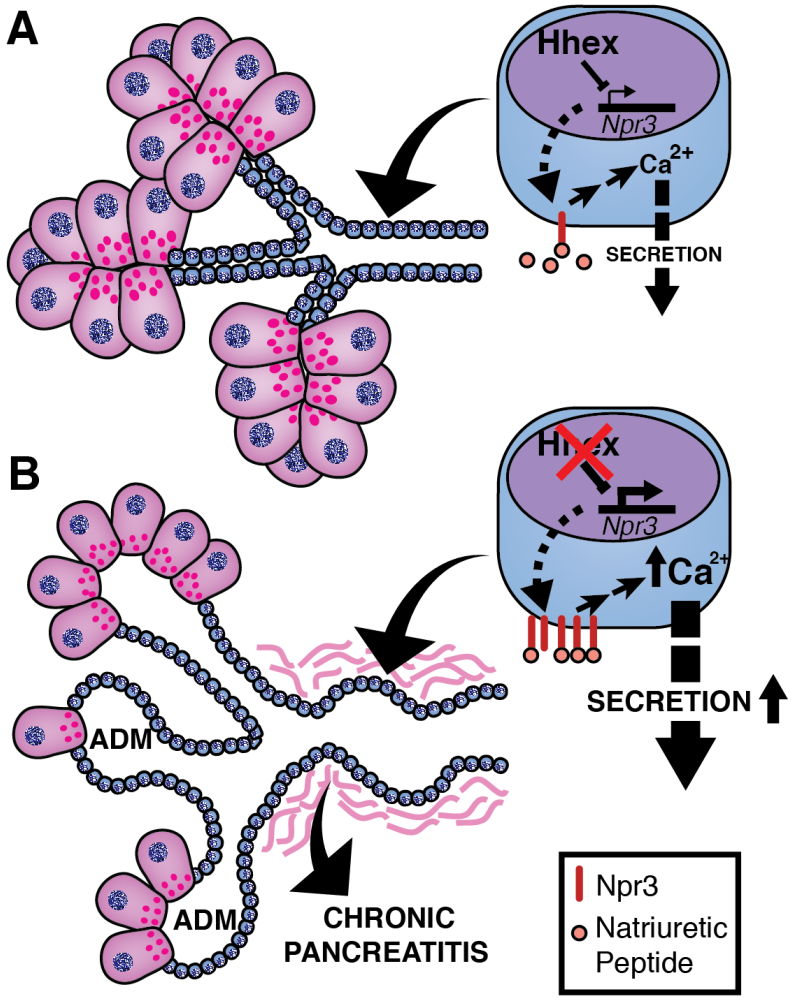

Figure 19. Model of Hhex molecular function in the pancreatic ductal epithelium. (A) In control pancreata, Hhex functions to repress expression from the *Npr3* locus. Signaling pathways in the ductal cell contribute to physiologically-appropriate secretion that maintains homeostasis of the exocrine pancreas. (B) When *Hhex* is ablated in pancreatic progenitors, however, Npr3 protein levels are increased specifically in ductal cells. Upon postnatal activation of the exocrine pancreas, the effective concentration of natriuretic peptide ligand at the ductal cell surface is raised, resulting in hypersecretion. Consistent with primary ductal hypertension, ectatic ducts with periductal fibrosis are evident, and disruption of exocrine homeostasis results in acinar-to-ductal metaplasia. Ultimately, destruction and remodeling of parenchyma will manifest as chronic pancreatitis.

and centroacinar cells (Chabot et al., 1987, Chabot et al., 1988). Intravenous administration of ANP in rats results in decreased chloride and increased bicarbonate concentrations in pancreatic juice (Sabbatini et al., 2003). Consistent with these molecular studies, ANP signaling, mediated via the phosphatidylinositol pathway downstream of Npr3, synergizes with secretin signaling to increase pancreatic flow rate, a physiologic metric that is contingent upon active transport of bicarbonate across the ductal epithelium (Sabbatini et al., 2003). Our transcriptome analysis of primary ductal cells is the first to indicate that Npr3 is the most highly expressed natriuretic peptide receptor in this cell type, thus likely accounting for the aforementioned physiologic functions (average normalized expression [RPKM] values of control PDCs: Npr1 0.16; Npr2 0.94; Npr3 2.86).

Identification of paracrine signaling molecules released from acinar cells and determining their relevance to pancreatic function and pathology is an ongoing effort. Proteomic analysis of pancreatic acinar zymogen granules identified 371 proteins, many of which are secreted and/or have unknown function (Rindler et al., 2007). In addition to peptides, an extensive list of other signaling molecules has been described; among these are Ca^{2+} and adenosine-5'-triphosphate (ATP), capable of mediating signals on ductal cells via luminal calcium-sensing G-protein coupled and iono-/metabotropic purinergic receptors, respectively (Hede et al., 1999, Racz et al., 2002). Moreover, Behrendorff and colleagues reported that exaggerated intraluminal acidification caused by proton release from secretory granules of acinar cells in response to supraphysiologic activation directly contributes to pancreatitis via perturbation of tight junctions (Behrendorff et al., 2010). Although the function of intraluminal acinar acidification is not entirely clear at this time,

it may serve as a negative feedback mechanism to prevent acinar hypersecretion by inhibiting acinar cell endocytosis (Freedman et al., 1998); thus, this report highlights a direct link between paracrine mediators and disease pathogenesis. To the best of our knowledge, our study is the first to describe a pathogenic mechanism in the exocrine pancreas implicating a paracrine signaling pathway as the primary defect.

It is important to note that a morphological defect of the ductal tree is not formally excluded in our study, but this possibility is unlikely for several reasons. First, genetic ablation of loci encoding transcription factors, such as *Sox9* or *Hnf6*, that result in morphological phenotypes often manifest in early- or mid-pancreatic development (Pierreux et al., 2006, Seymour et al., 2007). Second, our data indicate that ductal ectasia in *Hhex*-deficient mice occurs only after birth, and thus is coincident with exocrine activation upon feeding. Hezel and colleagues described a similar scenario in which conditional pancreatic ablation of *Lkb1* resulted in apparently normal pancreata at birth (Hezel et al., 2008); however, mice rapidly developed pancreatic inflammation and acinar degeneration only after birth due to defective acinar cell polarity and tight junctions. Likewise, in our study, a phenotype contingent upon paracrine signaling would manifest only after activation of the exocrine system postnatally. Finally, the overall progression of pancreatic pathology we observed is consistent with the primary ductal hypertension model (Yamamoto et al., 2006). Together, these data establish a role for Hhex and highlight the importance of paracrine signaling in maintaining normal pancreatic duct secretion, particularly in neonates.

Although Hhex is crucial for maintenance of exocrine homeostasis in early life, it is dispensable in the mature duct. According to our model, ductal hypersecretion in

Hhex$^{loxP/loxP}$*;Pdx1-Cre*^{Early} mice is sufficient to elevate interstitial pressure to a level that results in PSC activation, yet not in *Hhex*$^{loxP/loxP}$*;Sox9-CreER*^{T2} mice (see Figure 20). It remains unclear why elevated Npr3 levels in the ductal epithelium of *Hhex*$^{loxP/loxP}$*;Sox9-CreER*^{T2} mice do not result in ductal ectasia or fibrosis. We propose at least four possibilities to account for the discrepancy between our genetic models: (1) Newborn animals are fed a diet consisting exclusively of milk, which has a much higher fat content than normal rodent chow. Cholecystokinin levels – and thus acinar paracrine signals – would presumably be increased on a high fat diet, thereby exacerbating Npr3-mediated ductal hypersecretion. (2) The smaller average caliber of the perinatal ductal tree relative to that of the adult mouse may predispose younger mice to the sequelae of hypersecretion. Resistance to flow, and thus pressure, is inversely related to the fourth power of the radius of a tube; therefore, minor increases in the volume of secretion in early life may lead to a more drastic increase in pressure compared to adulthood, and this increase may pass a critical threshold for activation of pancreatic stellate cells. (3) The extracellular matrix of perinatal ducts may not be able to safeguard against increased pressure compared to a mature duct and/or the adult duct is more responsive to adapt to pressure fluctuations by altering extracellular matrix through posttranslational modification (such as collagen crosslinking). More compliant ducts in perinatal mice would become ectatic in response to intraductal hypertension caused by *Hhex* ablation, and this force would be more readily transmitted to the interstitial space, thus resulting in PSC activation. (4) The mature exocrine pancreas, including both acinar and ductal cells, may contain a negative feedback control mechanism lacking in the immature pancreas that is responsive to the volume of secretions. Of course, these possibilities are not

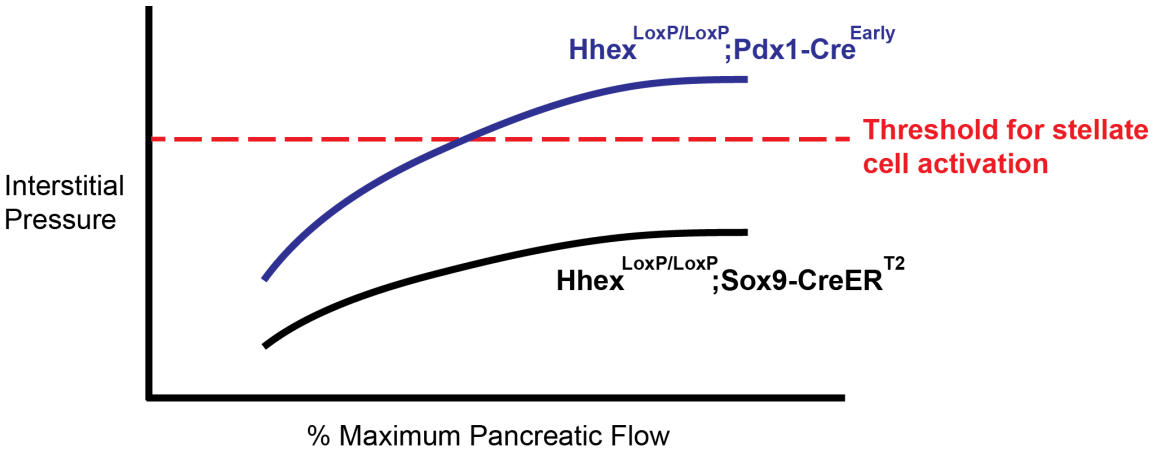

Figure 20. Conceptual model of interstitial pressure as a function of pancreatic flow in the genetic models of this study. Interstitial pressure within pancreata of *Hhex*$^{loxP/loxP}$*;Pdx1-Cre*^{Early} mice crosses a threshold that results in activation of pancreatic stellate cells, consequently leading to periductal fibrosis. Pressure within pancreata of *Hhex*$^{loxP/loxP}$*;Sox9-CreER*^{T2} mice, however, does not cross this threshold; thus, pancreatic homeostasis is preserved.

mutually exclusive, and some or all may contribute to the propagation of ductal ectasia and fibrosis in early life only.

Given the early onset and progressive nature of the phenotype in *Hhex*-ablated pancreata, it is tempting to speculate whether mutations in *HHEX* or other loci that result in ductal hypersecretion are plausible etiologies of hereditary or idiopathic chronic pancreatitis in humans. Often, hereditary chronic pancreatitis (HCP) presents in childhood or adolescence, and a majority of patients with hereditary pancreatitis possess a mutation (or rarely an amplification) in the cationic trypsinogen gene (*PRSS1*) (Applebaum-Shapiro et al., 2001, Rebours et al., 2009, Ceppa et al., 2013). Gain-of-function mutations in PRSS1 lower the threshold for autoactivation of trypsinogen into active trypsin within the pancreas, thus resulting in pancreatitis (Whitcomb et al., 1996). Mutations of PRSS1, however, are found only in 52%-68% of patients with HCP, leaving a large contingent of patients with unexplained etiology (Applebaum-Shapiro et al., 2001, Rebours et al., 2009, Ceppa et al., 2013).

Since the time mutations of the *PRSS1* locus were identified as a cause of HCP, other loci have been implicated as genetic modifiers of both HCP and idiopathic chronic pancreatitis (ICP), most notably those encoding cystic fibrosis transmembrane conductance regulator (*CFTR*), serine protease inhibitor Kazal type 1 (*SPINK1*), and chymotrypsin C (*CTRC*) (Whitcomb et al., 1996, Cohn et al., 1998, Sharer et al., 1998, Pfutzer et al., 2000, Witt et al., 2000, Rosendahl et al., 2008, Schneider et al., 2011). Sequencing analysis has determined 40%-50% of adults with ICP have a mutation in PRSS1, SPINK1, and/or CFTR, and the prevalence is as high as 79% in a pediatric cohort (Keiles and Kammesheidt, 2006, Joergensen et al., 2010, Gasiorowska et al., 2011, Sultan

et al., 2012). This raises the possibility that these risk loci may in fact be causative in some cases of ICP, especially when two or more loci carry mutations. Based on these epidemiological studies and the established role of trypsinogen autoactivation in pancreatitis pathogenesis, it is believed that dysfunction of either ductal secretion or the inhibition of trypsinogen autoactivation predisposes individuals to pancreatitis. These studies employed targeted sequencing of risk loci, precluding the discovery of novel loci; therefore, as genome-wide approaches in HCP and ICP patient cohorts become more commonplace, risk loci related to ductal hypersecretion may indeed be identified.

CHAPTER 4
DISCUSSION & FUTURE DIRECTIONS

The data presented above indicate a novel role for Hhex in the maintenance of the perinatal exocrine pancreas that results in dramatic organ pathology in adulthood, thus providing the field of pancreatic biology with a novel model of chronic pancreatitis. Transcriptome analysis revealed that the G-protein coupled receptor *Npr3* was significantly upregulated upon *Hhex* ablation in primary ductal cells. Follow-up immunostaining analyses supported this finding, evidenced by increased levels of Npr3 specifically in pancreatic ducts of both genetic models of *Hhex* ablation (Figure 18). Previous findings by Sabbatini and colleagues demonstrated that natriuretic peptide signaling is able to enhance the effects of secretin, thereby augmenting pancreatic flow (Sabbatini et al., 2003); further, this synergism is mediated specifically via Npr3. Taken together, elevated Npr3 levels within ductal cells may be a key component of driving pancreatic pathogenesis in $Hhex^{loxP/loxP}$;$Pdx1\text{-}Cre^{Early}$ mice.

Significance of Natriuretic Peptide Signaling in Pancreatic Ductal Cells

To test the conclusion put forth in this dissertation more rigorously, it would be of interest to cross our genetic model of early, conditional *Hhex* ablation with one of several genetic models of altered natriuretic peptide signaling, which include mice with *Npr3* ablation, ANP ablation (*Nppa* locus), or ANP-overexpression driven by the transthyretin promoter (*TTR-ANP*) (Steinhelper et al., 1990, John et al., 1995, Matsukawa et al., 1999).

Unfortunately, no mouse models of conditional *Npr3* or *Nppa* ablation or overexpression are currently in existence. Germline disruption of the *Npr3* locus in mice results in pleiotropic effects, ranging from skeletal deformities to hemodynamic alterations secondary to increased natriuresis, and half die before weaning (Matsukawa et al., 1999); these phenotypes, however, are not observed in $Npr3^{+/-}$ heterozygotes. Generation of $Hhex^{loxP/loxP}$;$Pdx1\text{-}Cre^{Early}$;$Npr3^{+/-}$ or $Hhex^{loxP/loxP}$;$Pdx1\text{-}Cre^{Early}$;$Npr3^{-/-}$ mice will reveal whether Npr3 is required for the pathologic changes observed in pancreata of $Hhex^{loxP/loxP}$;$Pdx1\text{-}Cre^{Early}$ mice, with the former more useful for longterm study and both models for the perinatal period.

As a complementary approach, novel genetic models can be derived by crossing $Hhex^{loxP/loxP}$;$Pdx1\text{-}Cre^{Early}$ mice with *TTR-ANP* or $Nppa^{-/-}$ mice (Steinhelper et al., 1990, John et al., 1995). To date, no pancreatic pathology has been described in either of these ANP models, but it is important to note that the overwhelming majority of reports utilizing these genetic models focus on the cardiovascular and renal effects of altered ANP levels. Therefore, *TTR-ANP* mice may in fact exhibit unappreciated pancreatic pathology. Regardless, I would hypothesize that $Hhex^{loxP/loxP}$;$Pdx1\text{-}Cre^{Early}$;*TTR-ANP* would show an accelerated pancreatic phenotype relative to $Hhex^{loxP/loxP}$;$Pdx1\text{-}Cre^{Early}$ mice. *TTR-ANP* transgenic mice express ANP under the transthyretin promoter, which leads to hepatic secretion of ANP and a 10-fold increase plasma levels (Steinhelper et al., 1990). Given that intravenous infusion of ANP in rats is sufficient for augmenting pancreatic flow in conjunction with secretin via Npr3, the increased level of ANP in plasma would cooperate with the elevated levels of Npr3 in ductal cells, further exacerbating hypersecretion (Sabbatini et al., 2003).

The converse experiment, i.e. the generation of *Hhex*$^{loxP/loxP}$*;Pdx1-Cre*^{Early}*;Nppa*$^{-/-}$ mice, may further support the conclusion that Npr3-mediated hypersecretion is required for pathogenesis in *Hhex*$^{loxP/loxP}$*;Pdx1-Cre*^{Early} mice. It is likely that mice lacking ANP only would not display any significant pancreatic pathology because of redundancy hardwired into the mechanism of acinar-ductal cell crosstalk; other paracrine mediators that signal via Ca^{2+}/PLCβ would be able to compensate for loss of ANP. According to my hypothesis, however, hypersecretion in *Hhex*$^{loxP/loxP}$*;Pdx1-Cre*^{Early} mice is driven by binding of natriuretic peptide ligands to Npr3. Therefore, *Hhex*$^{loxP/loxP}$*;Pdx1-Cre*^{Early}*;Nppa*$^{-/-}$ mice would not display pathology consistent with hypersecretion. An important caveat of this approach, however, is that ANP may not be the sole natriuretic peptide expressed in the pancreas. Although BNP and CNP expression has not been described in the rodent pancreas, Burgess and colleagues reported that CNP is expressed in α-cells of human islets (Burgess et al., 2009).

Will genome-wide methodologies link paracrine signaling to human ductal pathology?

The advent of genome-wide technologies and personalized medicine will undoubtedly continue to unmask unappreciated pathological mechanisms. To date, virtually all studies analyzing risk alleles for acute and chronic pancreatitis have been limited by the use of outdated technologies, such as linkage analysis within specific pedigrees and directed sequencing. Notwithstanding, risk alleles have been identified in *PRSS1*, *CFTR*, *SPINK1*, *CTRC*, and *CASR* (Whitcomb et al., 1996, Masson et al., 2008a, Muddana et al., 2008, Murugaian et al., 2008, Schneider et al., 2011). Furthermore, these

studies have begun to unravel the complexity of the etiology of pancreatitis, as they suggest *CFTR* and *SPINK1* mutations are more consistent with genetic modifiers of risk and that ductal dysfunction in general contributes to autoactivation of trypsinogen (Schneider et al., 2011).

To discover novel risk loci associated with alcohol-related and sporadic chronic pancreatitis, David Whitcomb and colleagues performed a two-stage, multicenter genome wide association study (GWAS) (Whitcomb et al., 2012). In the first stage (discovery stage), 676 patients with chronic pancreatitis (264 alcohol-related, 411 sporadic) were genotyped at 625,739 single nucleotide polymorphisms (SNPs), along with 4,514 controls. SNPs identified at two loci, 7q34 (*PRSS1-PRSS2* locus; cationic and anionic trypsinogen, respectively) and Xq23.3 (*CLDN2* locus; claudin-2), were significantly associated with risk of chronic pancreatitis. In the second stage (replication stage), 331 cases of chronic pancreatitis (70 alcohol-related, 256 sporadic), 579 cases of recurrent acute pancreatitis (113 alcohol-related, 462 sporadic), and 4,170 controls were genotyped, and significant associations with these two loci were validated.

Sequencing the *PRSS1* locus in a cohort of 418 chronic pancreatitis patients, 350 patients with recurrent acute pancreatitis, and 379 control subjects uncovered mutations in only 23 cases, thus implicating an alternative mechanism for the risk association identified. The authors determined that the risk-associated SNP, which resides in the 5' promoter region of *PRSS1*, is associated with higher expression levels of *PRSS1* transcript. This establishes a novel mechanism of increased risk of chronic pancreatitis in humans and corroborates previous studies identifying amplification of the *PRSS1* locus as causative in some patients (Masson et al., 2008b, LaRusch et al., 2012).

This GWAS also identified risk-associated SNPs at the *CLDN2* locus (Whitcomb et al., 2012). Although the study authors were unable to correlate *CLDN2* expression with risk genotype, they determined that moderate-to-strong CLDN2 expression was evident in acinar cells of patients with chronic pancreatitis and high-risk genotype only. The biological significance of this is unclear at this time, but Whitcomb and colleagues propose that it may affect the inflammatory response.

Since the publication of the study described above, other groups have undertaken GWA studies in pancreatitis. Derikx and colleagues replicated the finding of risk-associated SNPs in the *PRSS1-PRSS2* and *CLDN2* loci in a European cohort (Derikx et al., 2014). Two other GWA studies have identified risk-associated SNPs in the loci encoding γ-glutamyltransferase 1 (*GGT1*; OR=1.36, 95% CI 1.03-1.80), fucosyltransferase 2 (*FUT2*; OR=1.53), and the ABO-B blood antigen (*ABO*; OR=1.69), yet a direct contribution to pancreatitis pathogenesis remains to be defined (Brand et al., 2013, Weiss et al., 2014).

The data presented in this dissertation support a model in which mice with pancreatic *Hhex* ablation in pancreatic progenitors exhibit pathology consistent with hypersecretion, ultimately resulting in chronic pancreatitis. Furthermore, hypersecretion is dependent upon paracrine mediators of signaling, mediated by increased Npr3 expression in ductal cells. Ductal hypersecretion, however, has not yet been implicated in pancreatic pathology in humans. Future genome-wide studies, such as GWAS and whole-exome sequencing, may associate loci implicated in paracrine signaling and/or ductal hypersecretion with pancreatitis. It is important to note that although the aforementioned studies did indeed identify SNPs associated with increased risk of pancreatitis, the

relatively small sample sizes (n<1000 patients in each) likely render these studies underpowered. Power of a GWAS, defined by Spencer and colleagues as the probability of at least 1 SNP reaching genome-wide significance, is contingent upon multiple factors, such as relative allele frequency (rare vs. common), sample size, coverage established by choice of genotyping chip, and the magnitude of the effect conferred by the risk allele (Spencer et al., 2009). Extrapolating this definition, it is clear that the same variables listed above will determine whether an association will be uncovered at any given risk-associated SNP (as opposed to the GWAS as a whole). Therefore, despite the small sample size of the GWAS performed by Whitcomb and colleagues (n of approximately 1000), the authors were able to identify risk-associated SNPs because of the common allele frequencies identified at the *PRSS1-PRSS2* and *CLDN2* loci, use of the Illumina 1M genotyping chip (high coverage), and the magnitude of the effect of the risk allele, especially in the case of the SNP associated with increased *PRSS1* expression (Whitcomb et al., 2012). This does not exclude the possibility of the study being underpowered in regards to discovering other disease-associated SNPs, especially if the biological effect associated with the SNP is small. Thus, future GWA studies of pancreatitis will likely require larger sample sizes to determine novel risk-associated loci.

Instead of conducting a large, multicenter GWAS, an alternative approach would be to perform whole exome sequencing on patients with idiopathic or hereditary chronic pancreatitis, particularly if disease manifests at a young age, as this may be suggestive of a genetic defect. Although one group has adopted this methodology for a specific pedigree, they confined their interpretation of sequencing analysis to only those loci already associated with pancreatitis (i.e. *PRSS1*, *CFTR*, *SPINK1*, *CTRC*), as their

intention was to establish whole exome sequencing as a screening approach (LaRusch et al., 2012). Thus, the potential for whole-exome sequencing in this context has not been fully realized. Future whole-exome sequencing studies (or reinterpretation of existing data) may yield mutations in genes involved with regulation of pancreatic ductal secretion. It is worth noting that this approach does not have the capacity to detect specific mutations in intronic or intergenic regulatory regions, and a prospective pipeline to filter both polymorphisms/variants from *bona fide* mutations and disease-causing from incidental mutations would need to be in place.

Does HHEX play a role in pancreatic ductal adenocarcinoma tumorigenesis?

The requirement for the ductal-specific transcription factors Hnf6 and Sox9 in the processes of acinar-to-ductal metaplasia (ADM) and pancreatic ductal adenocarcinoma (PDAC) tumorigenesis has been established previously (Kopp et al., 2012, Prevot et al., 2012). The pattern of Hhex expression is similar to these factors in development and adulthood (see Figure 9), which begs the question whether Hhex affects ADM development and/or PDAC initiation or progression. To formulate a hypothesis regarding the potential role of Hhex in PDAC, Hhex expression was determined within pancreatic intraepithelial neoplasia (PanIN) lesions, readily identified by Alcian Blue positivity, of 6-month-old $Kras^{LSL\text{-}G12D};Pdx1\text{-}Cre^{Early}$ pancreata (Figure 21). The majority of lesions exhibited decreased Hhex expression, especially within Alcian Blue-positive cells (Figure 21B,B',D,D'). Morphologically normal-appearing, cuboidal cells within PanIN lesions

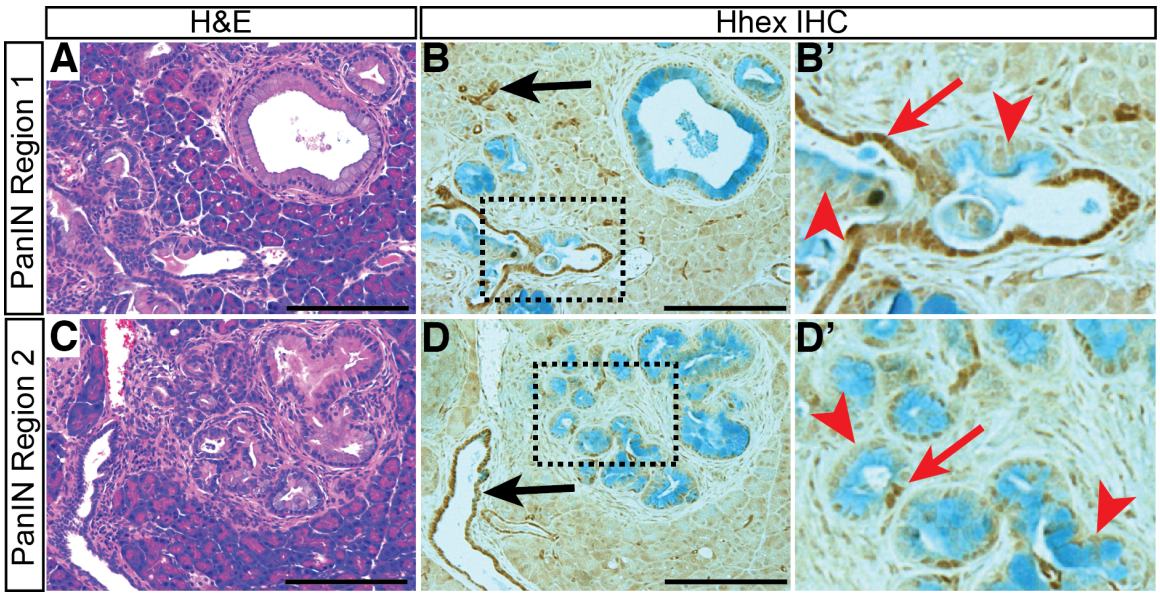

Figure 21. Hhex expression in pancreatic intraepithelial neoplasia. Immunostaining for Hhex in 6-month-old *Kras*$^{LSL\text{-}G12D}$*;Pdx1-Cre*^{Early} pancreata (n=2). Hhex is expressed in morphologically normal ducts within the field, serving as an internal positive control (*black arrows*). Within PanINs, Hhex is typically expressed at a much lower lever in Alcian Blue^{+} cells (*red arrowheads*) compared to morphologically normal-appearing within the same PanIN (*red arrows*). *Scale bars*, 200μm.

often expressed Hhex. These data, although preliminary, support the hypothesis that Hhex expression abrogates oncogenic Kras-driven tumorigenesis, and therefore, its downregulation is a requisite step in transformation. It is unclear at this time whether Hhex expression is upregulated in ADM and subsequently downregulated in transformation or if expression is never activated by metaplastic, transformed acinar cells, akin to Hnf1β (Jensen, 2005 #219)(Prevot, 2012 #41).

Cross-referencing the list of differentially regulated transcripts upon acute *Hhex* ablation in primary ductal cells (Appendix B) with the list generated using pancreata of *Hhex*-ablated mice (Appendix A; experiment performed by Dr. Jia Zhang) yielded Sox9 as one of six gene regulated by Hhex in both contexts (Figure 22). In the latter approach, pregnant dams were injected with tamoxifen at E13.5, and $Hhex^{loxP/loxP}$;$Sox9\text{-}CreER^{T2}$ mutants along with $Hhex^{loxP/loxP}$ littermate controls were dissected at E15.5. RNA-seq analysis was performed using RNA extracted from whole pancreas.

Identifying Sox9 as a possible Hhex target is intriguing because Kopp and colleagues reported that Sox9 is not only upregulated in human PDAC/PanIN tissues, but also plays a pivotal role in the progression to PanIN stages (Kopp, 2012 #26). Using a tamoxifen-inducible *Ptf1aCreER* driver, the authors were able to simultaneously activate expression of oncogenic Kras and ablate *Sox9*; loss of Sox9 significantly retarded the transformation process. Conversely, Sox9 overexpression greatly accelerated the tumorigenic potential of oncogenic Kras, especially in the context of inflammation. Given our comparative transcriptome data, I would hypothesize that Hhex, either directly or indirectly, represses *Sox9* expression. This hypothesis is also supported by the Hhex immunostaining in PanIN tissue – Hhex appears to be downregulated (and thus Sox9

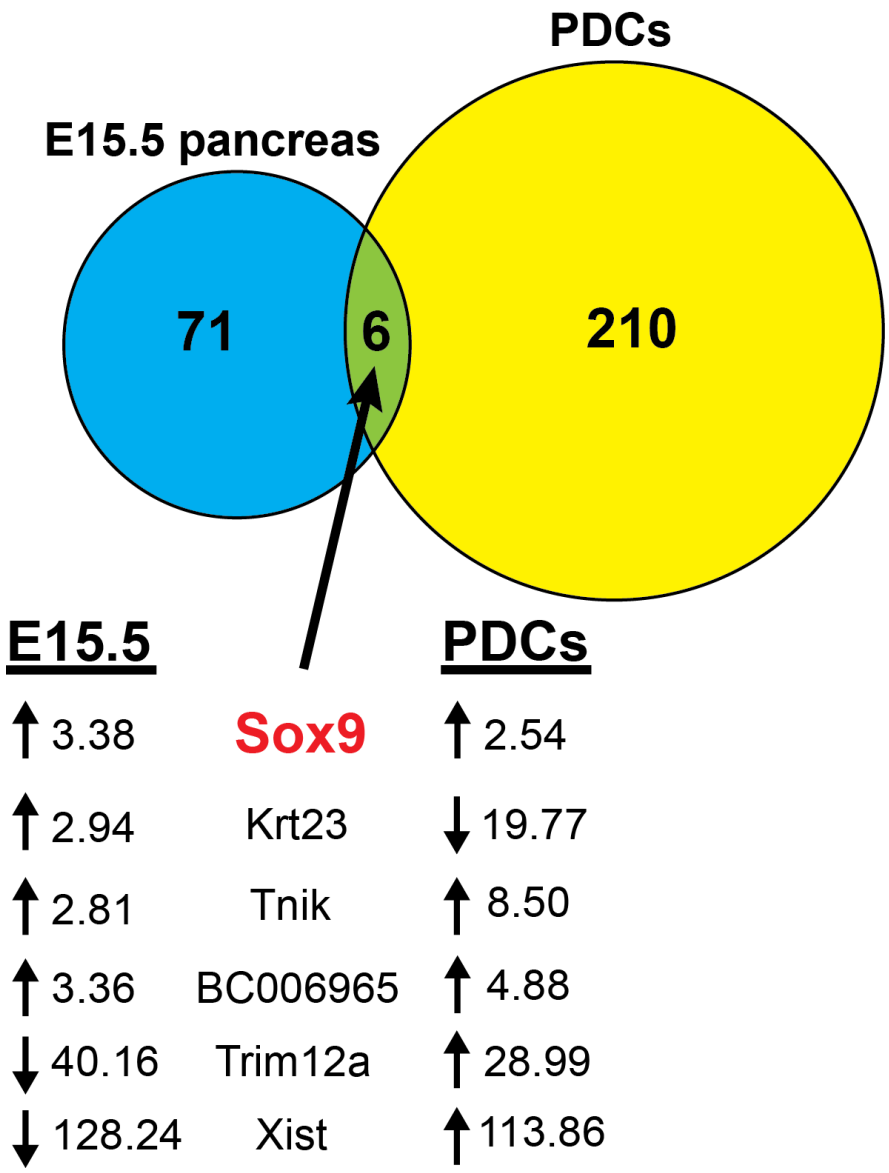

Figure 22. Cross-referencing of differentially expressed gene lists. For embryonic transcriptome analysis (*blue*), pregnant dams were intraperoteneally injected with tamoxifen at E13.5. *Hhex*$^{loxP/loxP}$*;Sox9-CreER*^{T2} mutants and *Hhex*$^{loxP/loxP}$ littermate controls were dissected at E15.5, and whole pancreas was used to construct libraries for RNA-seq. Transcriptome analysis for primary ductal cells (*yellow*) was described in Chapter II. Six genes were found to overlap, and expression fold change (presented as mutant/control) in each study is indicated.

would be upregulated) frequently in transformed, Alcian Blue^{+} cells. When Hhex is present, the ductal cell retains morphology similar to a normal cell.

To further support a possible link between Hhex and regulation of *Sox9*, microarray data available on the NCBI Gene Expression Omnibus comparing 36 PDAC samples to 16 control samples was analyzed for *SOX9* and *HHEX* expression (Figure 23) (Accession GSE16515) (Pei, 2009 #220). In agreement with Kopp and colleagues, *SOX9* expression was significantly upregulated in PDAC (means ± SEM: Control 288 ± 33; PDAC 436 ± 31; *p=0.0055* Student's t-test; *p=0.010* Mann-Whitney rank sum test). *HHEX* expression was reduced by approximately 33% reduction in PDAC samples (means ± SEM: Control 153.1 ± 18.0; PDAC 103.7 ± 12.7; *p=0.033* Student's t-test; *p=0.004* Mann-Whitney rank sum test). Thus, downregulation of *HHEX* expression in PDAC is conserved between mice and humans.

Generation of genetic mouse models of PDAC with simultaneous ablation of *Hhex* will provide much stronger evidence whether loss of *Hhex* plays a role in tumorigenesis. If Hhex is indeed a repressor of the Sox9 locus, with which the data presented above are consistent, *Hhex* ablation with oncogenic Kras should accelerate transformation. Therefore, the most appropriate model would be similar to that used by Kopp and colleagues, as the risk of a ceiling effect would be low in *Kras$^{LSL\text{-}G12D}$; Ptf1aCreER* mice induced at P10 (Kopp, 2012 #26).

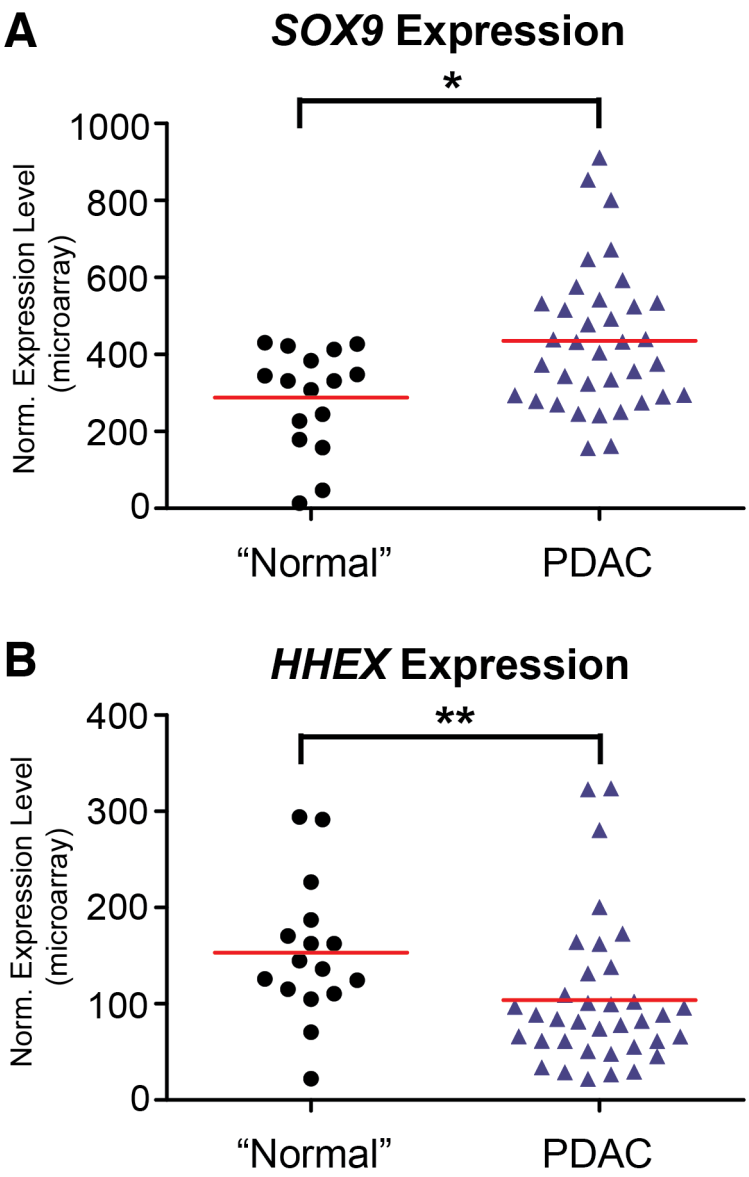

Figure 23. Microarray data for *SOX9* and *HHEX* expression in PDAC. (A) *SOX9* expression mean ± SEM: Control 288 ± 33; PDAC 436 ± 31; *p=0.0055* Student's t-test; *p=0.010* Mann-Whitney rank sum test. (B) *HHEX* expression mean ± SEM: Control 153.1 ± 18.0; PDAC 103.7 ± 12.7; *p=0.033* Student's t-test; *p=0.004* Mann-Whitney rank sum test. *Red bar*, mean of group. *$p<0.05$, **$p<0.01$, Mann-Whitney rank sum test.

APPENDIX A

Complete list of transcripts that are differentially expressed (FDR<0.1) between *Hhex*$^{loxP/loxP}$;*Sox9-CreER*^{T2} mutants and *Hhex*$^{loxP/loxP}$ littermate controls at E15.5. Embryos were induced with tamoxifen at E13.5. Fold change is reported as mutant/control, and genes are arranged in descending order of fold change.

Gene	Accession No.	Fold Change	p-value
Ftl1	NM_010240	75.59928556	1.9111E-205
Klk14	NM_174866	8.284418837	9.18144E-16
Klk13	NM_001039042	8.06429634	1.28545E-15
Klk4	NM_019928	6.863427483	0.000252443
Rpl21	NM_019647	6.37631659	5.33878E-09
Lect1	NM_010701	6.104465348	3.90852E-06
Tceal7	NM_001127169	5.215138061	0.000280228
Hfe2	NM_027126	5.193066875	0.00018541
Mylpf	NM_016754	5.091792659	5.53742E-05
Actc1	NM_009608	4.656159253	5.48011E-05
Col9a1	NM_007740	4.52537673	4.02882E-19
Gm6878	NM_001037931	4.358513907	0.000384405
Tnnc2	NM_009394	4.264769002	0.000345148
Klk10	NM_133712	4.207549011	2.92192E-09
Cym	NM_001111143	3.89855934	0.000141622
Tnnc1	NM_009393	3.819691725	0.000249675
Selenbp2	NM_019414	3.622208236	1.14078E-06
BC021891	NM_145608	3.604033071	4.62849E-06
Sox9	NM_011448	3.377209885	3.11694E-09
BC006965	NR_024085	3.357631535	2.44794E-13
Crp	NM_007768	3.246991565	6.2271E-12
D430050G20	NR_030701	3.184515136	3.72985E-05
AU015836	NR_028320	3.012340036	7.59084E-07
Tulp2	NM_001045555	2.993409147	2.22069E-07
Krt23	NM_033373	2.940875001	0.000254286
Tnik	NM_001163007	2.812046857	2.16166E-23
Col9a3	NM_009936	2.696374536	5.90294E-06
Ush1c	NM_001163733	2.563273085	3.15631E-05
Abcc8	NM_011510	2.530043589	4.6827E-06
BC021767	NR_033629	2.508824392	0.000379671

Sgpp2	NM_001004173	2.372834638	2.65087E-05
Trpc5	NM_009428	2.309615976	0.000164115
Gja6	NM_001001496	2.250659756	0.000270459
Gria1	NM_008165	2.154934321	3.51466E-05
Vnn1	NM_011704	2.138235567	3.65714E-07
Fxyd3	NM_008557	2.124795427	6.14794E-07
Abcc9	NM_021041	2.004505291	0.000109908
Rpl26	NM_009080	1.999766296	9.99903E-15
Gm15772	NR_003373	1.999766296	9.98262E-15
Col2a1	NM_031163	1.991689467	3.64699E-05
Dsg2	NM_007883	1.88572836	6.76144E-07
Zfp174	NM_001081217	1.846452283	4.73639E-05
Plekhb1	NM_001163183	1.819698834	3.90887E-05
Ugt8a	NM_011674	1.81228496	5.57514E-05
Pamr1	NM_173749	1.793158914	7.35084E-06
Dcx	NM_001110222	1.720396486	1.08778E-05
Klk8	NM_008940	1.679646252	0.000202641
Zfp597	NM_001033159	1.625057028	3.40212E-06
Ap4b1	NM_026193	1.553062449	3.19765E-06
Dclre1b	NM_133865	1.542462163	7.16863E-05
Spp1	NM_001204201	1.487129958	0.000307208
Epha7	NM_010141	1.466554401	0.000171411
Zim1	NM_011769	1.445699123	9.80974E-05
Plvap	NM_032398	-1.492659046	0.000156116
Madcam1	NM_013591	-1.493979413	0.000310552
Uvrag	NM_178635	-1.516259972	0.000311652
Slc40a1	NM_016917	-1.571256072	0.000159451
Lor	NM_008508	-1.617114385	0.000351805
Kazald1	NM_178929	-1.690212957	0.000258058
Tlx1	NM_021901	-1.736700434	0.000281177
Cldn5	NM_013805	-1.791219371	1.46674E-05
Ctsk	NM_007802	-1.793833398	0.000341905
Frzb	NM_011356	-1.84325909	0.000194188
Sox18	NM_009236	-1.843279274	0.00013648
Bcat1	NM_007532	-1.871656117	2.23345E-05
Myo7a	NM_008663	-2.26132133	8.47319E-05
Arntl2	NM_172309	-2.445814573	7.96026E-05
Gm3716	NR_045078	-2.802293489	7.47332E-06
A730046J19Rik	NR_040271	-3.038943425	4.25033E-05
Xlr4b	NM_021365	-3.816092478	2.44471E-05

Gm5801	NR_002889	-5.272262709	2.55208E-06
Ltf	NM_008522	-6.090648756	0.0002431
Lcn2	NM_008491	-7.231854796	6.22849E-05
Ngp	NM_008694	-8.41338379	0.000188328
Trim12a	NM_023835	-40.15613919	6.39692E-10
Tsix	NR_002844	-108.9912947	9.55998E-08
Xist	NR_001463	-128.2366506	1.14965E-06

APPENDIX B

Complete list of transcripts that are differentially expressed (FDR<0.1) between primary ductal cells (PDCs) isolated from uninduced adult *Hhex*$^{loxP/loxP}$;*Sox9-CreER*^{T2} and *Hhex*$^{loxP/loxP}$ mice. PDCs were induced with 4-hydroxytamoxifen *ex vivo* for 96 hours. Fold change is reported as mutant/control, and genes are arranged in descending order of fold change.

Gene	Accession No.	Fold Change	p-value
Xist	NR_001463	113.8569223	1.88791E-05
Trim12a	NM_023835	28.99393636	0.000585421
2210010C17Rik	NM_027308	27.23863707	2.61372E-05
Fam5c	NM_153539	17.75627125	1.15794E-21
Zscan4c	NM_001013765	16.07600509	0.000539122
Aqp5	NM_009701	14.25533873	0.000940888
Igfbp2	NM_008342	13.14170074	1.79755E-07
Vmn2r29	NR_003555	9.663032422	0.000435133
Lox	NM_010728	8.650634913	6.08513E-11
Tnik	NM_001163007	8.497121341	1.9864E-18
Rpl29	NM_009082	8.452552601	0.000269195
Col11a1	NM_007729	8.03939368	6.40295E-05
Scnn1g	NM_011326	7.568274204	9.99869E-10
Elmod1	NM_177769	7.260224317	0.00066971
Gldc	NM_138595	6.313325304	4.99535E-05
Scel	NM_022886	6.205373914	3.24611E-14
Bex4	NM_212457	6.147270805	1.82339E-05
Upk1b	NM_178924	5.731144883	9.27091E-06
Cpxm2	NM_018867	5.657575142	2.88642E-06
Cpvl	NM_027749	5.646693018	0.000181535
Cd109	NM_153098	5.594273651	1.84806E-05
Gm13109	NM_001126315	5.228339195	3.28831E-05
D730005E14Rik	NR_030675	5.057699965	0.000896308
4930503E14Rik	NM_029131	4.924027423	8.77231E-05
BC006965	NR_024085	4.88152449	0.000104394
Npr3	NM_001039181	4.696058437	8.16798E-06
Cd200	NM_010818	4.604156325	2.65681E-08
Gm5039	NR_003647	4.511213096	0.00010993
Rasl12	NM_001033158	4.424043145	0.000968148

Wfdc3	NM_027961	4.398442922	0.000393976
Sod3	NM_011435	4.240812166	3.16354E-07
Tmem117	NM_178789	4.150220939	0.000485233
Dclk1	NM_001111053	4.117983949	1.19759E-09
Itm2a	NM_008409	4.08462762	0.000382634
Klra18	NM_053153	3.902491086	8.86461E-14
Tram1l1	NM_146140	3.893812218	0.000397161
Pcsk9	NM_153565	3.877142927	7.62558E-05
Klra15	NM_013793	3.875541525	4.74596E-13
Klra12	NM_010646	3.813255825	2.47265E-14
Klra33	NM_001039118	3.813101307	3.4394E-13
Klra4	NM_010649	3.809714985	3.488E-13
Klra22	NM_053152	3.737284258	3.98042E-11
Sult1a1	NM_133670	3.663784588	3.60643E-12
Slc25a48	NM_177809	3.637659711	3.24684E-05
Akr1e1	NM_018859	3.613855541	0.000137783
Lass3	NM_001164201	3.519636493	7.28187E-11
Wisp1	NM_018865	3.475386242	6.18108E-05
Klra23	NM_024470	3.468977304	9.26798E-07
Klra13-ps	NR_033451	3.468977284	9.25965E-07
Tlr3	NM_126166	3.410129347	2.87588E-11
Efemp1	NM_146015	3.286879928	2.58189E-05
Porcn	NM_023638	3.268430001	1.42132E-11
1700016C15Rik	NM_027077	3.244302319	6.03102E-05
Htra1	NM_019564	3.129039556	3.75257E-08
Emp1	NM_010128	3.060372772	9.19125E-08
Slc16a12	NM_172838	3.053842136	8.84934E-05
Cited4	NM_019563	3.038069853	0.000425535
Sema3c	NM_013657	2.946023181	1.74825E-10
Colec12	NM_130449	2.88788971	0.000664521
Vim	NM_011701	2.77559648	5.07587E-07
Aldh1a1	NM_013467	2.767933422	7.21287E-06
Ehd2	NM_153068	2.715109821	7.33776E-06
Serpinb9b	NM_011452	2.678921671	0.000372921
Gcnt3	NM_028087	2.670187724	4.84315E-07
Cnr1	NM_007726	2.660483838	0.000550771
Anxa8	NM_013473	2.637154718	0.000495789
Igfbp4	NM_010517	2.631658401	0.000930292
Pgcp	NM_018755	2.626958886	1.8324E-05
Nid1	NM_010917	2.622074048	2.26411E-06

Lrrk2	NM_025730	2.610954118	0.000105067
Mtap2	NM_001039934	2.597206815	2.37294E-06
Eya4	NM_010167	2.579702834	6.41217E-06
Gsta3	NM_001077353	2.57126931	0.000709483
D830031N03Rik	NM_001167918	2.566728929	8.82604E-08
Pdgfc	NM_019971	2.551954748	0.000713833
Sox9	NM_011448	2.539148371	1.60444E-07
Fam190a	NM_001164316	2.528370955	0.000503216
Gm15441	NR_040409	2.511604021	1.59479E-06
Dclk3	NM_172928	2.426277156	0.000830892
Gclc	NM_010295	2.392556942	1.93662E-05
2310007B03Rik	NM_001159940	2.38915615	2.10957E-06
Txnip	NM_001009935	2.387666986	3.3732E-06
Mmp7	NM_010810	2.381091149	0.000352058
Ablim1	NM_178688	2.379903302	0.000130581
Scnn1a	NM_011324	2.374471295	1.46151E-06
S100a14	NM_001163525	2.367345796	0.000150423
Epn3	NM_027984	2.291867109	2.43044E-06
Ugt1a6a	NM_145079	2.287234571	1.19699E-05
Ugt1a7c	NM_201642	2.277793101	4.20198E-06
Suox	NM_173733	2.275497715	1.11769E-05
Gcnt1	NM_001136484	2.272780983	0.000395199
Tcp11l2	NM_146008	2.267043824	0.000407896
Ugt1a5	NM_201643	2.266903707	2.23152E-05
Ugt1a10	NM_201641	2.255762294	2.47542E-05
Ugt1a9	NM_201644	2.254442365	2.54043E-05
Ugt1a6b	NM_201410	2.243111468	2.58197E-05
Mbnl3	NM_134163	2.235951968	0.000846753
Bcar3	NM_013867	2.234435039	1.25556E-05
Ppl	NM_008909	2.230216737	0.0002782
Stard13	NM_001163493	2.212668683	2.18174E-06
Nbeal2	NM_183276	2.211010915	0.00039017
Prss23	NM_029614	2.206208206	2.57738E-05
Ugt1a2	NM_013701	2.200801092	4.45302E-05
Timp3	NM_011595	2.193765956	8.51052E-06
Slc43a3	NM_021398	2.186854949	0.000163081
Msln	NM_018857	2.181897735	1.7621E-05
Il33	NM_001164724	2.166889387	0.000395121
Abcb1b	NM_011075	2.157641855	3.27902E-06
Oat	NM_016978	2.157398692	8.75559E-06

B4galt4	NM_019804	2.126945355	3.7172E-05
Fam126a	NM_053090	2.125136289	0.000165107
Id2	NM_010496	2.119951952	0.000199284
Klhl13	NM_026167	2.08299522	2.61023E-05
Bst1	NM_009763	2.08249731	0.000302286
Ugt1a1	NM_201645	2.081794637	9.05854E-05
Arhgef26	NM_001081295	2.079454967	0.000591259
Ppat	NM_172146	2.07529945	4.18986E-05
Tmem37	NM_019432	2.069859828	0.000562666
Pak3	NM_001195049	2.069365686	1.19952E-05
Cd55	NM_010016	2.055377094	2.24991E-05
Sorl1	NM_011436	2.053841023	0.000618999
Paics	NM_025939	2.048193438	1.70378E-05
Tinagl1	NM_023476	2.040413451	1.12028E-05
Sema3e	NM_011348	2.019451132	5.01697E-05
Cryab	NM_009964	2.007477278	0.00016055
Ahnak	NM_009643	2.004640581	7.73349E-05
Pgap2	NM_145583	2.004265662	0.000320059
Serpinb8	NM_011459	1.972325639	9.74217E-05
Degs1	NM_007853	1.969117819	2.09099E-05
Vgll3	NM_028572	1.92647075	0.000629339
Ccnd1	NM_007631	1.912476505	4.22123E-05
2310016C08Rik	NM_023516	1.910008097	7.6811E-05
Sdc2	NM_008304	1.876646006	0.000619109
Plau	NM_008873	1.867437185	0.000295546
Epdr1	NM_134065	1.858274776	0.000252883
Gja1	NM_010288	1.852530587	0.000759776
Fam188a	NM_024185	1.850939123	0.000295533
Wnt7b	NM_009528	1.848941718	0.000137193
Iqgap2	NM_027711	1.844627583	0.000167023
Ptgs1	NM_008969	1.840517843	0.000971355
Anxa2	NM_007585	1.836270041	0.000367673
Macf1	NM_001199136	1.832578522	0.000281026
Usp46	NM_177561	1.825001318	0.000343264
Abcc5	NM_013790	1.823849088	0.000449644
S100a6	NM_011313	1.813917034	0.000944117
Klf10	NM_013692	1.804904031	0.00061197
Jam2	NM_023844	1.795644928	0.000648211
Cd97	NM_011925	1.774027332	0.00082041
Wnk1	NM_001199084	1.76422851	0.000624881

Prrg4	NM_178695	1.753444391	0.000519547
Adk	NM_001243041	1.743100892	0.000643887
Zbtb38	NM_175537	1.733748746	0.000756178
5730469M10Rik	NM_027464	-1.710962167	0.000801002
Gsta4	NM_010357	-1.776113564	0.000915488
Odc1	NM_013614	-1.817902788	0.000140961
Cotl1	NM_028071	-1.851395881	0.000636137
Rabgap1l	NM_001038621	-1.867787846	0.000237604
Gpc2	NM_172412	-1.890427225	0.00064813
8430408G22Rik	NM_145980	-1.916054146	0.000680987
Syne1	NM_001079686	-1.992705388	0.000335079
Ecscr	NM_001033141	-2.006850667	0.000112998
Rgs16	NM_011267	-2.07238794	0.00012927
Rgs2	NM_009061	-2.079206807	7.00253E-05
Tnc	NM_011607	-2.194425504	1.25895E-06
Plat	NM_008872	-2.207901804	0.000801777
Hspb8	NM_030704	-2.279976383	0.000119612
Ccdc3	NM_028804	-2.315081591	2.76834E-06
Gdf15	NM_011819	-2.427779742	0.000418609
Atp6v1c2	NM_001159632	-2.463395309	0.000472462
Fstl1	NM_008047	-2.471208687	1.73705E-05
Neurl3	NM_153408	-2.488207387	8.4488E-05
Dok2	NM_010071	-2.503898654	5.48134E-05
6430598A04Rik	NM_175521	-2.545082265	0.000880863
Ifitm3	NM_025378	-2.702530263	1.85074E-06
Nradd	NM_026012	-2.794774695	9.61222E-06
Il23a	NM_031252	-2.851205011	1.70934E-07
Slc22a4	NM_019687	-2.91866048	1.26141E-06
Sparc	NM_009242	-2.992795186	9.93959E-06
Mx1	NM_010846	-2.999675859	0.000789926
Rbp1	NM_011254	-3.051561507	0.00012886
Fam167a	NM_177628	-3.07007693	8.45069E-06
Gbp9	NM_172777	-3.089477598	1.73212E-10
Tm4sf4	NM_145539	-3.098900297	1.23751E-10
Uts2d	NM_198166	-3.190574557	0.000180002
Mxra8	NM_024263	-3.450673252	0.000250912
Efhd1	NM_028889	-3.479373112	9.25462E-05
Gpr161	NM_001081126	-3.659659811	2.79281E-08
Slfn2	NM_011408	-3.67862078	1.12919E-10
Anks4b	NM_028085	-3.755520681	0.000689102

Thsd1	NM_019576	-3.928442011	2.10853E-05
AI507597	NR_033566	-3.978987473	1.15608E-06
Slc28a3	NM_022317	-4.077627775	6.49863E-06
Slc16a3	NM_001038653	-4.222835956	4.41054E-07
Nes	NM_016701	-4.286025403	1.70643E-07
Tmem82	NM_145987	-4.364057391	2.67834E-07
Il11	NM_008350	-4.36438257	1.18854E-05
Cacna1h	NM_001163691	-4.39414167	0.000213543
Tmem35	NM_026239	-4.451600972	7.25674E-07
Muc1	NM_013605	-4.464156929	1.74634E-05
Themis	NM_178666	-4.485153825	5.586E-05
Akr1c12	NM_013777	-4.59155662	0.000123524
Tmprss11a	NM_001033233	-4.604022541	8.66881E-05
Gbp8	NM_029509	-4.631712318	5.26104E-09
Bdkrb2	NM_009747	-4.822841048	2.50198E-05
Mtus2	NM_029920	-4.960890639	9.51203E-05
Akr1c13	NM_013778	-5.218830777	4.8859E-08
Xkrx	NM_183319	-5.299581132	9.36659E-05
Oas1g	NM_011852	-5.3042016	4.77174E-05
Sp5	NM_022435	-6.032262723	0.000209367
Steap4	NM_054098	-6.388779551	6.17834E-08
AW112010	NM_001177351	-6.465777303	0.000819386
Tm4sf1	NM_008536	-8.361470907	6.1516E-31
Krt17	NM_010663	-8.986343002	2.27082E-09
3830403N18Rik	NM_027510	-11.61855443	4.19061E-06
Tfpi	NM_001177319	-14.24461953	1.83669E-44
Krt23	NM_033373	-19.77163187	1.15434E-15

BIBLIOGRAPHY

Abuladze N, Lee I, Newman D, Hwang J, Boorer K, Pushkin A, Kurtz I (1998) Molecular cloning, chromosomal localization, tissue distribution, and functional expression of the human pancreatic sodium bicarbonate cotransporter. The Journal of biological chemistry 273:17689-17695.

Afelik S, Chen Y, Pieler T (2006) Combined ectopic expression of Pdx1 and Ptf1a/p48 results in the stable conversion of posterior endoderm into endocrine and exocrine pancreatic tissue. Genes & development 20:1441-1446.

Anderson MP, Berger HA, Rich DP, Gregory RJ, Smith AE, Welsh MJ (1991) Nucleoside triphosphates are required to open the CFTR chloride channel. Cell 67:775-784.

Anderson MP, Welsh MJ (1992) Regulation by ATP and ADP of CFTR chloride channels that contain mutant nucleotide-binding domains. Science 257:1701-1704.

Andoh A, Takaya H, Saotome T, Shimada M, Hata K, Araki Y, Nakamura F, Shintani Y, Fujiyama Y, Bamba T (2000) Cytokine regulation of chemokine (IL-8, MCP-1, and RANTES) gene expression in human pancreatic periacinar myofibroblasts. Gastroenterology 119:211-219.

Apelqvist A, Ahlgren U, Edlund H (1997) Sonic hedgehog directs specialised mesoderm differentiation in the intestine and pancreas. Current biology : CB 7:801-804.

Apelqvist A, Li H, Sommer L, Beatus P, Anderson DJ, Honjo T, Hrabe de Angelis M, Lendahl U, Edlund H (1999) Notch signalling controls pancreatic cell differentiation. Nature 400:877-881.

Applebaum-Shapiro SE, Finch R, Pfutzer RH, Hepp LA, Gates L, Amann S, Martin S, Ulrich CD, 2nd, Whitcomb DC (2001) Hereditary pancreatitis in North America: the Pittsburgh-Midwest Multi-Center Pancreatic Study Group Study. Pancreatology : official journal of the International Association of Pancreatology 1:439-443.

Asaumi H, Watanabe S, Taguchi M, Tashiro M, Otsuki M (2007) Externally applied pressure activates pancreatic stellate cells through the generation of intracellular reactive oxygen species. American journal of physiology Gastrointestinal and liver physiology 293:G972-978.

Ashton N, Argent BE, Green R (1990) Effect of vasoactive intestinal peptide, bombesin and substance P on fluid secretion by isolated rat pancreatic ducts. The Journal of physiology 427:471-482.

Ashton N, Argent BE, Green R (1991) Characteristics of fluid secretion from isolated rat pancreatic ducts stimulated with secretin and bombesin. The Journal of physiology 435:533-546.

Ashton N, Evans RL, Elliott AC, Green R, Argent BE (1993) Regulation of fluid secretion and intracellular messengers in isolated rat pancreatic ducts by acetylcholine. The Journal of physiology 471:549-562.

Bayliss WM, Starling EH (1902) The mechanism of pancreatic secretion. The Journal of physiology 28:325-353.

Bedford FK, Ashworth A, Enver T, Wiedemann LM (1993) HEX: a novel homeobox gene expressed during haematopoiesis and conserved between mouse and human. Nucleic acids research 21:1245-1249.

Behrendorff N, Floetenmeyer M, Schwiening C, Thorn P (2010) Protons released during pancreatic acinar cell secretion acidify the lumen and contribute to pancreatitis in mice. Gastroenterology 139:1711-1720, 1720 e1711-1715.

Bhushan A, Itoh N, Kato S, Thiery JP, Czernichow P, Bellusci S, Scharfmann R (2001) Fgf10 is essential for maintaining the proliferative capacity of epithelial progenitor cells during early pancreatic organogenesis. Development 128:5109-5117.

Bogue CW, Ganea GR, Sturm E, Ianucci R, Jacobs HC (2000) Hex expression suggests a role in the development and function of organs derived from foregut endoderm. Developmental dynamics : an official publication of the American Association of Anatomists 219:84-89.

Bohn S, Thomas H, Turan G, Ellard S, Bingham C, Hattersley AT, Ryffel GU (2003) Distinct molecular and morphogenetic properties of mutations in the human HNF1beta gene that lead to defective kidney development. Journal of the American Society of Nephrology : JASN 14:2033-2041.

Bort R, Martinez-Barbera JP, Beddington RS, Zaret KS (2004) Hex homeobox gene-dependent tissue positioning is required for organogenesis of the ventral pancreas. Development 131:797-806.

Bort R, Signore M, Tremblay K, Martinez Barbera JP, Zaret KS (2006) Hex homeobox gene controls the transition of the endoderm to a pseudostratified, cell emergent epithelium for liver bud development. Developmental biology 290:44-56.

Brand H, Diergaarde B, O'Connell MR, Whitcomb DC, Brand RE (2013) Variation in the gamma-glutamyltransferase 1 gene and risk of chronic pancreatitis. Pancreas 42:836-840.

Brenner BM, Ballermann BJ, Gunning ME, Zeidel ML (1990) Diverse biological actions of atrial natriuretic peptide. Physiological reviews 70:665-699.

Burgess MD, Moore KD, Carter GM, Alli AA, Granda CS, Ichii H, Ricordi C, Gower WR, Jr. (2009) C-type natriuretic peptide receptor expression in pancreatic alpha cells. Histochemistry and cell biology 132:95-103.

Burghardt B, Elkaer ML, Kwon TH, Racz GZ, Varga G, Steward MC, Nielsen S (2003) Distribution of aquaporin water channels AQP1 and AQP5 in the ductal system of the human pancreas. Gut 52:1008-1016.

Burlison JS, Long Q, Fujitani Y, Wright CV, Magnuson MA (2008) Pdx-1 and Ptf1a concurrently determine fate specification of pancreatic multipotent progenitor cells. Developmental biology 316:74-86.

Cano DA, Murcia NS, Pazour GJ, Hebrok M (2004) Orpk mouse model of polycystic kidney disease reveals essential role of primary cilia in pancreatic tissue organization. Development 131:3457-3467.

Cano DA, Sekine S, Hebrok M (2006) Primary cilia deletion in pancreatic epithelial cells results in cyst formation and pancreatitis. Gastroenterology 131:1856-1869.

Ceppa EP, Pitt HA, Hunter JL, Leys CM, Zyromski NJ, Rescorla FJ, Sandrasegaran K, Fogel EL, McHenry LW, Watkins JL, Sherman S, Lehman GA (2013) Hereditary pancreatitis: endoscopic and surgical management. Journal of gastrointestinal surgery : official journal of the Society for Surgery of the Alimentary Tract 17:847-856; discussion 856-847.

Chabot JG, Morel G, Belles-Isles M, Jeandel L, Heisler S (1988) ANF and exocrine pancreas: ultrastructural autoradiographic localization in acinar cells. The American journal of physiology 254:E301-309.

Chabot JG, Morel G, Kopelman H, Belles-Isles M, Heisler S (1987) Atrial natriuretic factor and exocrine pancreas: autoradiographic localization of binding sites and ultrastructural evidence for internalization of endogenous ANF. Pancreas 2:404-413.

Chen G, Courey AJ (2000) Groucho/TLE family proteins and transcriptional repression. Gene 249:1-16.

Cockell M, Stevenson BJ, Strubin M, Hagenbuchle O, Wellauer PK (1989) Identification of a cell-specific DNA-binding activity that interacts with a transcriptional activator of genes expressed in the acinar pancreas. Molecular and cellular biology 9:2464-2476.

Coffinier C, Barra J, Babinet C, Yaniv M (1999) Expression of the vHNF1/HNF1beta homeoprotein gene during mouse organogenesis. Mechanisms of development 89:211-213.

Cohn JA, Friedman KJ, Noone PG, Knowles MR, Silverman LM, Jowell PS (1998) Relation between mutations of the cystic fibrosis gene and idiopathic pancreatitis. The New England journal of medicine 339:653-658.

Cong R, Jiang X, Wilson CM, Hunter MP, Vasavada H, Bogue CW (2006) Hhex is a direct repressor of endothelial cell-specific molecule 1 (ESM-1). Biochemical and biophysical research communications 346:535-545.

Crompton MR, Bartlett TJ, MacGregor AD, Manfioletti G, Buratti E, Giancotti V, Goodwin GH (1992) Identification of a novel vertebrate homeobox gene expressed in haematopoietic cells. Nucleic acids research 20:5661-5667.

de Bold AJ, Bruneau BG, Kuroski de Bold ML (1996) Mechanical and neuroendocrine regulation of the endocrine heart. Cardiovascular research 31:7-18.

Denson LA, Karpen SJ, Bogue CW, Jacobs HC (2000) Divergent homeobox gene hex regulates promoter of the Na(+)-dependent bile acid cotransporter. American journal of physiology Gastrointestinal and liver physiology 279:G347-355.

Derikx MH, Kovacs P, Scholz M, Masson E, Chen JM, Ruffert C, Lichtner P, Te Morsche RH, Cavestro GM, Algul H, Berg T, Bodeker H, Bluher M, Bruno MJ, Buch S, Bugert P, Cichoz-Lach H, Dabrowski A, Farre A, Frank J, Gasiorowska A, Geisz A, Goni E, Grothaus J, Grutzmann R, Haas S, Hampe J, Hellerbrand C, Hegyi P, Huster D, Ioana M, Iordache S, Jurkowska G, Keim V, Landt O, Di Leo M, Lerch MM, Levy P, Lohr MJ, Macek M, Malats N, Malecka-Panas E, Mariani A, Martorana D, Mayerle J, Mora J, Mossner J, Muller S, Ockenga J, Paderova J, Pedrazzoli S, Pereira SP, Pfutzer R, Real FX, Rebours V, Ridinger M, Rietschel M, Rohde K, Sack S, Saftoiu A, Schneider A, Schulz HU, Soyka M, Simon P, Skipworth J, Stickel F, Stumvoll M, Testoni PA, Tonjes A, Treiber M, Weiss FU, Werner J, Wodarz N, Ferec C, Drenth JP, Witt H, Rosendahl J (2014) Polymorphisms at PRSS1-PRSS2 and CLDN2-MORC4 loci associate with alcoholic and non-alcoholic chronic pancreatitis in a European replication study. Gut.

Deschamps J, van den Akker E, Forlani S, De Graaff W, Oosterveen T, Roelen B, Roelfsema J (1999) Initiation, establishment and maintenance of Hox gene expression patterns in the mouse. The International journal of developmental biology 43:635-650.

Deutsch G, Jung J, Zheng M, Lora J, Zaret KS (2001) A bipotential precursor population for pancreas and liver within the embryonic endoderm. Development 128:871-881.

Dubois CL, Shih HP, Seymour PA, Patel NA, Behrmann JM, Ngo V, Sander M (2011) Sox9-haploinsufficiency causes glucose intolerance in mice. PloS one 6:e23131.

Ferec C, Cutting GR (2012) Assessing the Disease-Liability of Mutations in CFTR. Cold Spring Harbor perspectives in medicine 2:a009480.

Folsch UR, Fischer H, Soling HD, Creutzfeldt W (1980) Effects of gastrointestinal hormones and carbamylcholine on cAMP accumulation in isolated pancreatic duct fragments from the rat. Digestion 20:277-292.

Freedman SD, Kern HF, Scheele GA (1998) Cleavage of GPI-anchored proteins from the plasma membrane activates apical endocytosis in pancreatic acinar cells. European journal of cell biology 75:163-173.

Freedman SD, Scheele GA (1993) Regulated secretory proteins in the exocrine pancreas aggregate under conditions that mimic the trans-Golgi network. Biochemical and biophysical research communications 197:992-999.

Fry AM, Leaper MJ, Bayliss R (2014) The primary cilium: guardian of organ development and homeostasis. Organogenesis 10:62-68.

Gao N, White P, Kaestner KH (2009) Establishment of intestinal identity and epithelial-mesenchymal signaling by Cdx2. Developmental cell 16:588-599.

Gasiorowska A, Talar-Wojnarowska R, Czupryniak L, Smolarz B, Romanowicz-Makowska H, Kulig A, Malecka-Panas E (2011) The prevalence of cationic trypsinogen (PRSS1) and serine protease inhibitor, Kazal type 1 (SPINK1) gene mutations in Polish patients with alcoholic and idiopathic chronic pancreatitis. Digestive diseases and sciences 56:894-901.

Georgia S, Soliz R, Li M, Zhang P, Bhushan A (2006) p57 and Hes1 coordinate cell cycle exit with self-renewal of pancreatic progenitors. Developmental biology 298:22-31.

Ghosh B, Ganea GR, Denson LA, Iannucci R, Jacobs HC, Bogue CW (2000) Immunocytochemical characterization of murine Hex, a homeobox-containing protein. Pediatric research 48:634-638.

Gower WR, Jr., Dietz JR, Vesely DL, Finley CL, Skolnick KA, Fabri PJ, Cooper DR, Chalfant CE (1994) Atrial natriuretic peptide gene expression in the rat gastrointestinal tract. Biochemical and biophysical research communications 202:562-570.

Gower WR, Jr., Salhab KF, Foulis WL, Pillai N, Bundy JR, Vesely DL, Fabri PJ, Dietz JR (2000) Regulation of atrial natriuretic peptide gene expression in gastric antrum by fasting. American journal of physiology Regulatory, integrative and comparative physiology 278:R770-780.

Grant GR, Farkas MH, Pizarro AD, Lahens NF, Schug J, Brunk BP, Stoeckert CJ, Hogenesch JB, Pierce EA (2011) Comparative analysis of RNA-Seq alignment algorithms and the RNA-Seq unified mapper (RUM). Bioinformatics 27:2518-2528.

Gray MA, Greenwell JR, Garton AJ, Argent BE (1990) Regulation of maxi-K+ channels on pancreatic duct cells by cyclic AMP-dependent phosphorylation. The Journal of membrane biology 115:203-215.

Gray MA, Plant S, Argent BE (1993) cAMP-regulated whole cell chloride currents in pancreatic duct cells. The American journal of physiology 264:C591-602.

Greenwood AL, Li S, Jones K, Melton DA (2007) Notch signaling reveals developmental plasticity of Pax4(+) pancreatic endocrine progenitors and shunts them to a duct fate. Mechanisms of development 124:97-107.

Gresh L, Fischer E, Reimann A, Tanguy M, Garbay S, Shao X, Hiesberger T, Fiette L, Igarashi P, Yaniv M, Pontoglio M (2004) A transcriptional network in polycystic kidney disease. The EMBO journal 23:1657-1668.

Gross E, Fedotoff O, Pushkin A, Abuladze N, Newman D, Kurtz I (2003) Phosphorylation-induced modulation of pNBC1 function: distinct roles for the amino- and carboxy-termini. The Journal of physiology 549:673-682.

Gu G, Dubauskaite J, Melton DA (2002) Direct evidence for the pancreatic lineage: NGN3+ cells are islet progenitors and are distinct from duct progenitors. Development 129:2447-2457.

Guiral M, Bess K, Goodwin G, Jayaraman PS (2001) PRH represses transcription in hematopoietic cells by at least two independent mechanisms. The Journal of biological chemistry 276:2961-2970.

Guo Y, Chan R, Ramsey H, Li W, Xie X, Shelley WC, Martinez-Barbera JP, Bort B, Zaret K, Yoder M, Hromas R (2003) The homeoprotein Hex is required for hemangioblast differentiation. Blood 102:2428-2435.

Haanes KA, Novak I (2010) ATP storage and uptake by isolated pancreatic zymogen granules. The Biochemical journal 429:303-311.

Hallaq H, Pinter E, Enciso J, McGrath J, Zeiss C, Brueckner M, Madri J, Jacobs HC, Wilson CM, Vasavada H, Jiang X, Bogue CW (2004) A null mutation of Hhex results in abnormal cardiac development, defective vasculogenesis and elevated Vegfa levels. Development 131:5197-5209.

Hart A, Papadopoulou S, Edlund H (2003) Fgf10 maintains notch activation, stimulates proliferation, and blocks differentiation of pancreatic epithelial cells. Developmental dynamics : an official publication of the American Association of Anatomists 228:185-193.

Haumaitre C, Barbacci E, Jenny M, Ott MO, Gradwohl G, Cereghini S (2005) Lack of TCF2/vHNF1 in mice leads to pancreas agenesis. Proceedings of the National Academy of Sciences of the United States of America 102:1490-1495.

Hebrok M, Kim SK, Melton DA (1998) Notochord repression of endodermal Sonic hedgehog permits pancreas development. Genes & development 12:1705-1713.

Hebrok M, Kim SK, St Jacques B, McMahon AP, Melton DA (2000) Regulation of pancreas development by hedgehog signaling. Development 127:4905-4913.

Hede SE, Amstrup J, Christoffersen BC, Novak I (1999) Purinoceptors evoke different electrophysiological responses in pancreatic ducts. P2Y inhibits K(+) conductance, and P2X stimulates cation conductance. The Journal of biological chemistry 274:31784-31791.

Hezel AF, Gurumurthy S, Granot Z, Swisa A, Chu GC, Bailey G, Dor Y, Bardeesy N, Depinho RA (2008) Pancreatic LKB1 deletion leads to acinar polarity defects and cystic neoplasms. Molecular and cellular biology 28:2414-2425.

Hromas R, Radich J, Collins S (1993) PCR cloning of an orphan homeobox gene (PRH) preferentially expressed in myeloid and liver cells. Biochemical and biophysical research communications 195:976-983.

Hunter MP, Wilson CM, Jiang X, Cong R, Vasavada H, Kaestner KH, Bogue CW (2007) The homeobox gene Hhex is essential for proper hepatoblast differentiation and bile duct morphogenesis. Developmental biology 308:355-367.

Ishiguro H, Naruse S, Kitagawa M, Hayakawa T, Case RM, Steward MC (1999) Luminal ATP stimulates fluid and HCO3- secretion in guinea-pig pancreatic duct. The Journal of physiology 519 Pt 2:551-558.

Ishiguro H, Steward MC, Lindsay AR, Case RM (1996a) Accumulation of intracellular HCO3- by Na(+)-HCO3- cotransport in interlobular ducts from guinea-pig pancreas. The Journal of physiology 495 (Pt 1):169-178.

Ishiguro H, Steward MC, Wilson RW, Case RM (1996b) Bicarbonate secretion in interlobular ducts from guinea-pig pancreas. The Journal of physiology 495 (Pt 1):179-191.

Jacquemin P, Durviaux SM, Jensen J, Godfraind C, Gradwohl G, Guillemot F, Madsen OD, Carmeliet P, Dewerchin M, Collen D, Rousseau GG, Lemaigre FP (2000) Transcription factor hepatocyte nuclear factor 6 regulates pancreatic endocrine cell differentiation and controls expression of the proendocrine gene ngn3. Molecular and cellular biology 20:4445-4454.

Jacquemin P, Lemaigre FP, Rousseau GG (2003) The Onecut transcription factor HNF-6 (OC-1) is required for timely specification of the pancreas and acts upstream of Pdx-1 in the specification cascade. Developmental biology 258:105-116.

Jaffe AB, Kaji N, Durgan J, Hall A (2008) Cdc42 controls spindle orientation to position the apical surface during epithelial morphogenesis. The Journal of cell biology 183:625-633.

Jalleh RP, Aslam M, Williamson RC (1991) Pancreatic tissue and ductal pressures in chronic pancreatitis. The British journal of surgery 78:1235-1237.

Jensen J, Pedersen EE, Galante P, Hald J, Heller RS, Ishibashi M, Kageyama R, Guillemot F, Serup P, Madsen OD (2000) Control of endodermal endocrine development by Hes-1. Nature genetics 24:36-44.

Joergensen MT, Brusgaard K, Cruger DG, Gerdes AM, Schaffalitzky de Muckadell OB (2010) Genetic, epidemiological, and clinical aspects of hereditary pancreatitis: a population-based cohort study in Denmark. The American journal of gastroenterology 105:1876-1883.

John SW, Krege JH, Oliver PM, Hagaman JR, Hodgin JB, Pang SC, Flynn TG, Smithies O (1995) Genetic decreases in atrial natriuretic peptide and salt-sensitive hypertension. Science 267:679-681.

Jonsson J, Ahlgren U, Edlund T, Edlund H (1995) IPF1, a homeodomain protein with a dual function in pancreas development. The International journal of developmental biology 39:789-798.

Jonsson J, Carlsson L, Edlund T, Edlund H (1994) Insulin-promoter-factor 1 is required for pancreas development in mice. Nature 371:606-609.

Jung J, Zheng M, Goldfarb M, Zaret KS (1999) Initiation of mammalian liver development from endoderm by fibroblast growth factors. Science 284:1998-2003.

Kasamatsu S, Sato A, Yamamoto T, Keng VW, Yoshida H, Yamazaki Y, Shimoda M, Miyazaki J, Noguchi T (2004) Identification of the transactivating region of the homeodomain protein, hex. Journal of biochemistry 135:217-223.

Kawaguchi Y, Cooper B, Gannon M, Ray M, MacDonald RJ, Wright CV (2002) The role of the transcriptional regulator Ptf1a in converting intestinal to pancreatic progenitors. Nature genetics 32:128-134.

Keiles S, Kammesheidt A (2006) Identification of CFTR, PRSS1, and SPINK1 mutations in 381 patients with pancreatitis. Pancreas 33:221-227.

Keng VW, Fujimori KE, Myint Z, Tamamaki N, Nojyo Y, Noguchi T (1998) Expression of Hex mRNA in early murine postimplantation embryo development. FEBS letters 426:183-186.

Kesavan G, Sand FW, Greiner TU, Johansson JK, Kobberup S, Wu X, Brakebusch C, Semb H (2009) Cdc42-mediated tubulogenesis controls cell specification. Cell 139:791-801.

Kim SK, Hebrok M, Melton DA (1997) Notochord to endoderm signaling is required for pancreas development. Development 124:4243-4252.

Kim SK, Melton DA (1998) Pancreas development is promoted by cyclopamine, a hedgehog signaling inhibitor. Proceedings of the National Academy of Sciences of the United States of America 95:13036-13041.

Ko SB, Naruse S, Kitagawa M, Ishiguro H, Furuya S, Mizuno N, Wang Y, Yoshikawa T, Suzuki A, Shimano S, Hayakawa T (2002) Aquaporins in rat pancreatic interlobular ducts. American journal of physiology Gastrointestinal and liver physiology 282:G324-331.

Kopelman H, Corey M, Gaskin K, Durie P, Weizman Z, Forstner G (1988) Impaired chloride secretion, as well as bicarbonate secretion, underlies the fluid secretory defect in the cystic fibrosis pancreas. Gastroenterology 95:349-355.

Kopp JL, Dubois CL, Schaffer AE, Hao E, Shih HP, Seymour PA, Ma J, Sander M (2011) Sox9+ ductal cells are multipotent progenitors throughout development but do not produce new endocrine cells in the normal or injured adult pancreas. Development 138:653-665.

Kopp JL, von Figura G, Mayes E, Liu FF, Dubois CL, Morris JPt, Pan FC, Akiyama H, Wright CV, Jensen K, Hebrok M, Sander M (2012) Identification of Sox9-dependent acinar-to-ductal reprogramming as the principal mechanism for initiation of pancreatic ductal adenocarcinoma. Cancer cell 22:737-750.

Krapp A, Knofler M, Ledermann B, Burki K, Berney C, Zoerkler N, Hagenbuchle O, Wellauer PK (1998) The bHLH protein PTF1-p48 is essential for the formation of the exocrine and the correct spatial organization of the endocrine pancreas. Genes & development 12:3752-3763.

Kumar M, Jordan N, Melton D, Grapin-Botton A (2003) Signals from lateral plate mesoderm instruct endoderm toward a pancreatic fate. Developmental biology 259:109-122.

LaRusch J, Barmada MM, Solomon S, Whitcomb DC (2012) Whole exome sequencing identifies multiple, complex etiologies in an idiopathic hereditary pancreatitis kindred. JOP : Journal of the pancreas 13:258-262.

Le Lay J, Tuteja G, White P, Dhir R, Ahima R, Kaestner KH (2009) CRTC2 (TORC2) contributes to the transcriptional response to fasting in the liver but is not required for the maintenance of glucose homeostasis. Cell metabolism 10:55-62.

Lee MG, Choi JY, Luo X, Strickland E, Thomas PJ, Muallem S (1999a) Cystic fibrosis transmembrane conductance regulator regulates luminal Cl-/HCO3- exchange in mouse submandibular and pancreatic ducts. The Journal of biological chemistry 274:14670-14677.

Lee MG, Wigley WC, Zeng W, Noel LE, Marino CR, Thomas PJ, Muallem S (1999b) Regulation of Cl-/ HCO3- exchange by cystic fibrosis transmembrane conductance regulator expressed in NIH 3T3 and HEK 293 cells. The Journal of biological chemistry 274:3414-3421.

Maestro MA, Boj SF, Luco RF, Pierreux CE, Cabedo J, Servitja JM, German MS, Rousseau GG, Lemaigre FP, Ferrer J (2003) Hnf6 and Tcf2 (MODY5) are linked in a gene network operating in a precursor cell domain of the embryonic pancreas. Human molecular genetics 12:3307-3314.

Martin-Belmonte F, Gassama A, Datta A, Yu W, Rescher U, Gerke V, Mostov K (2007) PTEN-mediated apical segregation of phosphoinositides controls epithelial morphogenesis through Cdc42. Cell 128:383-397.

Martinez Barbera JP, Clements M, Thomas P, Rodriguez T, Meloy D, Kioussis D, Beddington RS (2000) The homeobox gene Hex is required in definitive endodermal tissues for normal forebrain, liver and thyroid formation. Development 127:2433-2445.

Masson E, Chen JM, Scotet V, Le Marechal C, Ferec C (2008a) Association of rare chymotrypsinogen C (CTRC) gene variations in patients with idiopathic chronic pancreatitis. Human genetics 123:83-91.

Masson E, Le Marechal C, Chandak GR, Lamoril J, Bezieau S, Mahurkar S, Bhaskar S, Reddy DN, Chen JM, Ferec C (2008b) Trypsinogen copy number mutations in patients with idiopathic chronic pancreatitis. Clinical gastroenterology and hepatology : the official clinical practice journal of the American Gastroenterological Association 6:82-88.

Matsukawa N, Grzesik WJ, Takahashi N, Pandey KN, Pang S, Yamauchi M, Smithies O (1999) The natriuretic peptide clearance receptor locally modulates the physiological effects of the natriuretic peptide system. Proceedings of the National Academy of Sciences of the United States of America 96:7403-7408.

Matthews EK, Petersen OH, Williams JA (1973) Pancreatic acinar cells: acetylcholine-induced membrane depolarization, calcium efflux and amylase release. The Journal of physiology 234:689-701.

Meda P, Findlay I, Kolod E, Orci L, Petersen OH (1983) Short and reversible uncoupling evokes little change in the gap junctions of pancreatic acinar cells. Journal of ultrastructure research 83:69-84.

Metzger RJ, Klein OD, Martin GR, Krasnow MA (2008) The branching programme of mouse lung development. Nature 453:745-750.

Miralles F, Lamotte L, Couton D, Joshi RL (2006) Interplay between FGF10 and Notch signalling is required for the self-renewal of pancreatic progenitors. The International journal of developmental biology 50:17-26.

Morck C, Rauthan M, Wagberg F, Pilon M (2004) pha-2 encodes the C. elegans ortholog of the homeodomain protein HEX and is required for the formation of the pharyngeal isthmus. Developmental biology 272:403-418.

Muddana V, Lamb J, Greer JB, Elinoff B, Hawes RH, Cotton PB, Anderson MA, Brand RE, Slivka A, Whitcomb DC (2008) Association between calcium sensing receptor gene polymorphisms and chronic pancreatitis in a US population: role of serine protease inhibitor Kazal 1type and alcohol. World journal of gastroenterology : WJG 14:4486-4491.

Murtaugh LC, Stanger BZ, Kwan KM, Melton DA (2003) Notch signaling controls multiple steps of pancreatic differentiation. Proceedings of the National Academy of Sciences of the United States of America 100:14920-14925.

Murugaian EE, Premkumar RM, Radhakrishnan L, Vallath B (2008) Novel mutations in the calcium sensing receptor gene in tropical chronic pancreatitis in India. Scandinavian journal of gastroenterology 43:117-121.

Norgaard GA, Jensen JN, Jensen J (2003) FGF10 signaling maintains the pancreatic progenitor cell state revealing a novel role of Notch in organ development. Developmental biology 264:323-338.

O'Reilly DA, Yang BM, Creighton JE, Demaine AG, Kingsnorth AN (2001) Mutations of the cationic trypsinogen gene in hereditary and non-hereditary pancreatitis. Digestion 64:54-60.

Oliver-Krasinski JM, Kasner MT, Yang J, Crutchlow MF, Rustgi AK, Kaestner KH, Stoffers DA (2009) The diabetes gene Pdx1 regulates the transcriptional network of pancreatic endocrine progenitor cells in mice. The Journal of clinical investigation 119:1888-1898.

Park S, Shcheynikov N, Hong JH, Zheng C, Suh SH, Kawaai K, Ando H, Mizutani A, Abe T, Kiyonari H, Seki G, Yule D, Mikoshiba K, Muallem S (2013) Irbit mediates synergy between ca(2+) and cAMP signaling pathways during epithelial transport in mice. Gastroenterology 145:232-241.

Pellizzari L, D'Elia A, Rustighi A, Manfioletti G, Tell G, Damante G (2000) Expression and function of the homeodomain-containing protein Hex in thyroid cells. Nucleic acids research 28:2503-2511.

Petersen OH, Findlay I (1987) Electrophysiology of the pancreas. Physiological reviews 67:1054-1116.

Petersen OH, Ueda N (1975) Pancreatic acinar cells: effect of acetylcholine, pancreozymin, gastrin and secretin on membrane potential and resistance in vivo and in vitro. The Journal of physiology 247:461-471.

Petrucco S, Wellauer PK, Hagenbuchle O (1990) The DNA-binding activity of transcription factor PTF1 parallels the synthesis of pancreas-specific mRNAs during mouse development. Molecular and cellular biology 10:254-264.

Pfutzer RH, Barmada MM, Brunskill AP, Finch R, Hart PS, Neoptolemos J, Furey WF, Whitcomb DC (2000) SPINK1/PSTI polymorphisms act as disease modifiers in familial and idiopathic chronic pancreatitis. Gastroenterology 119:615-623.

Pictet RL, Clark WR, Williams RH, Rutter WJ (1972) An ultrastructural analysis of the developing embryonic pancreas. Developmental biology 29:436-467.

Pierreux CE, Poll AV, Kemp CR, Clotman F, Maestro MA, Cordi S, Ferrer J, Leyns L, Rousseau GG, Lemaigre FP (2006) The transcription factor hepatocyte nuclear factor-6 controls the development of pancreatic ducts in the mouse. Gastroenterology 130:532-541.

Pirro N, Sielezneff I, Ouaissi M, Weber D, Consentino B, Sastre B (2003) [Coelioscopic treatment of pancreatic polycystic disease]. Annales de chirurgie 128:109-111.

Prevot PP, Simion A, Grimont A, Colletti M, Khalaileh A, Van den Steen G, Sempoux C, Xu X, Roelants V, Hald J, Bertrand L, Heimberg H, Konieczny SF, Dor Y, Lemaigre FP, Jacquemin P (2012) Role of the ductal transcription factors HNF6 and Sox9 in pancreatic acinar-to-ductal metaplasia. Gut 61:1723-1732.

Puppin C, Puglisi F, Pellizzari L, Manfioletti G, Pestrin M, Pandolfi M, Piga A, Di Loreto C, Damante G (2006) HEX expression and localization in normal mammary gland and breast carcinoma. BMC cancer 6:192.

Que J, Okubo T, Goldenring JR, Nam KT, Kurotani R, Morrisey EE, Taranova O, Pevny LH, Hogan BL (2007) Multiple dose-dependent roles for Sox2 in the patterning and differentiation of anterior foregut endoderm. Development 134:2521-2531.

Racz GZ, Kittel A, Riccardi D, Case RM, Elliott AC, Varga G (2002) Extracellular calcium sensing receptor in human pancreatic cells. Gut 51:705-711.

Raimondi S, Lowenfels AB, Morselli-Labate AM, Maisonneuve P, Pezzilli R (2010) Pancreatic cancer in chronic pancreatitis; aetiology, incidence, and early detection. Best practice & research Clinical gastroenterology 24:349-358.

Rebours V, Boutron-Ruault MC, Schnee M, Ferec C, Le Marechal C, Hentic O, Maire F, Hammel P, Ruszniewski P, Levy P (2009) The natural history of hereditary pancreatitis: a national series. Gut 58:97-103.

Reichert M, Rustgi AK (2011) Pancreatic ductal cells in development, regeneration, and neoplasia. The Journal of clinical investigation 121:4572-4578.

Reichert M, Takano S, Heeg S, Bakir B, Botta GP, Rustgi AK (2013) Isolation, culture and genetic manipulation of mouse pancreatic ductal cells. Nature protocols 8:1354-1365.

Rindler MJ, Xu CF, Gumper I, Smith NN, Neubert TA (2007) Proteomic analysis of pancreatic zymogen granules: identification of new granule proteins. Journal of proteome research 6:2978-2992.

Riordan JR, Rommens JM, Kerem B, Alon N, Rozmahel R, Grzelczak Z, Zielenski J, Lok S, Plavsic N, Chou JL, et al. (1989) Identification of the cystic fibrosis gene: cloning and characterization of complementary DNA. Science 245:1066-1073.

Robinson MD, McCarthy DJ, Smyth GK (2010) edgeR: a Bioconductor package for differential expression analysis of digital gene expression data. Bioinformatics 26:139-140.

Rosendahl J, Witt H, Szmola R, Bhatia E, Ozsvari B, Landt O, Schulz HU, Gress TM, Pfutzer R, Lohr M, Kovacs P, Bluher M, Stumvoll M, Choudhuri G, Hegyi P, te Morsche RH, Drenth JP, Truninger K, Macek M, Jr., Puhl G, Witt U, Schmidt H, Buning C, Ockenga J, Kage A, Groneberg DA, Nickel R, Berg T, Wiedenmann B, Bodeker H, Keim V, Mossner J, Teich N, Sahin-Toth M (2008) Chymotrypsin C (CTRC) variants that diminish activity or secretion are associated with chronic pancreatitis. Nature genetics 40:78-82.

Rossi JM, Dunn NR, Hogan BL, Zaret KS (2001) Distinct mesodermal signals, including BMPs from the septum transversum mesenchyme, are required in combination for hepatogenesis from the endoderm. Genes & development 15:1998-2009.

Rukstalis JM, Habener JF (2007) Snail2, a mediator of epithelial-mesenchymal transitions, expressed in progenitor cells of the developing endocrine pancreas. Gene expression patterns : GEP 7:471-479.

Sabbatini ME, Villagra A, Davio CA, Vatta MS, Fernandez BE, Bianciotti LG (2003) Atrial natriuretic factor stimulates exocrine pancreatic secretion in the rat through NPR-C receptors. American journal of physiology Gastrointestinal and liver physiology 285:G929-937.

Schneider A, Larusch J, Sun X, Aloe A, Lamb J, Hawes R, Cotton P, Brand RE, Anderson MA, Money ME, Banks PA, Lewis MD, Baillie J, Sherman S, Disario J, Burton FR, Gardner TB, Amann ST, Gelrud A, George R, Rockacy MJ, Kassabian S, Martinson J, Slivka A, Yadav D, Oruc N, Barmada MM, Frizzell R, Whitcomb DC (2011) Combined bicarbonate conductance-impairing variants in CFTR and SPINK1 variants are associated with chronic pancreatitis in patients without cystic fibrosis. Gastroenterology 140:162-171.

Seymour PA, Freude KK, Dubois CL, Shih HP, Patel NA, Sander M (2008) A dosage-dependent requirement for Sox9 in pancreatic endocrine cell formation. Developmental biology 323:19-30.

Seymour PA, Freude KK, Tran MN, Mayes EE, Jensen J, Kist R, Scherer G, Sander M (2007) SOX9 is required for maintenance of the pancreatic progenitor cell pool. Proceedings of the National Academy of Sciences of the United States of America 104:1865-1870.

Seymour PA, Shih HP, Patel NA, Freude KK, Xie R, Lim CJ, Sander M (2012) A Sox9/Fgf feed-forward loop maintains pancreatic organ identity. Development 139:3363-3372.

Sharer N, Schwarz M, Malone G, Howarth A, Painter J, Super M, Braganza J (1998) Mutations of the cystic fibrosis gene in patients with chronic pancreatitis. The New England journal of medicine 339:645-652.

Shek FW, Benyon RC, Walker FM, McCrudden PR, Pender SL, Williams EJ, Johnson PA, Johnson CD, Bateman AC, Fine DR, Iredale JP (2002) Expression of transforming growth factor-beta 1 by pancreatic stellate cells and its implications for matrix secretion and turnover in chronic pancreatitis. The American journal of pathology 160:1787-1798.

Shih HP, Kopp JL, Sandhu M, Dubois CL, Seymour PA, Grapin-Botton A, Sander M (2012) A Notch-dependent molecular circuitry initiates pancreatic endocrine and ductal cell differentiation. Development 139:2488-2499.

Smanio T (1969) Proposed nomenclature and classification of the human pancreatic ducts and duodenal papillae. Study based on 200 post mortems. International surgery 52:125-141.

Smith ZD, Caplan MJ, Forbush B, 3rd, Jamieson JD (1987) Monoclonal antibody localization of Na+-K+-ATPase in the exocrine pancreas and parotid of the dog. The American journal of physiology 253:G99-109.

Solar M, Cardalda C, Houbracken I, Martin M, Maestro MA, De Medts N, Xu X, Grau V, Heimberg H, Bouwens L, Ferrer J (2009) Pancreatic exocrine duct cells give rise to insulin-producing beta cells during embryogenesis but not after birth. Developmental cell 17:849-860.

Soufi A, Smith C, Clarke AR, Gaston K, Jayaraman PS (2006) Oligomerisation of the developmental regulator proline rich homeodomain (PRH/Hex) is mediated by a novel proline-rich dimerisation domain. Journal of molecular biology 358:943-962.

Spencer CC, Su Z, Donnelly P, Marchini J (2009) Designing genome-wide association studies: sample size, power, imputation, and the choice of genotyping chip. PLoS genetics 5:e1000477.

Spooner BS, Walther BT, Rutter WJ (1970) The development of the dorsal and ventral mammalian pancreas in vivo and in vitro. The Journal of cell biology 47:235-246.

Stanger BZ, Tanaka AJ, Melton DA (2007) Organ size is limited by the number of embryonic progenitor cells in the pancreas but not the liver. Nature 445:886-891.

Steinhelper ME, Cochrane KL, Field LJ (1990) Hypotension in transgenic mice expressing atrial natriuretic factor fusion genes. Hypertension 16:301-307.

Stewart AK, Yamamoto A, Nakakuki M, Kondo T, Alper SL, Ishiguro H (2009) Functional coupling of apical Cl-/HCO3- exchange with CFTR in stimulated HCO3- secretion by guinea pig interlobular pancreatic duct. American journal of physiology Gastrointestinal and liver physiology 296:G1307-1317.

Stimec B, Bulajic M, Korneti V, Milosavljevic T, Krstic R, Ugljesic M (1996) Ductal morphometry of ventral pancreas in pancreas divisum. Comparison between clinical and anatomical results. The Italian journal of gastroenterology 28:76-80.

Stoffers DA, Ferrer J, Clarke WL, Habener JF (1997a) Early-onset type-II diabetes mellitus (MODY4) linked to IPF1. Nature genetics 17:138-139.

Stoffers DA, Zinkin NT, Stanojevic V, Clarke WL, Habener JF (1997b) Pancreatic agenesis attributable to a single nucleotide deletion in the human IPF1 gene coding sequence. Nature genetics 15:106-110.

Sultan M, Werlin S, Venkatasubramani N (2012) Genetic prevalence and characteristics in children with recurrent pancreatitis. Journal of pediatric gastroenterology and nutrition 54:645-650.

Swingler TE, Bess KL, Yao J, Stifani S, Jayaraman PS (2004) The proline-rich homeodomain protein recruits members of the Groucho/Transducin-like enhancer of split protein family to co-repress transcription in hematopoietic cells. The Journal of biological chemistry 279:34938-34947.

Tabcharani JA, Chang XB, Riordan JR, Hanrahan JW (1991) Phosphorylation-regulated Cl- channel in CHO cells stably expressing the cystic fibrosis gene. Nature 352:628-631.

Thomas PQ, Brown A, Beddington RS (1998) Hex: a homeobox gene revealing peri-implantation asymmetry in the mouse embryo and an early transient marker of endothelial cell precursors. Development 125:85-94.

Topisirovic I, Culjkovic B, Cohen N, Perez JM, Skrabanek L, Borden KL (2003) The proline-rich homeodomain protein, PRH, is a tissue-specific inhibitor of eIF4E-dependent cyclin D1 mRNA transport and growth. The EMBO journal 22:689-703.

Ulrich CD, 2nd, Holtmann M, Miller LJ (1998) Secretin and vasoactive intestinal peptide receptors: members of a unique family of G protein-coupled receptors. Gastroenterology 114:382-397.

Vankeerberghen A, Wei L, Jaspers M, Cassiman JJ, Nilius B, Cuppens H (1998) Characterization of 19 disease-associated missense mutations in the regulatory domain of the cystic fibrosis transmembrane conductance regulator. Human molecular genetics 7:1761-1769.

Veel T, Villanger O, Holthe MR, Cragoe EJ, Jr., Raeder MG (1992) Na(+)-H+ exchange is not important for pancreatic HCO3- secretion in the pig. Acta physiologica Scandinavica 144:239-246.

Villasenor A, Chong DC, Henkemeyer M, Cleaver O (2010) Epithelial dynamics of pancreatic branching morphogenesis. Development 137:4295-4305.

Vollmar AM, Paumgartner G, Gerbes AL (1997) Differential gene expression of the three natriuretic peptides and natriuretic peptide receptor subtypes in human liver. Gut 40:145-150.

Wang Y, Soyombo AA, Shcheynikov N, Zeng W, Dorwart M, Marino CR, Thomas PJ, Muallem S (2006) Slc26a6 regulates CFTR activity in vivo to determine pancreatic duct HCO3- secretion: relevance to cystic fibrosis. The EMBO journal 25:5049-5057.

Weiss FU, Schurmann C, Guenther A, Ernst F, Teumer A, Mayerle J, Simon P, Volzke H, Radke D, Greinacher A, Kuehn JP, Zenker M, Volker U, Homuth G, Lerch MM (2014) Fucosyltransferase 2 (FUT2) non-secretor status and blood group B are associated with elevated serum lipase activity in asymptomatic subjects, and an increased risk for chronic pancreatitis: a genetic association study. Gut.

Wells JM, Melton DA (2000) Early mouse endoderm is patterned by soluble factors from adjacent germ layers. Development 127:1563-1572.

Wessells NK, Cohen JH (1967) Early Pancreas Organogenesis: Morphogenesis, Tissue Interactions, and Mass Effects. Developmental biology 15:237-270.

Whitcomb DC, Ermentrout GB (2004) A mathematical model of the pancreatic duct cell generating high bicarbonate concentrations in pancreatic juice. Pancreas 29:e30-40.

Whitcomb DC, Gorry MC, Preston RA, Furey W, Sossenheimer MJ, Ulrich CD, Martin SP, Gates LK, Jr., Amann ST, Toskes PP, Liddle R, McGrath K, Uomo G, Post JC, Ehrlich GD (1996) Hereditary pancreatitis is caused by a mutation in the cationic trypsinogen gene. Nature genetics 14:141-145.

Whitcomb DC, LaRusch J, Krasinskas AM, Klei L, Smith JP, Brand RE, Neoptolemos JP, Lerch MM, Tector M, Sandhu BS, Guda NM, Orlichenko L, Alzheimer's Disease Genetics C, Alkaade S, Amann ST, Anderson MA, Baillie J, Banks PA, Conwell D, Cote GA, Cotton PB, DiSario J, Farrer LA, Forsmark CE, Johnstone M, Gardner TB, Gelrud A, Greenhalf W, Haines JL, Hartman DJ, Hawes RA, Lawrence C, Lewis M, Mayerle J, Mayeux R, Melhem NM, Money ME, Muniraj T, Papachristou GI, Pericak-Vance MA, Romagnuolo J, Schellenberg GD, Sherman S, Simon P, Singh VP, Slivka A, Stolz D, Sutton R, Weiss FU, Wilcox CM, Zarnescu NO, Wisniewski SR, O'Connell MR, Kienholz ML, Roeder K, Barmada MM, Yadav D, Devlin B (2012) Common genetic variants in the CLDN2 and PRSS1-PRSS2 loci alter risk for alcohol-related and sporadic pancreatitis. Nature genetics 44:1349-1354.

Wiebe PO, Kormish JD, Roper VT, Fujitani Y, Alston NI, Zaret KS, Wright CV, Stein RW, Gannon M (2007) Ptf1a binds to and activates area III, a highly conserved region of the Pdx1 promoter that mediates early pancreas-wide Pdx1 expression. Molecular and cellular biology 27:4093-4104.

Witt H, Luck W, Hennies HC, Classen M, Kage A, Lass U, Landt O, Becker M (2000) Mutations in the gene encoding the serine protease inhibitor, Kazal type 1 are associated with chronic pancreatitis. Nature genetics 25:213-216.

Wu G, D'Agati V, Cai Y, Markowitz G, Park JH, Reynolds DM, Maeda Y, Le TC, Hou H, Jr., Kucherlapati R, Edelmann W, Somlo S (1998) Somatic inactivation of Pkd2 results in polycystic kidney disease. Cell 93:177-188.

Wu G, Markowitz GS, Li L, D'Agati VD, Factor SM, Geng L, Tibara S, Tuchman J, Cai Y, Park JH, van Adelsberg J, Hou H, Jr., Kucherlapati R, Edelmann W, Somlo S (2000) Cardiac defects and renal failure in mice with targeted mutations in Pkd2. Nature genetics 24:75-78.

Yamamoto M, Otani M, Otsuki M (2006) A new model of chronic pancreatitis in rats. American journal of physiology Gastrointestinal and liver physiology 291:G700-708.

Yang D, Li Q, So I, Huang CL, Ando H, Mizutani A, Seki G, Mikoshiba K, Thomas PJ, Muallem S (2011) IRBIT governs epithelial secretion in mice by antagonizing the WNK/SPAK kinase pathway. The Journal of clinical investigation 121:956-965.

Yang D, Shcheynikov N, Zeng W, Ohana E, So I, Ando H, Mizutani A, Mikoshiba K, Muallem S (2009) IRBIT coordinates epithelial fluid and HCO3- secretion by stimulating the transporters pNBC1 and CFTR in the murine pancreatic duct. The Journal of clinical investigation 119:193-202.

Zeng W, Lee MG, Yan M, Diaz J, Benjamin I, Marino CR, Kopito R, Freedman S, Cotton C, Muallem S, Thomas P (1997) Immuno and functional characterization of CFTR in submandibular and pancreatic acinar and duct cells. The American journal of physiology 273:C442-455.

Zhang H, Ables ET, Pope CF, Washington MK, Hipkens S, Means AL, Path G, Seufert J, Costa RH, Leiter AB, Magnuson MA, Gannon M (2009) Multiple, temporal-specific roles for HNF6 in pancreatic endocrine and ductal differentiation. Mechanisms of development 126:958-973.

Zhang J, McKenna LB, Bogue CW, Kaestner KH (2014) The diabetes gene Hhex maintains delta-cell differentiation and islet function. Genes & development 28:829-834.

Zhao H, Star RA, Muallem S (1994) Membrane localization of H+ and HCO3- transporters in the rat pancreatic duct. The Journal of general physiology 104:57-85.

Zhou Q, Law AC, Rajagopal J, Anderson WJ, Gray PA, Melton DA (2007) A multipotent progenitor domain guides pancreatic organogenesis. Developmental cell 13:103-114.